MORPHOLOGICAL AND BIOCHEMICAL EVIDENCE FOR THE EVOLUTION OF HYPO-OSMOREGULATION IN SNAKES

By

LESLIE S. BABONIS

A DISSERTATION PRESENTED TO THE GRADUATE SCHOOL
OF THE UNIVERSITY OF FLORIDA IN PARTIAL FULFILLMENT
OF THE REQUIREMENTS FOR THE DEGREE OF
DOCTOR OF PHILOSOPHY

UNIVERSITY OF FLORIDA

2011

To all my mentors: official and unofficial, past, present, and future

ACKNOWLEDGMENTS

First, I would like to thank my doctoral advisory committee: David H. Evans, Martin J. Cohn, Karen A. Bjorndal, Daniel A. Hahn, and Colette M. St. Mary, for their commitment to my success in my PhD, their guidance along my path to a career in science, and the endless stream of letters of recommendation they provided. In addition to my official committee, several faculty members both in the Department of Biology and elsewhere contributed much to my development during this period. Among these, Harvey Lillywhite and Ming-Chung Tu (National Taiwan Normal University) were absolutely instrumental in introducing me to my field sites and enabling me to develop a project that focused on the physiological ecology of marine snakes. As my project became more molecular and less ecological (and more confusing), the intellectual and technical guidance offered to me by Ed Braun and Rebecca Kimball became indispensible. I would also like to recognize Lou Guillette and David Reed for always making the time to offer me professional advice on top of making their labs totally available to me and the lab of Charles Wingo for allowing me to use their vapor pressure osmometer and pHOx machine. Lastly, I am forever indebted to Ben Bolker for his patience in helping me to develop my quantitative and analytic skills.

Beyond the contributions of the faculty members listed above, there are several graduate and undergraduate students without whom I simply would not have been able to put these pieces together. Molly Womack and Stephanie Miller (my last two undergraduate assistants) were indispensable as I was putting together the gut/cloaca and kidney chapters (respectively). Though these two earned co-authorship through their efforts, the following people (ordered alphabetically) also made notable

contributions to this dissertation: Julie Allen, David Butcher, Chelsey Campbell, David Hall, Ryan McCleary, Brandon Moore, Coleman Sheehy, and Mike Thompson.

I also offer my deepest and most sincere thanks to Kelly Hyndman and Mike and Krista McCoy. These three people directly and significantly contributed to the conception, development, and completion of this project as well as my development as a scientist in ways that I can never fully represent on paper. Kelly, Mike, and Krista were my mentors, editors, teachers, listeners, voices of reason, and friends throughout this whole process; I wouldn't be where I am without them. Lastly, I would like to thank my parents for supporting all of my oscillating interests over the years and always encouraging me to work hard for what I want. This work was funded by the National Geographic Society (8058-06 to Harvey B. Lillywhite), the National Science Foundation (IOB-0519579 to DHE; EAPSI Fellowship to LSB), the Society for Integrative and Comparative Biology (LSB), Sigma Xi (LSB), the American Physiological Society (LSB), and several internal/departmental awards (LSB).

TABLE OF CONTENTS

page

LIST OF TABLES

LIST OF FIGURES

LIST OF ABBREVIATIONS

α5	monoclonal antibody directed against the α subunit of NKA
AB^+	alcian blue positive
Ach	acetylcholine
ANOVA	analysis of variance
AQP	aquaporin
AVMA	American Veterinary Medical Association
AVT	arginine vasotocin
BLAST	basic local alignment search tool
bp	base pair
C	celsius
Cl^-	chloride ion
cDNA	complimentary DNA
CFTR	cystic fibrosis transmembrane conductance regulator
DNA	deoxyribonucleic acid
DI	deionized water
EF1a1	eukaryotic translation elongation factor 1 α 1
ENaC	epithelial Na^+ channel
FL	Florida
g	grams
h	hours
Hc-3	polyclonal antibody detecting c-tail of AQP3
IACUC	Institutional Animal Care and Use Committee
IgG	immunoglobulin G
IHC	immunohistochemistry

K^+	potassium ion
kDa	kilo-Dalton
L8	ribosomal gene L8
lsAQP3	*Laticauda semifasciata* isoform of AQP3
lsCFTR	*Laticauda semifasciata* isoform of CFTR
min	minutes
mM	milimolar
mmol/L	milimoles per liter
mOsm	miliosmoles
mRNA	messenger RNA
N	sample size
Na^+	sodium ion
NaCl	sodium chloride
NCBI	National Center for Biotechnology Information
NCC	Na^+/Cl^- symporter
NHE	Na^+/H^+ exchanger
NKA	Na^+/K^+-ATPase
NKCC	$Na^+/K^+/2Cl^-$ cotransporter
NPA	asparagine-proline-alanine (motif)
PAS^+	periodic acid Schiff positive
PBS	phosphate buffered saline
PCR	polymerase chain reaction
ppt	parts per thousand
qRT-PCR	quantitative real-time PCR
RACE	rapid amplification of cDNA ends

RNA	ribonucleic acid
RPM	rotations per minute
RT	room temperature
s.e.m	standard error of the mean
SW	seawater
T4	monoclonal antibody detecting the C-tail in NKCC1, NKCC2, NCC
TBS	tris buffered saline
TTBS	tBS with Tween-20
µm	micrometer
V	volts
VIP	vasoactive intestinal peptide

Abstract of Dissertation Presented to the Graduate School
of the University of Florida in Partial Fulfillment of the
Requirements for the Degree of Doctor of Philosophy

MORPHOLOGICAL AND BIOCHEMICAL EVIDENCE FOR THE EVOLUTION OF HYPO-OSMOREGULATION IN SNAKES

By

Leslie S. Babonis

May 2011

Chair: Martin J. Cohn
Cochair: David H. Evans
Major: Zoology

Vertebrates inhabiting marine environments experience salt accumulation and water loss. Accordingly, several physiological specializations have evolved to combat these challenges. Among reptiles, salt glands have evolved multiple times but, interestingly, many species of reptiles use marine habitats without any known physiological specializations. By comparing the physiology of specialized marine species with that of species without such specializations, it is possible to develop hypotheses about the evolution of marine habitat use in reptiles. Here, I examine the morphology and biochemistry of the secretory epithelia in the salt glands of three species of Laticaudine sea snake and then compare the salt glands of one species (*Laticauda semifasciata*) with the cellular morphology, biochemistry, and response to salinity in the cephalic glands from semi-marine (*Nerodia clarkii clarkii*) and freshwater (*Nerodia fasciata*) watersnakes to make predictions about the steps leading to the evolution of salt glands. To then understand the renal and post-renal responses to salinity change in reptiles from marine and freshwater environments, I examined the structure/function of the kidney in these same three species of snakes and the

gut/cloacal complex in the two species of watersnake only. Specifically, I examined the epithelia of each tissue for evidence of water/ion secretion or absorption when acclimated to 0, 50 or 100% seawater. Since I found no differences in renal or gut/cloacal morphology or in the distribution of ion transporters/water channels between the two species of watersnake, renal and gut/cloacal reclamation of ions/water cannot be responsible for the differential success of *N. c. clarkii* and *N. fasciata* in marine habitats. Additionally, only minor/equivocal differences in the cephalic glands were detected in *N. c. clarkii*, suggesting that the ability of this species to tolerate marine environments may reflect behavioral rather than physiological innovations.

CHAPTER 1
INTRODUCTION

Evolution of Marine Habitat Use

The vast majority of marine vertebrates are hypo-osmoregulators, maintaining body fluids which are more dilute than the surrounding environment (compare typical vertebrate plasma osmolality of ~300mOsm with typical seawater osmolality of ~1000mOsm). Accordingly, animals invading marine environments face two major osmoregulatory challenges: minimizing the accumulation of salt and maximizing the retention of water. Salt accumulation in marine vertebrates occurs primarily through oral intake; while some species actively drink seawater (e.g., many teleosts and some birds and mammals; Ortiz, 2001; Goldstein, 2002; Evans and Claiborne, 2009), most marine reptiles that have been studied are known to avoid ingestion of saltwater (Bentley et al., 1967; Dunson and Dunson, 1979; Taplin, 1985; Lillywhite et al., 2008; but, see: Holmes and McBean, 1964; Reina et al., 2002). Among many vertebrates, then, seawater influx occurs only incidentally, while feeding on marine prey (Shoemaker and Nagy, 1984; Dunson, 1985). By contrast, water loss occurs via several routes: across the respiratory and cutaneous membranes, in the production of urinary and fecal wastes, and in the production of an aqueous salt solution secreted from salt-regulatory organs (e.g., salt glands). Thus, in the evolution of marine habitat use, traits that reduce the intake of salt or increase the excretion of salt (while still minimizing the loss of water) might have provided a selective advantage. In this light, it might be expected that behavioral traits, like a dietary shift from isosmotic to hypo-osmotic prey or from small prey items to large prey items (which requires fewer feeding events and, therefore, less incidental intake of salt water), might have been associated with early stages of marine invasion (Dunson

and Mazzotti, 1989). The evolution of the salt-secretory gill, in marine teleosts, as well as the salt glands of reptiles and birds, and the specialized kidney of mammals may, therefore, have occurred only after initial modifications to the behavior of the animals invading these new environments.

Although the physiology of the gills varies considerably among extant taxa, all marine teleosts have this organ suggesting, parsimoniously, that this complex structure evolved once and was retained in all descendents. Additionally, despite the fact that marine habitat use is patchy in birds, three pieces of evidence suggest that the specialized salt regulatory organs of birds (the nasal salt glands) are a synapomorphy of this group: (i) the skull morphology of the extinct taxa *Hesperornis* and *Ichthyornis* suggests that salt glands were present in these taxa (Marples, 1932), (ii) the recently revised avian phylogeny places the Struthioniformes (ostriches and their allies), which are thought to have a salt gland (Hughes, 1970; Peaker and Linzell, 1975; but see: Bennett and Hughes, 2003), as the most basal taxon (Hackett et al., 2008), (iii) the salt gland appears to be developmentally homologous in all extant and extinct taxa (i.e., it is a modified nasal gland; Marples, 1932). Likewise, the complicated nephron structure and associated concentrating capacity of the kidney is a unifying feature of the mammals, marine or otherwise. From an evolutionary perspective, reptiles, which have likely undergone several independent invasion events leading to the diversity of modern marine taxa and of modern salt glands, are, therefore, a much more interesting group in which to ask questions about the relationship between marine invasion and the evolution of specialized salt-secreting tissues.

Among reptiles, salt glands have evolved *at least* five times: there is a lachrymal salt gland in the marine and estuarine turtles (Schmidt-Nielsen and Fange, 1958), a nasal salt gland in marine iguanas (Schmidt-Nielsen and Fange, 1958) and many desert lizards (Dunson, 1969), a sublingual salt gland in the truly marine sea snakes (Dunson et al., 1971) and the marine file snakes (Dunson and Dunson, 1973), a premaxillary salt gland in the old world watersnakes that inhabit estuarine and coastal marine environments (Dunson and Dunson, 1979), and lingual salt glands in marine crocodilians (Taplin and Grigg, 1981). Though these occurrences represent the minimum number of independent origins of salt glands in reptiles, the actual number of independent evolutionary events may actually be much higher than this, a claim supported by (i) the polyphyly of extant marine taxa within any given lineage, (ii) the presence of salt glands in an independently marine lineage of fossil turtles (Billon-Bruyat et al., 2005), and (iii) evidence of *nasal* salt glands in fossil crocodilians (Fernandez and Gasparini, 2000), which are, necessarily, not homologous to the *lingual* salt glands of extant species. Importantly, though many desert lizards are also known to possess salt glands (although these glands appear to be specialized for the excretion of KCl rather than NaCl), salt glands have never been identified in the freshwater or terrestrial (including desert) species of snake. Among crocodilians, only those species in the Crocodylidae, not the Alligatoridae, are known to have salt glands (Taplin et al., 1982).

Salt Gland Physiology

Salt glands are specialized organs that, among marine taxa, function primarily in the excretion of NaCl (the exception to this is the high K^+ load excreted by the herbivorous marine iguana). In tetrapods, the salt glands are located in the cephalic

region where they are perfused by abundant blood vessels, enabling them to remove excess salts keeping plasma ion loads low. All salt glands studied thus far are known to be compound tubular in shape and to be populated by specialized ionosecretory cells – the prinicipal cells. Principal cells are defined by their ability to secrete net NaCl, which they do through the combined action of the basolaterally positioned Na^+/K^+-ATPase (NKA) and $Na^+/K^+/Cl^-$ cotransporter (NKCC) and the apically positioned cystic fibrosis transmembrane conductance regulator (CFTR). Although the identity and localization of these components of NaCl secretion in the principal cell have long been known in the salt glands of elasmobranchs and birds (Shuttleworth and Hildebrandt, 1999), much less is known about the details of ion secretion from the salt glands of reptiles. Furthermore, the ways in which the anatomy/physiology of salt glands differ from unspecialized glands (i.e., the traits that make salt glands unique) have gone largely unstudied, especially among reptilian taxa. Finally, the relationship between the possession of salt glands and the anatomy/physiology of other osmoregulatory organs, like the kidneys, has been almost completely ignored among reptilian taxa.

Other Salt-Regulatory Organs

While the salt glands appear to be the primary organs used in the excretion of excess salts in marine reptiles, some studies of marine bird physiology suggest that the integrated whole-animal response to high environmental salinity may also involve the kidneys, gut, and cloaca (Braun, 1999; Hughes, 2003). Early studies of kidney function in reptiles revealed the poor concentrating capacity of this organ, which is likely a function of the organization of the nephron relative to the collecting duct (Dantzler and Bradshaw, 2009). In the context of marine habitat use, excretion of enough salt to prevent its accumulation would also involve the loss of a large amount of water; thus,

the reptilian kidney cannot function in net salt excretion. Despite this inability to secrete concentrated salts, the contribution of the reptilian kidneys to whole animal homeostasis may still be important. Though many important advancements in our understanding of renal physiology in non-mammalian taxa have come from detailed studies of water and ion transport across the various segments of the nephron in reptilian taxa (reviewed in: Dantzler and Bradshaw, 2009), still much remains to be learned about the mechanisms by which reptilian kidneys regulate salt and water balance and, importantly, the relationship between these salt/water regulatory mechanisms and the possession of an extra-renal means for salt secretion.

Considering that salt accumulation in marine reptiles is, in part, a result of oral influx (while feeding) followed by salt absorption across the lining of the gut and, potentially, the cloaca, it might reasonably be assumed that modifications to the ionoregulatory function of the gut/cloaca may be an important part of the integrated salt regulatory response of the whole animal. In particular, animals with a means of excreting concentrated salt solution (e.g., those species with a salt gland) might be expected to absorb salt across the gut, even during salt loading, to facilitate greater reabsorption of water (via solute-mediated processes). By contrast, the response to salt loading in those species without a specialized salt-secretory organ might be assumed to follow either of two patterns: (i) animals might minimize the reabsorption of salt across the gut/cloaca and sacrifice the associated water (animals following this pattern would be expected to tolerate low blood volume and high plasma osmolality), or (ii) animals might continue to absorb salt even during salt loading, and tolerate the high blood volume that would result from the associated reabsorption of water. Both strategies

have been observed in extant reptile taxa (Bentley, 1959; Bradshaw and Shoemaker, 1967; Nagy and Medica, 1986), though the relationship between the ionoregulatory function of the gut and the possession of a salt gland is far from clear among reptiles. Despite the particular strategy employed by any given taxon, in the evolution of marine habitat use, modifications to the gut/cloaca have likely been coincident with or closely tied to the evolution of specialized salt-secreting tissues.

Model Organisms

Understanding the evolutionary trajectory of specific anatomical and/or physiological traits can be difficult, in part, because the species in which these traits are expressed contemporaneously are snap-shots of their evolutionary history. Comparing multiple species that are known to experience similar ecological pressures (i.e., multiple species that have invaded marine environments), however, can provide additional power for evolutionary inference in that they provide a measure of replication on an evolutionary scale. Thus, traits that are common in multiple independent lineages that have evolved to use similar habitats can be assumed to have evolved in concert with the pressures of that habitat. There have been many studies of the physiology of marine birds and elasmobranchs, providing opportunities to examine commonalities in the physiology/anatomy of distantly related marine vertebrates, yet many fewer data are available for marine reptiles. Studies of reptiles are of particular interest because, (i) several estuarine species exist and may provide information about the stages through which the fully marine species progressed during their evolution, (ii) salt gland diversity (i.e., the identity of the precursor gland from which the salt gland likely evolved) is greatest among reptiles, and (iii) due to their phylogenetic position between elasmobranchs and birds, reptiles may reasonably provide evidence to link what is

known about these, otherwise, divergent taxa. Furthermore, unlike birds, there are no reptile taxa that are known to have the mammalian-type nephrons that enable the kidney to serve as a primary regulator of NaCl secretion; thus, reptiles must rely entirely on extra-renal organs to excrete NaCl solutions that are hypertonic to the blood plasma.

To understand the integration of various putative osmoregulatory organs and, ultimately, the evolution of marine habitat use in reptiles, it is important to compare fully marine species with semi-marine (estuarine) species and both of these with freshwater species. Laticaudine sea snakes (Elapidae) are marine specialists. Though they must return to land to reproduce (they are oviparous), Laticaudine sea snakes feed on marine fish, live in rock crevices under water, and have fully functional salt glands specialized for the excretion of NaCl (Dunson et al., 1971). By contrast, snakes in the genus *Nerodia* (Colubridae) do not have specialized glands for the excretion of excess salt (Schmidt-Nielsen and Fange, 1958). Despite this, marine/estuarine habitat use appears to have evolved at least twice in this group, once in the *Nerodia clarkii* complex (including three subspecies: *N. c. clarkii*, *N. c. compressicauda*, and *N. c. taeniata*) and once in a subspecies of *Nerodia sipedon* (*N. s. williamengelsi*); all other species in the genus *Nerodia* are known to be freshwater specialists. Though these two lineages (Elapidae and Colubridae) are only distantly related, by comparing the physiology of the "semi-marine" species of *Nerodia* with its freshwater congener, it may be possible to generate hypotheses about which traits are associated with marine habitat use in this genus. Further, pairing these studies with comparisons of the semi-marine species of *Nerodia* with the fully marine sea snake, *Laticauda semifasciata*, enables formulation of

broader hypotheses about the repeated evolutionary events resulting in diverse marine snake lineages.

Objectives of this Research

To begin to examine the relationships among various organ systems and, ultimately, to attempt to understand the evolution of marine specialization in reptiles, I first examined the physiology/anatomy of specialized salt-secreting glands in sea snakes (three species in the genus *Laticauda*; Chapter 1) and then compared the function of the salt gland in *Laticauda semifasciata* with the function of unspecialized glands in the same species and in the semi-marine *Nerodia clarkii clarkii* and the freshwater *Nerodia fasciata* (Chapter 2). To then understand how other putative osmoregulatory organs may be contributing to whole-animal ion and water balance in species with and without salt glands and in species from marine and freshwater habitats, I compared the anatomy and physiology of the kidneys in *L. semifasciata* with the kidneys of *N. c. clarkii* and *N. fasciata* after acclimation to 0%, 50%, and 100% seawater (Chapter 3) and the anatomy/physiology of the gut/cloaca in *N. c. clarkii* and *N. fasciata* in these same treatments (Chapter 4). Despite dramatic differences in the survival of *N. c. clarkii* and *N. fasciata* in seawater, I find little evidence for specialization in *N. c. clarkii* for marine habitats. The implications of these results in the context of the evolutionary trajectory of marine reptiles are discussed in the conclusions (Chapter 5).

CHAPTER 2
IMMUNOLOCALIZATION OF NA^+/K^+-ATPASE AND $NA^+/K^+/2CL^-$ COTRANSPORTER IN THE TUBULAR EPITHELIA OF SEA SNAKE SALT GLANDS[1]

Marine Invasion and the Evolution of Salt Glands

Marine invasions have occurred, independently, multiple times among vertebrates. As most marine vertebrates maintain blood plasma at approximately 300mOsm (about 1/3 the concentration of seawater), they experience salt accumulation and dehydration in marine environments (Evans and Claiborne, 2009). The evolution of specialized ionoregulatory tissues has, therefore, likely been responsible for ameliorating this ionic challenge, permitting the successful habitation of marine environments. One such specialized tissue, the salt gland, has evolved multiple times throughout the evolution of marine vertebrates. Among reptiles alone, five different cephalic salt glands have been described: the lachrymal gland in sea turtles and terrapins, the nasal gland in the marine iguana, the posterior sub-lingual and pre-maxillary glands in marine snakes, and the lingual gland in crocodilians (Dantzler and Bradshaw, 2009). While reptilian salt glands exhibit the greatest diversity and number of independent evolutionary origins among vertebrates, little is known about the mechanism of ion secretion in this group.

The anatomy and physiology of the rectal salt gland of marine elasmobranchs and the nasal salt glands of marine birds have been studied in great detail (for recent reviews, see: Hildebrandt, 2001; Evans et al., 2004). Glands from both groups have a compound tubular morphology composed of a series of branched secretory tubules that are bound by vascularized connective tissue arranged radially around the perimeter of a

[1] Reprinted with permission from: Babonis LS, Hyndman KA, Lillywhite HB, Evans DH. 2009. Immunolocalization of Na^+/K^+-ATPase and $Na^+/K^+/2Cl^-$ cotransporter in the tubular epithelia of sea snake salt glands. Comp Biochem Physiol Part A Mol Integr Physiol 154(4):535-540.

central duct (Sullivan, 1907; Marples, 1932). Secretory tubules bound into groups by connective tissue constitute the individual “lobules” of the gland; multiple such lobules are joined by the connection of their central ducts to a main duct, which serves to transfer the salt secretion from the mass of lobules to either the ileum of the intestine (elasmobranchs) or the nasal passage (birds) from where it is expelled. The salt secretory function of these glands is thought to be mediated by the specialized cells comprising the individual secretory tubules (reviewed by: Shuttleworth and Hildebrandt, 1999). Two cell types are typically found in the tubules: “principal” cells are often the most abundant as they populate the length of the secretory epithelium, while “peripheral” cells comprise the blind ends of the tubules. Principal cells have dense mitochondria and either deeply invaginated basal membranes (birds) or extensive lateral evaginations (elasmobranchs) which provide the surface area necessary to house the suite of membrane-bound, ion transport proteins that typify vertebrate secretory cells (Kirschner, 1980; Lowy et al., 1989; Ernst et al., 1994; Riordan et al., 1994). In contrast, the peripheral cells are non-secretory and have little, if any, specialization of the plasma membrane. Among birds, the peripheral cells are thought to be generative in nature and have therefore been implicated in the “adaptive differentiation” of salt glands undergoing salt stress (Ellis et al., 1963). Although adult salt gland morphology has also been shown to vary with salinity in some species of elasmobranchs (Oguri, 1964; Gerzeli et al., 1976), a role for the peripheral cells in regulating this process remains to be demonstrated. No such investigation of the function of the peripheral cells has been undertaken in any reptilian taxon.

Excretion of NaCl from the salt glands of elasmobranchs and birds, as well as the gills of marine teleosts, is effected primarily by three ion transport proteins: Na^+/K^+-ATPase (NKA), $Na^+/K^+/2Cl^-$ cotransporter isoform 1 (NKCC1), and cystic fibrosis transmembrane conductance regulator (CFTR) (Shuttleworth and Hildebrandt, 1999; Evans and Claiborne, 2009). Upon phosphorylation, NKA asymmetrically exchanges 3 Na^+ ions for 2 K^+ ions resulting in the extracellular accumulation of Na^+ ions and a potential difference across the basolateral membrane. Together, these phenomena create an electrochemical gradient which drives the uptake of Na^+, K^+, and Cl^- from the extracellular fluid at the basolateral surface of the cell via NKCC1. Ultimately, this process potentiates the apical loss of Cl^- through CFTR and the paracellular secretion of Na^+ through the leaky tight junctions between epithelial cells. While this model of ion transport across secretory epithelia appears to be conserved across taxa, the localization of the above ion transport proteins has yet to be identified in the secretory epithelia of marine reptile salt glands.

The objective of this study was to examine the secretory epithelia of marine snake salt glands to determine if the localization of NKA and NKCC in a marine reptile is consistent with the localization of these proteins in the vertebrate secretory cell model described above. Among marine snakes, two separate salt-secreting cephalic glands have been described: the posterior sublingual gland in sea snakes (Hydrophiidae and Laticaudidae; Dunson et al., 1971) and file snakes (Acrochordidae; Dunson and Dunson, 1973) and the premaxillary gland in old world watersnakes (Colubridae: Homalopsinae; Dunson and Dunson, 1979). Both are compound tubular glands, like those of elasmobranchs and birds, and both are comprised almost entirely of principal

cells exhibiting the lateral evaginations typical of elasmobranch principal cells (Dunson and Dunson, 1973; 1979). Preliminary studies by Dunson and Dunson (1974; 1975) suggested that NKA activity is high in the salt glands of several sea snake taxa, including one freshwater species, and remains high even as environmental salinity is decreased. Further studies of salt gland function in estuarine turtles utilized NKA- and NKCC-specific blocking agents to demonstrate the involvement of these two ion transporters in activating NaCl excretion (Shuttleworth and Thompson, 1987). While no further investigation into ion transport mechanisms has been conducted in marine reptiles, studies of desert iguanas also demonstrate basolateral localizations of NKA and NKCC (Ellis and Goertemiller, 1974; Hazard, 1999), consistent with their role in activating ion secretion.

In this study I build on the work of my predecessors by immunolocalizing NKA and NKCC in the secretory epithelia of salt glands from three species of laticaudine sea snake: *Laticauda semifasciata*, *L. Laticaudata*, and *L. colubrina*. These three species are of special interest because they are commonly found in coastal areas and frequently experience fluctuations in environmental salinity. Furthermore, observations of their daily activity patterns suggest slight differences in habitat use whereby *L. semifasciata* tends to be more aquatic than either *L. laticaudata* or *L. colubrina* (Lillywhite et al., 2008). Thus, in addition to examining the localization of NKA and NKCC in the secretory epithelia, I aimed to determine if the ecological differences among these species were reflected in the anatomy of their salt glands. I found that, as in other vertebrates, NKA and NKCC localize to the basolateral membranes of the principal cells of the secretory

tubules in all three species. Neither the gross anatomy, nor the localization of the examined ion transporters were found to differ among species.

Methods

Animal Collection

In June of 2006, three species of laticaudine sea snake (*Laticauda semifasciata*, *L. laticaudata*, and *L. colubrina*) were collected from the shallow coastal inlets around the perimeter of Orchid Island, Taiwan. Animals (N = 6 per species) were captured by hand and maintained in mesh bags during transportation to the laboratory at National Taiwan Normal University in Taipei. In the laboratory, animals remained in the mesh bags and were allowed to dehydrate in air for 14 days (for the experiment published in: Lillywhite et al. 2008). All animals were fasted through the entire dehydration period. Throughout the experimentation period, all animals were treated in accordance with the standard of ethics put forth by the University of Florida's Institutional Animal Care and Use Committee.

Tissue Collection

Following the 14-day dehydration period, each animal was euthanized and the posterior sub-lingual salt gland was excised and cut in half lengthwise. Half of each gland was snap frozen in liquid nitrogen, transported back to the University of Florida, and stored at -80˚C for Western blot analysis. The other half of each gland was fixed in Bouin's solution (71% saturated picric acid, 24% Formaldehyde (37%), 5% glacial acetic acid) for 24 hours at room temperature (RT, 27˚C). Following fixation, tissues were washed in three rinses of 10 mM phosphate buffered saline (PBS) and stored in 75% ethanol for transport back to the University of Florida. In preparation for histology and immunohistochemistry, fixed salt glands were dehydrated through a series of ethanol

washes of increasing concentration (75 to 100%). Following dehydration, tissues were cleared in Citrisolv (Fisher Scientific, Pittsburgh, PA USA), embedded in paraffin wax (Tissue Prep 2, Fisher Scientific), and sectioned at 7µm perpendicular to the long axis of the gland. Sections were mounted on charged glass microscope slides (Superfrost Plus, Fisher Scientific) and dried for 24 hours at 30˚C.

Histology

For analysis of salt gland tissue morphology, I used the Lillie (1940) modification of the Masson Trichrome technique (Humason, 1972). To further examine the secretory nature of the various cell types I used a modified Periodic Acid Schiff (PAS) technique (Humason, 1972). In brief, tissue sections were de-paraffinized in Citrisolv and rehydrated through a series of ethanol baths of decreasing concentration (100 to 35%). Rehydrated sections were then rinsed in 10 mM PBS for 5 minutes followed by a 1 min rinse in de-ionized (DI) water. Sections were then placed into 0.5% periodic acid (in DI water) for 5 min at RT, rinsed for 1 min in DI water, and placed into Schiff's reagent (Sigma Aldrich, St. Louis, MO USA) for 1 min at RT. Hematoxylin was used to counter-stain before sections were dehydrated through a series of ethanol baths of increasing concentration, cleared with Citrisolv, and mounted with coverslips using Permount (Fisher Scientific). Alcian blue was used to detect acidic mucopolysaccharides following a modification of the protocol outlined in Humason (1972). Briefly, rehydrated sections were incubated in 3% acetic acid (in DI water) for 3 min at RT and then placed directly into 1% Alcian blue 8GX (in 3% acetic acid, pH 2.5) for an additional 30 min at RT. Sections were then rinsed in running tap water for 5 min, rinsed in DI water for 1 min, dehydrated, cleared, and mounted.

Immunohistochemistry

To localize specific ion transporters in tubular epithelia, I followed the immunohistochemical techniques of Piermarini et al. (2002). Briefly, rehydrated tissue sections were washed in 10 mM PBS, encircled with a hydrophobic barrier using a PAP pen (Electron Microscopy Sciences, Hatfield, PA USA), and incubated in 3% H_2O_2 (in DI water) for 30 min at RT. Tissues were again washed in 10 mM PBS and incubated in a Biogenex Protein Block (BPB; normal goat serum with 1% bovine serum albumin, 0.09% NaN_3, and 0.1% Tween-20; San Ramon CA USA) for an additional 20 min at RT. Tissues were again rinsed in 10 mM PBS followed by incubation in anti-NKA (1/100; diluted in BPB) or anti-NKCC (1/2,000) overnight at 4˚C. The primary antibody was then removed with 10 mM PBS and tissues were prepared for visualization using the horseradish peroxidase Super Sensitive™ Link-Label IHC Detection System (Biogenex). To begin, tissues were incubated in "Link" (peroxidase-conjugated streptavidin) for 20 min in a humidified chamber at RT. Following a 10 mM PBS wash, tissues were incubated in "Label" (biotinylated anti-immunoglobulins) for an additional 20 min. Visualization was achieved through a final 5–min incubation in 3, 3'-diaminobenzidine tetrahydrochloride (DAB) (Biogenex) at RT. Following visualization with DAB, tissue sections were dehydrated and mounted. Negative controls were produced following a modification of the aforementioned procedures whereby tissues were incubated in BPB rather than primary antibody.

Primary Antibodies

Monoclonal anti-NKA (α5) developed by Dr. Douglas Fambrough and monoclonal anti-NKCC (T4) developed by Drs. Christian Lytle and Bliss Forbush III were obtained from the Developmental Studies Hybridoma Bank developed under the auspices of the

National Institute of Child Health and Human Development and maintained by The University of Iowa, Department of Biological Sciences, Iowa City, IA 52242. While α5 recognizes an epitope specific to the α1 subunit of NKA (Takeyasu et al., 1988), T4 was made against a conserved epitope in the carboxyl tail of NKCC (Lytle et al., 1995) and is therefore unable to distinguish between NKCC isoforms 1 (NKCC1) and 2 (NKCC2).

Western Blot Analysis

Frozen salt glands were homogenized in ice-cold lysis buffer (10 mL of buffer per 1g of tissue; Cell Signaling Technology, Danvers, MA USA) and centrifuged at 14,000 RPM for 10 min at 4˚C. The supernatant was then removed and stored on ice. To quantify protein in each sample, I used the BCA detergent compatible protein assay kit (Pierce, Rockford, IL USA). Following addition of 2% β-mercaptoethanol and 0.01% Bromophenol Blue, each sample was heated at 65˚C for 10 mins. I then loaded 15 µg of total protein from each sample into a 7.5% Tris-HCl polyacrylamide gels (Bio-Rad, Hercules, CA USA) and electrophoresed each gel for 2 h at 100V. Separated proteins were then transferred to an Immuno-blot polyvinylidene fluoride (PVDF) membrane (Bio-Rad) following the manufacturer's protocol. Following transfer, membranes were rehydrated in 100% methanol for 5 min and rinsed twice in de-ionized water. To block non-specific proteins, membranes were incubated, while shaking, in Blotto: 5% non-fat dry milk in Tris-buffered saline (TBS 25 mmol/L Tris, 150 mmol/L NaCl; pH 7.4), for 1 hour at RT followed by an incubation with anti-NKA (α5, 1/100) or anti-NKCC (T4, 1/4,000) overnight at RT. Membranes were then washed three times (15 min each) with TTBS (0.1% Tween-20 in TBS; pH 7.4) and incubated in alkaline-phosphatase-conjugated goat anti-mouse IgG (1/3000 diluted in Blotto) at RT for 1 hour and washed in TTBS. To visualize antibody binding, membranes were incubated in a

chemiluminescent signal (Immun-star chemiluminescent kit, BioRad) following the manufacturer's protocol. Total protein present on the membranes was visualized by incubating membranes in 0.02% Coomassie blue stain (diluted in 50% methanol, 10% acetic acid, and 40% water) for 1 min. Exposed films and Coomassie blue stained membranes were digitally imaged using a flatbed scanner and brightened using Adobe Photoshop CS3 (San Jose, CA USA).

Results

Anatomical Description of Salt Glands

The sublingual salt gland in each species is typified by branched secretory tubules encased in a matrix of collagen fibers (Fig 2-1A-C). Abundant blood vessels populate the connective tissue surrounding each tubule. The central ducts can be distinguished from the secretory tubules by their pseudostratified columnar epithelia and large lumena (Fig 2-2A-C). In contrast, secretory tubules are simple and cuboidal to columnar, have relatively smaller lumena and thereby smaller apical than basal surfaces. Distally, ducts join and become continuous with the stratified squamous epithelium of the tongue sheath (Fig 2-2B); this provides the opportunity for the secreted salt solution to be expelled by tongue-flicking (Dunson and Taub, 1967; Dunson and Dunson, 1979). Both central ducts and secretory tubules are PAS^+ apically, suggesting the presence of polysaccharides (magenta coloration, Fig 2-2A-C). However, neither ducts nor tubules stained positively for mucopolysaccharides (all were Alcian blue-negative; Fig 2-3A-C).

Immunolocalization of Ion Transport Proteins in Salt Gland Epithelia

Immunolocalization of the α-subunit of NKA was detected in the basolateral membrane of the cuboidal cells of the secretory epithelia in all three species (brown coloration, Fig 2-4A-C). A similar basolateral localization was detected for NKCC (Fig 2-

4D-F). While there appears to be weak cytoplasmic staining in NKA^- and $NKCC^+$ cells, this likely reflects the localization of NKA and NKCC to the interdigitating lateral membranes of the secretory cells. The localization of these two proteins does not appear to differ among the species examined. Control sections lack staining for either NKA or NKCC (Fig 2-4G-I).

Primary Antibody Specificity

The anti-NKA antibody (α5) detected a protein with a molecular weight of approximately 110 kDa in each species (Fig 2-5A), which is consistent with the molecular weight of NKA in other vertebrates (Blanco and Mercer, 1998). Additionally, anti-NKCC (antibody T4) detected a single band of approximately 195 kDa (Fig 2-5B), also within the range published for the molecular weight of this protein in other vertebrates (Lytle et al., 1995). Coomassie blue stains total protein (Fig 2-5C) in the same lanes shown for primary antibody (Fig 2-5A-B). Detection of only a single product of the appropriate size (110 kDa and 195 kDa for α5 and T4, respectively) in the presence of the full complement of proteins extracted from the salt glands supports specificity of these antibodies for their target proteins.

Discussion

These results confirm that the morphology of salt glands from three species of laticaudine sea snake is similar to that of all other vertebrate salt glands studied to date (Hildebrandt, 2001; Evans et al., 2004; Dantzler and Bradshaw, 2009). While no peripheral cells were identified in this study, the principal cells, which comprise the tubular epithelium of the salt gland from all three species, were found to be predominantly serous in nature. In all three species the nuclei from the principal cells are round and positioned in the basal portion of the cell. The presence of PAS^+

polysaccharide granules throughout the cytoplasm of the secretory cells (Fig 2-2C) and the absence of mucopolysaccharides (Fig 2-3A-C) further confirms the serous nature of this gland. As most cephalic secretory glands (primarily salivary glands) are typified by more equivalent proportions of serous and mucous cells (Burns and Pickwell, 1972; Baccari et al., 2002), the primarily serous nature of vertebrate salt glands might, in fact, reflect a developmental pathway leading to the evolution of this gland type from an unspecialized seromucous precursor (Dunson, 1969; Peaker and Linzell, 1975; Barnitt and Goertemiller, 1985).

Additionally, I demonstrate that the localization of NKA and NKCC in marine snake salt glands is consistent with the localization of these proteins in all other vertebrate salt secreting tissues studied to date (Hildebrandt, 2001; Evans and Claiborne, 2009). In all three species of sea snake NKA and NKCC were localized to the basolateral membranes of the cuboidal/columnar cells comprising the epithelia of the salt gland tubules (Fig 2-4A-F). The localization of these two proteins is consistent with their roles in the active uptake of $Na^+/K^+/Cl^-$ across the basolateral membrane of the secretory cells (Shuttleworth and Thompson, 1987) and suggests conservation of a similar mechanism for ion transport at the level of the vertebrate secretory cell. While the identity of the putative apical Cl^- transporter remains to be determined, the presence of CFTR in taxa ranging from elasmobranchs to birds suggests that this ion transporter is also likely conserved among the reptiles. In fact, I have cloned a full mRNA sequence for CFTR from the salt gland of *L. semifasciata* (Chapter 3); however, my attempts to localize CFTR protein in the tubular epithelium have failed (despite the use of several antibodies both commercially available and donated from other laboratories). Thus,

further studies of the role of CFTR and other potential apical chloride channels are necessary before hypotheses about conservation of the full ion secretory mechanism can be evaluated.

Finally, despite apparent differences in both habitat use and dehydration rate (Lillywhite et al., 2008), no differences in either gross morphology or the localization of either NKA or NKCC were seen among the species examined. Furthermore, while my Western blots suggest that variation may exist in the abundance of both NKA and NKCC among species, further investigations aimed at quantifying this pattern are necessary before conclusions about the relationship between habitat use or dehydration rate and ion transporter abundance can be made.

The consistency with which salt gland form and function have been conserved throughout the evolution of marine vertebrates suggests that the genetic mechanism leading to the development of this tissue type may also be conserved. Indeed studies of the regulation of salt gland development may reveal a mechanism by which these glands have been co-opted from unspecialized gland precursors (Dunson, 1969; Peaker and Linzell, 1975; Barnitt and Goertemiller, 1985). In this context, studies aimed at understanding the development and distribution of principal cells in the secretory epithelia as well as the development of the compound tubular structure of the gland would be of special interest.

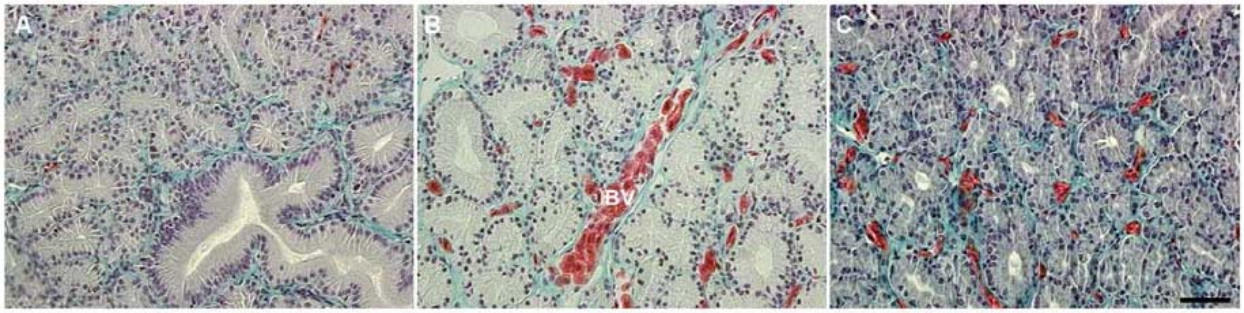

Figure 2-1. Cross sections of sublingual salt glands from (A) *L. semifasciata*, (B) *L. laticaudata*, and (C) *L. colubrina* (Masson Trichrome). Blood vessels (BV) are easily distinguishable by the presence of red blood cells. Collagen fibers (green) surround each secretory tubule. Scale bar = 50μm.

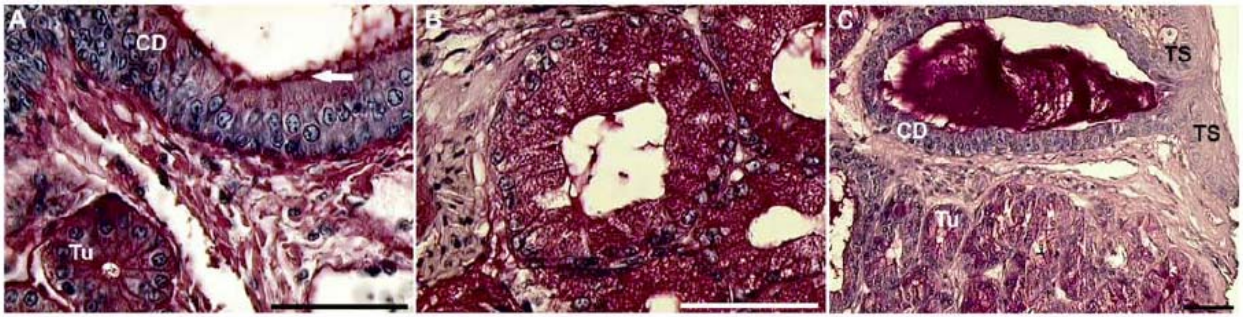

Figure 2-2. Periodic Acid Schiff (PAS) reaction reveals the presence of polysaccharide (magenta color) in the tubules of all three species. (A) Secretory tubules (Tu) can be distinguished from central ducts (CD) by the size of the lumena and the morphology of the epithelium. Tubules have relatively small lumena and simple cuboidal to columnar epithelia; ducts have large lumena and pseudostratified columnar epithelia. Additionally, while central duct epithelium is PAS^+ apically (arrow), (B) the PAS^+ material appears to be more evenly distributed through the cytoplasm of the secretory tubules. (C) Ultimately, central ducts join distally with the tongue sheath epithelium (TS) to facilitate passage of secreted products (magenta mass) into the tongue sheath. (A *L. semifasciata*, B *L. colubrina*, C *L. laticaudata*). Scale bar = 50μm.

Figure 2-3. Cross sections of salt glands from all three species. (A *L. semifasciata*, B *L. laticaudata,* C *L. colubrina*) Both tubules and ducts are negative for Alcian blue stain at pH 2.5, which indicates that these cells are not secreting acidic mucopolysaccharides. Scale bar = 50µm.

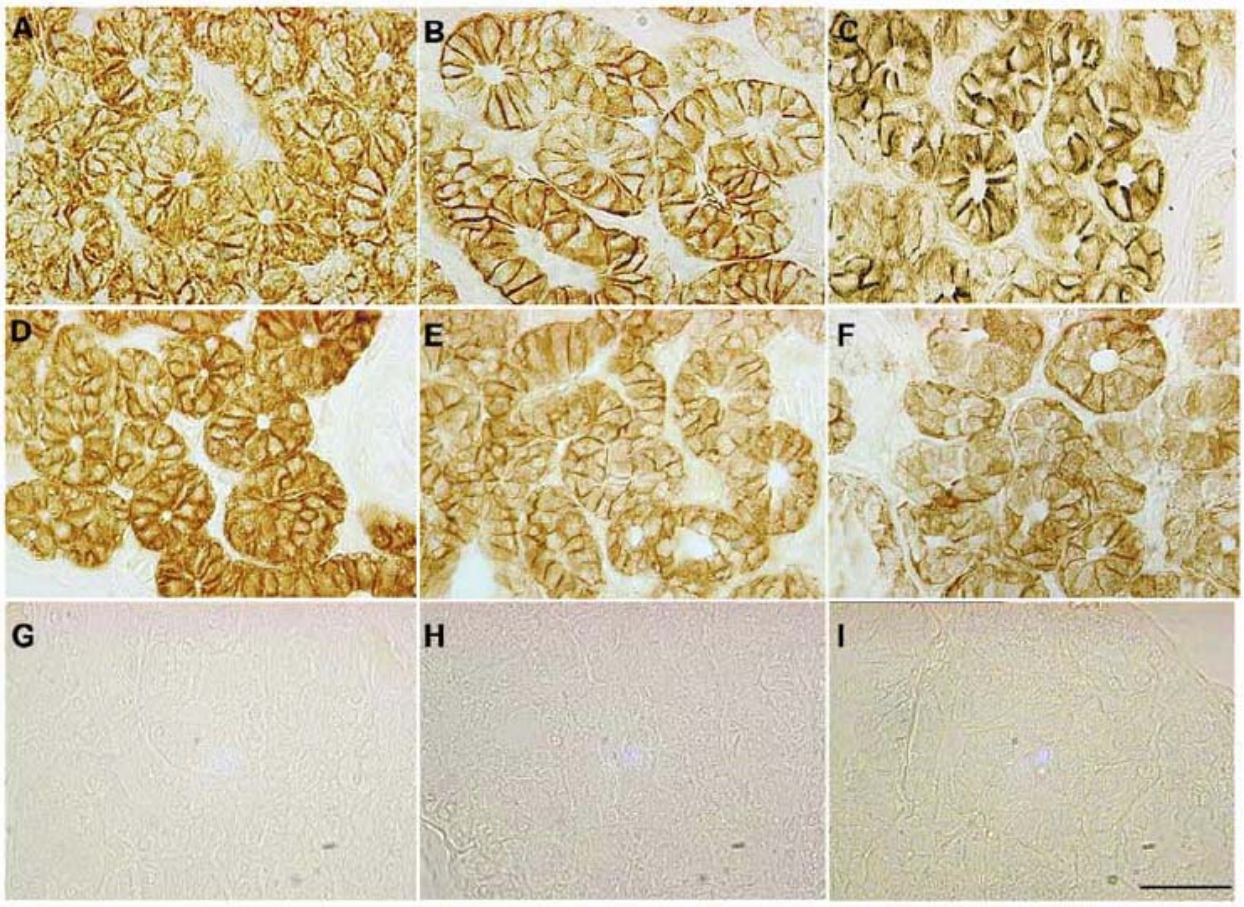

Figure 2-4. IHC showing the localization of (A-C) NKA and (D-F) NKCC to the basolateral membranes of the cells comprising the tubular epithelia in all three species (A/D/G *L. semifasciata*; B/E/H *L. laticaudata*; C/F/I *L. colubrina*). Negative controls for NKA and NKCC (D-F) show no staining. Scale bar = 50µm.

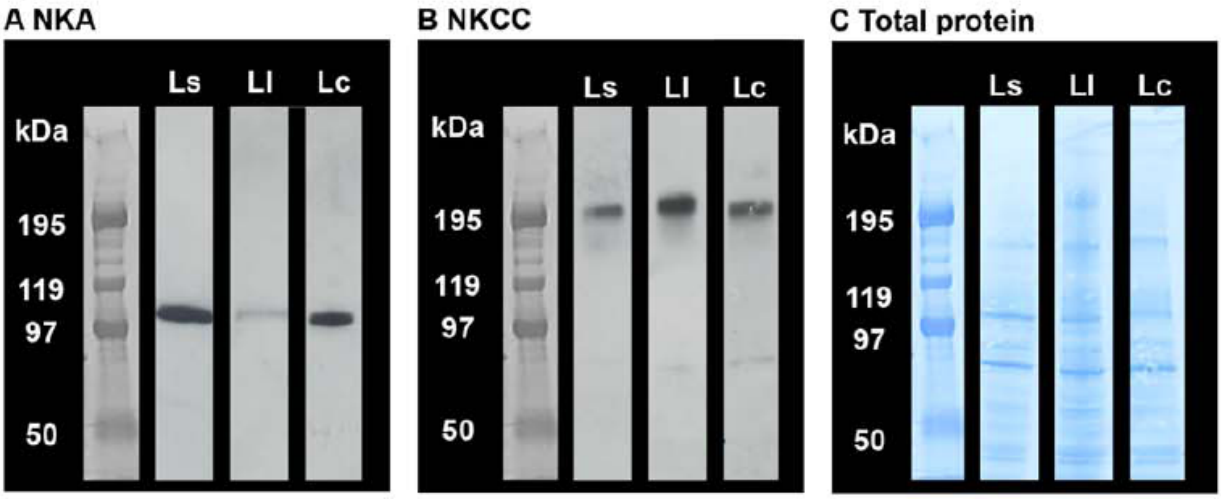

Figure 2-5. Western blots support the specificity of the antibodies used in IHC for all three species (Ls = *L. semifasciata*, Ll = *L. laticaudata*, Lc = *L. colubrina*.) (A) Antibody α5 (NKA) detects a protein of approximately 110 kDa in all three species of sea snake and (B) antibody T4 (NKCC) detects a protein of approximately 195 kDa. (C) Total protein is visualized on the same blot using Coomassie blue stain.

CHAPTER 3
ON THE ORIGINS OF REPTILIAN SALT GLANDS: MORPHOLOGICAL AND MOLECULAR COMPARISONS OF CEPHALIC GLANDS IN MARINE AND FRESHWATER SNAKES

Form and Function in the Evolution of Reptilian Salt Glands

Specialized salt-secreting glands have arisen multiple times, independently, in various vertebrate lineages that have invaded marine habitats. Hypotheses about the evolution of these specialized osmoregulatory organs have focused either on the relationship between gland size and diet in estuarine and marine species (Dunson and Mazzotti, 1989) or on the relative proportions of salt-secreting and mucus-secreting cells across marine taxa (Peaker and Linzell, 1975). The presence of embryologically homologous, though functionally divergent, glands in closely related marine and freshwater/terrestrial taxa suggests that specialized salt-secreting glands may have been co-opted from unspecialized (with regards to salt-secretion) precursors; however, the molecular mechanisms that might underlie such co-option are poorly understood. In order to propose a means by which glands specialized for the secretion of NaCl may have evolved from unspecialized precursors, it is first necessary to identify tissues that represent the stages through which salt glands may have passed during the evolution of their current form/function. Aquatic snakes are an ideal taxon in which to ask these questions; in addition to the fully marine lineages (Hydrophiidae and Laticaudidae) there are several snake taxa which lack a specialized salt gland but are thought to use behavioral and other physiological means to prevent desiccation and salt accumulation in marine environments, including at least two species in the Colubridae (Pettus, 1963; Conant and Lazell Jr, 1973; Dunson, 1980; Dunson and Mazzotti, 1989). Comparisons of the cephalic glands in fully marine and semi-marine species with the cephalic glands

in freshwater/terrestrial species may reveal the critical functional differences between a specialized salt gland and a gland incapable of secreting a concentrated NaCl solution.

Studies of salt gland form and function from diverse vertebrate lineages suggest that at least three elements of a salt gland's form are important for regulating its function: (i) Compound tubular shape. All vertebrate salt glands examined thus far (including those from elasmobranchs, birds, and reptiles) exhibit a compound tubular shape (for reviews, see: Hildebrandt, 2001; Dantzler and Bradshaw, 2009; Evans and Claiborne, 2009). Since the length of the secretory tubule has been correlated with the concentration of Cl^- in the secretion among shore birds (Staaland, 1967) and the maximum secretory rate of salt glands is known to vary with gland size among marine snakes (Dunson and Dunson, 1974), the importance of a tubular gland, as opposed to an acinar gland, may derive from the increased secretory surface area. (ii) Presence of principal cells. The distribution of specific ion transporting proteins in the membranes of a secretory cell is a good indication of the function of the cell. The basolateral membranes of the principal cells lining the tubules of salt glands express abundant ion transporters, notably: Na^+/K^+- ATPase (NKA) and $Na^+/K^+/2Cl^-$ cotransporter (NKCC) (Shuttleworth and Hildebrandt, 1999). When co-expressed with an apical Cl^- channel, known to be cystic fibrosis transmembrane conductance regulator (CFTR) in elasmobranchs and birds (Lowy et al., 1989; Riordan et al., 1994), these ion transporters facilitate the net secretion of NaCl to the apical membrane of the epithelium. By contrast, when NKCC localizes to the apical membrane of an epithelial cell expressing basolateral NKA, Na^+ transport is in the opposite direction (e.g., in the proximal tubule of the mammalian kidney; Kinne and Zeidel, 2009). (iii) Cell-type

homogeneity. Relative gland homogeneity, resulting from reduction/loss of mucus-secreting cells at the expense of NaCl secreting cells, suggests specialization for a single function – secretion of NaCl. The degree of homogeneity varies across taxa, from the presence of a single cell type in many sea snakes (Dunson et al., 1971; Dunson and Dunson, 1974; Chapter 2) to tubules interspersed with NaCl-secreting and mucus-secreting cells in lizards and turtles (summarized in Peaker and Linzell, 1975). Despite this, a general trend toward reduction in mucus-secreting cell types and relative increase in NaCl-secreting cell types appears conserved across taxa. Among many taxa, the blind endings of the secretory tubules are populated by an additional cell type (neither mucus-secreting nor NaCl-secreting). Among birds, these are thought to be a population of stem cells that are responsible for modulating the adaptive response of salt glands to increasing environmental salinity (Ellis et al., 1963). Peripheral stem cells have not been identified in the salt glands of any reptile, though it would be interesting to explicitly examine the potential for ontogenetic shifts in the size/function of the salt glands in reptiles to determine if a similar phenomenon occurs among non-avian taxa.

To understand the relationship between specialized and unspecialized cephalic glands in snakes, I examine the morphology and biochemistry of the salt gland and the harderian gland (unspecialized) in *Laticauda semifasciata* (marine), and compared these results with similar examinations of the various cephalic glands (Fig 3-1) in two species of watersnake from different habitats: *Nerodia clarkii* (semi-marine) and *Nerodia fasciata* (freshwater). Specifically, I examined the morphology/cellular anatomy of each gland, the localization and abundance of ion secreting cells (as indicated by NKA, NKCC, and CFTR), and the localization and abundance of two indicators of mucus

secretion: neutral mucins (detectable via Periodic acid Schiff staining; Humason, 1972) and AQP3, a water channel thought to be indicative of the water transport associated with mucus production in vertebrate epithelia (Lignot et al., 2002; Akabane et al., 2007). Further, I examined the effect of salinity acclimation on the expression of these ion/mucus regulating features in the salt and harderian glands of *L. semifasciata* to determine if, like the gills of many teleost fishes (see: Evans and Claiborne, 2009, and references therein), the biochemical phenotype of the salt gland is associated with changes in environmental salinity. I then summarize these results in a proposed model by which salt glands may have been co-opted from unspecialized glands.

Materials and Methods

Animal Collections and Experimental Procedures

Adult sea snakes (*L. semifasciata*; 497.4 ± 121.2 g initial mass) were collected from the coastal inlets around Orchid Island, Taiwan, and housed in individual plastic aquaria in 100% seawater (SW; 32 ppt) prior to the beginning of the experiment. The remaining procedures were described previously (Chapter 4). In brief, all animals were held in 100% SW at room temperature (RT; 29.67 ± 0.62˚C) for five days. Control animals (N = 6) were then selected randomly and sacrificed and all remaining animals were assigned to one of three treatments: 0, 50, or 100% SW (N = 6, per treatment). Cage water salinity was then reduced in small increments over a period of seven days until animals reached their final treatment salinity, where they were held for one week before being sacrificed. Cage water was mixed fresh daily using Instant Ocean (Spectrum Brands, Inc., Madison, WI, USA) and tapwater (from National Taiwan Normal University, Taipei, Taiwan) and salinity was checked daily using either an Atago S/Mill refractometer (Tokyo, Japan) or a YSI 85 salinity meter (Yellow Springs, OH, USA). Salt

marsh snakes (*N. c. clarkii*; 118.8 ± 79.7 g initial mass) and banded watersnakes (*N. fasciata*; 136.3 ± 95.2 g) were collected from Seahorse Key, FL (Levy Co.; permit #05-012) and the roadways near Paynes Prairie, FL (Alachua Co.), respectively, and held in 0% SW (Gainesville, FL tapwater) for the lab acclimation period (room temperature: 23.23 ± 0.65˚C). All animals were maintained in enough water such that all cutaneous surfaces were covered as they rested on the bottom of the cage, and fasted throughout the experiment. All animals were sacrificed by rapid decapitation, as outlined in the American Veterinary Medical Association's Guidelines on Euthanasia. The procedures described herein are in accordance with the guidelines of the Institutional Animal Care and Use Committee at the University of Florida.

Histology and Immunohistochemistry

Salt glands and harderian glands were removed from sea snake heads immediately following sacrifice and fixed in 4% paraformaldehyde for 24 h at 4˚C. Fixative was removed through three washes in phosphate buffered saline (PBS, 10mM) after which time tissues were transferred to 75% ethanol and stored at RT prior to embedding. I collected whole heads from watersnakes, rather than individual glands; as such, following fixation, watersnake heads were decalcified by continuous washing in a 1:1 solution of 8%HCl : 8%Formic Acid at RT for 4-5 weeks before being stored in 75% ethanol at RT. All tissues (individual glands and whole heads) were then dehydrated through a graded series of ethanol baths prior to embedding in paraffin wax (Tissue Prep 2, Fisher Scientific, Pittsburgh, PA USA). Prior to histological analysis, tissues were sectioned at 7μm and mounted on charged glass slides (Superfrost Plus, Fisher Scientific).

For a basic analysis of tissue morphology, I used the Lillie (1940) modification of the Masson Trichrome Technique (Humason, 1972). To detect the presence of neutral mucins, rehydrated tissues were pre-digested for 30 min at 37˚C in a 1.5% solution (in DI water) of α-amylase (Sigma Aldrich, St. Louis, MO USA). Control sections on adjacent slides were incubated for 30 min at 37˚C in DI water. Control and experimental sections were then stained using a modified Periodic Acid Schiff (PAS) technique with a hematoxylin counter stain (Chapter 2). To immunolocalize NKA, NKCC, CFTR, and AQP3, I followed the procedures previously described (Chapter 2) . Briefly, endogenous peroxidases were blocked in rehydrated sections by a 30 min incubation in 3% H_2O_2 and non-specific protein interactions were blocked by a 20 min incubation in protein block (normal goat serum with 1% bovine serum albumin, 0.09% NaN_3, and 0.1% Tween-20; BioGenex, San Ramon CA, USA), both at RT. Sections were then incubated in anti-NKA (α5; 1/100), anti-NKCC (T4; 1/1000), anti-CFTR (60; 1/500), or anti-AQP3 (Hc-3, 1/500) overnight at 4˚C. Visualization was achieved using the Supersensitive™ Link-Label universal secondary antibody kit (BioGenex) with a DAB (3, 3'-diaminobenzidine tetrahydrochloride) chromagen. At least one negative control section was produced on each slide by omitting the primary antibody and incubating sections in protein block (BioGenex) instead. Specificity of primary antibodies was previously confirmed via Western blot (anti-NKA, anti-NKCC; Chapter 2) or peptide preabsorption (anti-AQP3; Chapter 4). A minimum of three individuals per treatment were examined for each species.

Primary Antibodies

Monoclonal anti-NKA (α5), developed by Dr. Douglas Fambrough, and monoclonal anti-NKCC (T4), developed by Drs. Christian Lytle and Bliss Forbush III, were obtained

from the Developmental Studies Hybridoma Bank developed under the auspices of the National Institute of Child Health and Human Development and maintained by The University of Iowa, Department of Biological Sciences, Iowa City, IA 52242. Anti-NKA is directed against the α1 subunit of the NKA heterodimer (Takeyasu et al., 1988) and anti-NKCC is directed against a conserved region of the C-terminus in NKCC1, NKCC2, and the Na^+/Cl^- symporter, NCC (Lytle et al., 1995). The anti-CFTR antibodies (Table 3-1) were generous gifts from Dr. John Riordan at University of North Carolina and anti-AQP3 (Hc-3) and its blocking peptide were a generous gift from Dr. David Goldstein at Wright State University.

RNA Preparation and PCR

Salt glands and harderian glands were removed from *L. semifasciata* immediately following sacrifice and fixed in RNA*later* (Ambion, Woodward Austin, TX, USA) for 24 h at 4˚C. Tissues were stored at -20˚C in RNA*later* before being homogenized in ice-cold Tri-Reagent (Sigma Aldrich). Total RNA was then extracted following the protocol of Choe et al. (2005) and checked for purity and quality using a micro-volume spectrophotometer (Nanodrop ND-1000, Thermo Scientific, Wilmington, DE, USA) and agarose gel electrophoresis. cDNA was then synthesized using the Superscript III reverse transcription kit (Invitrogen, Carlsbad, CA, USA) and oligo-dT primers. Primers used for initial cDNA amplification and quantitative real-time PCR (qRT-PCR) for NKA and AQP3 were reported previously (Chapter 4). Additional primers for initial cDNA amplification of NKCC1, CFTR, and the reference gene (eukaryotic translation elongation factor 1α1; EF1a1) from *L. semifasciata* were designed using CODEHOP (Rose et al., 2003) and primers for qRT-PCR (NKCC1, CFTR, and EF1a1) and duplexing PCR (NKCC1, CFTR, and NKA) were designed using Primer 3 Plus

(Untergasser et al., 2007). Primer sequences for each application are listed in Table 3-2. I used standard cycles to amplify 0.5 µl oligo-dT cDNA using Ex-taq Hot Start DNA Polymerase (Takara Bio, Madison, WI, USA) in an Express thermocycler (ThermoHybaid, Franklin, MA, USA). Amplicons were cloned using the TOPO-TA cloning kit for sequencing (Invitrogen) and plasmids were sequenced in both directions by the Marine DNA sequencing facility at the Mount Desert Island Biological Laboratory (Salisbury Cove, ME, USA). Specific sequences for the *L. semifasciata* orthologs of NKCC1, CFTR, and EF1a1 were deposited in GenBank; accession numbers are as follows: NKCC1 HQ888849 (partial coding sequence), CFTR HQ888850 (complete coding sequence), EF1a1 HQ386012 (partial coding sequence).

Quantitative Real-time PCR and RACE PCR

Changes in the abundance of NKA, NKCC, CFTR, and AQP3 transcripts were measured using qRT-PCR, as has previously been described (Chapter 4). In brief, 24 µl triplicates of reaction mixture (1 µl of 1/10 diluted cDNA, 7.4 pmol specific primers, and SYBR® Green Mastermix; Applied Biosystems, Foster City, CA, USA) were loaded into 96-well optical plates (Bio-Rad, Hercules, CA USA) and PCR-amplified using an I-cycler IQ thermocycler (Bio-Rad). Amplification was accomplished using the following cycling protocol: step 1 - 95˚C for 10 min (initial denaturing step), step 2 - 95˚C for 35 s, 60˚C for 30 s, 72˚C for 30 s (repeat for a total of 40 cycles), step 3 - melting curve analysis (to ensure amplification of only a single product). I also loaded 24 µl triplicates of a 5-point dilution series, mixed fresh for each use from a mixed sample of undiluted species-specific cDNA, onto each plate. Two types of control reactions, either lacking cDNA template or made with RNA template, were amplified using the same procedures to ensure amplification occurred >10 cycles after the latest cycle of amplification for cDNA.

A random selection of samples from each plate were extracted, sequenced, and BLASTed (NCBI, Bethesda, MD, USA), to ensure specificity of products. The full-length mRNA sequence for CFTR from *L. semifasciata* was identified through amplification of both the 5' and 3' ends of the CFTR transcript following the manufacturer's protocol for the GeneRacer kit (Invitrogen).

Epitope Analysis of lsCFTR

Because I was unable to detect CFTR in the salt gland, where it is known to regulate apical Cl^- secretion in other vertebrate salt glands, I sequenced the full-length mRNA transcript and compared regions of the predicted amino acid sequence with the epitopes of a sample of the various anti-CFTR antibodies I tried. Epitope sequences from the taxa against which they were designed are listed in Table 3-1. To ensure the product was CFTR (and not a paralogous member of the ABC protein family), I searched the nucleotide sequence for the coding region against the nucleotide collection at NCBI using the blastn algorithm. The predicted amino acid sequence was the examined via pair-wise comparisons using NCBI's bl2seq function and the blastp algorithm with sequences from: *Gallus gallus*, *Homo sapiens*, and *Squalus acanthias* (see Table 3-3 for accession numbers).

Semi-quantitative Duplexing PCR

To examine the distribution and relative abundance of NKA, NKCC1, and CFTR across tissues, RNA was extracted (as described above) from the brain, duodenum, esophagus, harderian gland, kidney, liver, lung, muscle (skeletal), pancreas, salt gland, stomach, and testis of *L. semifasciata*, and reverse transcribed into cDNA using random hexamer primers (Superscript III kit, Invitrogen). For NKA and NKCC1, duplexing PCR was then performed by simultaneous amplification of cDNA by both gene specific

primers and control primers (Quantum RNA™ 18S internal standard primer kit; Ambion). Due to interference between the gene specific CFTR primers and the control primers, control and experimental amplification occurred in separate reactions. All reactions were terminated in the exponential phase of the PCR protocol to ensure accuracy of relative abundance values and PCR products were then electrophoresed at 60 V in a 2% agarose gel, stained with ethidium bromide, and digitized (Gel Doc™ XR system; Bio-Rad) for viewing. Negative control reactions were prepared with RNA rather than cDNA for each tissue and consistency in the relative abundance of 18S across samples was used as an indicator of low variability in the quality and quantity of total cDNA loaded into each sample.

qRT-PCR Statistical Analysis

An arbitrary threshold of 100 was used for comparison of cycle threshold values across treatments with the MyIQ Optical System software (version 1.0; Bio-Rad). Threshold values for each sample were adjusted to the plate-specific standard curve to account for plate-to-plate variation; resulting values were log-transformed to homogenize variance and normalized to the expression value for the reference gene (EF1a1), which was invariant across treatments (L. S. Babonis, unpublished). Normalized expression values were then standardized to the control treatment for each species such that expression values for the control treatment will always appear as 1.0. Error estimates were calculated from the log transformed data and rescaled to the standardized mean. All analyses were performed in the R statistical environment (R Development Core Team, 2008).

Results

Morphology

In contrast with the compound tubular shape of the sublingual salt gland in *L. semifasciata* (Chapter 2), the harderian gland is compound acinar in this species (Fig 3-2). The heterogeneity of the cells populating the ducts (d) and acini (a) can be easily seen, especially in areas where the ducts meet the acini (indicated by *; Fig 3-2A). Both cell types have basally positioned nuclei (white arrows; Fig 3-2B), however, while the duct cells are filled with light colored cytoplasm, like the secretory cells of the salt gland, the cytoplasm of the secretory acini is filled with dense, basophilic secretory granules (white arrowheads; Fig 3-2B).

Regarding the morphology of the cephalic glands in *Nerodia*, I found no difference between the semi-marine (*N. c. clarkii*) and freshwater (*N. fasciata*) species. Representative sections (from *N. c. clarkii*) of each cephalic gland outlined in Fig 3-1 are shown in Fig 3-3. Situated at the rostrum, the premaxillary gland (Fig 3-3A) is tubuloacinar and populated by at least two cell types: while the ducts/tubules appear light in color (arrows), the acinar cells are slightly darker in color (arrowheads) and are filled with secretory granules. In contrast to this, the nasal glands (Fig 3-3B) appear to be compound tubular in shape and populated by a single cell type: both duct (d) and tubule (t) cells are light in color with basally positioned nuclei. Ducts can be differentiated from tubules by their larger lumen and the presence of cells that are more columnar than cuboidal. On a morphological level, the harderian glands (Fig 3-3C) are nearly indistinguishable from the duvernoy's glands (Fig 3-3D) in *Nerodia*. Both glands are compound acinar, and, while duct cells (d) appear relatively light in color, acini (a) stain darkly with hematoxylin and contain abundant secretory vesicles (arrowheads).

Supralabial (Fig 3-3E) and infralabial (Fig 3-3F) glands are tubuloacinar and appear similar to the premaxillary gland with two cell types – light (arrows), populating the ducts and tubules, and dark (arrowheads), populating the acini. The anterior and posterior sublingual glands (Fig 3-3G,H, respectively) like the nasal gland in *Nerodia* and the sublingual glands of *L. semifasciata*, are compound tubular in shape. The anterior sublingual gland is populated by a single, light-staining cell type with basally/centrally position nuclei (arrowheads). By contrast, the ducts (d) of the posterior sublingual gland appear lighter in color and have basally positioned nuclei (arrow) whereas the tubule cells (t) stain slightly darker and have basally/centrally positioned nuclei (arrowheads).

Localization of NKA

NKA immunolocalized to the basal (arrows) and lateral (arrowheads) membranes (Fig 3-4A) of the ducts (d) and tubules (t) in the salt gland of *L. semifasciata*, but there was no effect of salinity on this localization (Fig 3-4B-D). By contrast, NKA was not detectable via IHC in either the ducts (d) or the acini (a) of the harderian gland (Fig 3-4E) in this species and this also did not change with treatment (Fig 3-4F-H). In *N. c. clarkii*, NKA immunolocalized to the basolateral membranes of both cell types in the premaxillary gland (Fig 3-5A), the ducts of the nasal gland (Fig 3-5B), the light colored cells in the supra- and infralabial glands (Fig 3-5E,F) and all cells of the anterior and posterior sublingual glands (Fig 3-5G,H). In *N. fasciata*, NKA appeared only in the ducts (d) and very weakly in the lateral membranes (arrowheads) of the tubules (t) in the premaxillary gland (Fig 3-6A); acini (a) were negative for NKA in this gland. In the nasal gland (Fig 3-6B), the ducts (d) were positive basolaterally for NKA while the tubules (t) were negative. Both the ducts and acini of the harderian gland (Fig 3-6C), the duvernoy's gland (Fig 3-6D), and the supralabial gland (Fig 3-6E) were negative for

NKA. The light staining cells of the ducts and tubules in the infralabial gland (Fig 3-6F), and all cells of the anterior (Fig 3-6G) and posterior (Fig 3-6H) sublingual glands were positive for NKA. The expression of NKA in the posterior sublingual gland, though apparently darker in the lateral membranes (arrowheads), was nearly undetectable via IHC in *N. fasciata*.

Localization of NKCC

NKCC was detected in the basolateral membranes of the salt gland (Fig 3-7A) of *L. semifasciata* and, like NKA, its localization was unaffected by salinity treatment (Fig 3-7B-D). In the harderian gland of this species, NKCC was detected in the basal membranes, and perhaps the basal cytoplasm (arrows), of the duct cells; weak positive reaction was also detected in the basolateral membranes (arrowheads) of the acini immediately adjacent to the ducts (Fig 3-7E). Expression of NKCC in the harderian gland was unaffected by salinity (Fig 3-7F-H).

In *N. c. clarkii*, NKCC is expressed in the basolateral membranes of the acini of the premaxillary gland (Fig 3-8A) and weakly in the ducts of the nasal glands (Fig 3-8B). NKCC is absent from the ducts/tubules of the premaxillary gland, the tubules of the nasal gland, all cell types in the harderian gland (Fig 3-8C) and duvernoy's gland (Fig 3-8D). Positive reaction was weak but basolateral in the acinar cells of the supralabial gland (Fig 3-8E) and weak/patchy in the acinar cells of the infralabial gland (Fig 3-8F) but strongly basolateral in the duct cells of the infralabial gland. NKCC was basolaterally positive in all cells of the anterior and posterior sublingual glands (Fig 3-8G,H). In *N. fasciata*, the pattern of expression of NKCC across glands was similar to that of *N. c. clarkii* (Fig 3-9), though, like NKA, the expression of NKCC in the posterior sublingual

gland of *N. fasciata* appears to be weaker than its expression in *N. c. clarkii* (compare Fig 3-8H with Fig 3-9H).

Localization of CFTR

CFTR was undetectable via IHC in both the salt gland and the harderian gland of *L. semifasciata* and in all glands of the *Nerodia* (data not shown). The mRNA, however, for the *L. semifasciata* ortholog of vertebrate CFTR (lsCFTR) is expressed together with NKA and NKCC1 in both the salt gland and harderian gland as well as a variety of other tissues (Fig 3-10). Both the amino acid and nucleotide sequences for lsCFTR shared high % identities with other vertebrates (Table 3-3), though % identity in the regions of the various antibodies I used were variable (Fig 3-11). Binding sequences for six of the seventeen antibodies used in attempts to immunolocalize CFTR are highlighted in grey in Fig 3-11 and the % identity shared between the predicted lsCFTR sequence and the epitope from taxon against which the antibody was made (Table 3-1) is indicated.

Mucus Secretion

Both the salt glands and harderian glands of *L. semifasciata* have secretory cells which are PAS^+ (Fig 3-12). In the salt glands, the PAS^+ material is found only at the apical most margin of the cytoplasm in both the secretory tubules and the ducts (Fig 3-12A) and this domain of PAS^+ expression does not change with salinity (Fig 3-12B-D). In the harderian gland, the domain of expression of PAS^+ material extends further into the cell (Fig 3-12E), in some cases all the way to the basal membrane (Fig 3-12G) but PAS^+ material is only present in the duct cells and is absent from the secretory acini. Like the salt gland, there was no effect of salinity on the domain of expression of PAS^+ material in the harderian gland (Fig 3-12F-H). In both gland types, pre-digestion with α-amylase had no effect on the domain of expression of PAS^+ material (see insets in Fig

3-12) suggesting that these glands secrete neutral mucins, rather than glycogen (Humason, 1972).

As was true of gland morphology, I find no difference in the domain of expression of PAS^+ material in the glands of *N. c. clarkii* and *N. fasciata*; thus, representative sections through each gland are shown for *N. c. clarkii* only (Fig 3-13). PAS^+ material was abundant throughout the cytoplasm of the light-staining tubule/duct cells of the premaxillary gland (Fig 3-13A) but was absent from the acini in this gland and from all cell types in the nasal gland (Fig 3-13B). The duct cells of the harderian gland were also PAS^+ (Fig 3-13C) but the duvernoy's gland was completely negative (Fig 3-13D). Both the supra- (Fig 3-13E) and infralabial (Fig 3-13F) glands exhibited strong positive reaction throughout the duct/tubule cells, similar to the staining pattern in the premaxillary gland. All cell types in the anterior (Fig 3-13G) and posterior (Fig 3-13H) sublingual glands were PAS^+.

Localization of AQP3

Though AQP3 is thought to be transcribed in both the salt gland and the harderian gland of *L. semifasciata* (Chapter 4), AQP3 protein was undetectable via IHC in the salt gland in any treatment (Fig 3-14A-D). By contrast, AQP3 localized to the basolateral membranes (arrows) of the ducts only in the harderian gland (Fig 3-14E). This localization was also not affected by treatment (Fig 3-14F-H). In *N. c. clarkii*, AQP3 is weak but basolateral in all cell types of the premaxillary gland (Fig 3-15A) and the ducts of the nasal gland (Fig 3-15B). AQP3 is restricted to the ducts of the harderian gland as well (Fig 3-15C), though the expression in this tissue appears to be stronger than in the nasal gland. All cell types of the duvernoy's (Fig 3-15D) and supralabial (Fig 3-15E) glands are negative for AQP3, whereas all cell types of the infralabial (Fig 3-15F),

anterior sublingual (Fig 3-15G) and posterior sublingual (Fig 3-15H) glands were positive. In *N. fasciata*, only the duct/tubule cells (d) of the premaxillary gland (Fig 3-16A) were positive for AQP3; the acinar cells (a) were negative in this species. The remaining glands of *N. fasciata* (Fig 3-16B-H) exhibited the same pattern of AQP3 reactivity as was seen in *N. c. clarkii*.

Salinity Acclimation

There was no significant effect of salinity on the abundance of NKA (Fig 3-17A), NKCC1 (Fig 3-17B), CFTR (Fig 3-17C), or AQP3 (Fig 3-17D) in either the salt gland or the harderian gland of *L. semifasciata*. There was, however, a slight non-significant trend toward increased abundance of each of these transcripts with increased salinity in the salt gland only. Expression of each transcript, particularly among control animals, tended to be higher in salt glands than in harderian glands.

Discussion

This study aimed to define the phenotype of a vertebrate salt gland using morphology, cellular anatomy, biochemistry, and, importantly, comparisons between distantly related taxa experiencing similar abiotic stressors. By comparing the salt gland of *L. semifasciata*, with an unspecialized gland in this same species, and all of the unspecialized cephalic glands in two species of watersnake (one semi-marine, the other freshwater), I further develop the hypothesis describing the evolution of a salt gland from an unspecialized precursor as proposed by Peaker and Linzell (1975). Although *N. c. clarkii* (the semi-marine watersnake) is not known to have a salt gland (no salt gland was found in the conspecific *N. c. compressicauda*; Schmidt-Nielsen and Fange, 1958), this species is much more tolerant of salt water than its freshwater congeners (Dunson, 1980). This disparity in salinity tolerance has been attributed to differences in behavior

(including the propensity of the freshwater species to consume salt water when dehydrated; Pettus, 1963) and the physiology of the integument (Dunson, 1978). Here, I suggest that minor differences in the biochemistry of the cephalic glands in these two species may also be related to habitat use and, further, may provide insights into the evolution of salt glands.

The observation that all known vertebrate salt glands are compound tubular in shape provides initial support for the hypothesis that this feature is a necessary component of salt gland phenotype. Indeed, the salt gland of *L. semifasciata* exhibits this morphology (Chapter 2) but, importantly, three cephalic glands in *Nerodia* (nasal, anterior sublingual, and posterior sublingual; Fig 3-3) share this form but do not appear to have the same function. Furthermore, the cell types populating the secretory tubules and ducts of snake salt glands are, largely, homogeneous in their biochemistry and putative function, a feature that appears to be true only of the anterior and posterior sublingual glands in *Nerodia*. Thus, in combination, the anterior and posterior sublingual glands appear, morphologically, to be most similar to the salt gland of *L. semifasciata*. Since the salt gland of *L. semifasciata* is also the posterior sublingual gland, it is difficult to determine whether the similarities in morphology are representative of more than shared ancestry. Thus, additional analyses of sublingual gland morphology in other snake taxa including analyses of the morphology of the sublingual gland in, for example, the homalopsid snakes which have a premaxillary salt gland, are necessary to further evaluate this putative similarity.

NKA and NKCC have previously been identified in the basolateral membranes of both the secretory tubules and ducts of the salt gland in *L. semifasciata* (Chapter 2).

Although NKA was completely absent (or present in an abundance too low to detect via IHC) from all parts of the harderian gland (Fig 3-4), NKCC localized to the basolateral membranes of the ducts in the harderian gland (Fig 3-7). NKA is known to play a critical role in activating the asymmetrical exchange of Na^+/K^+ that ultimately results in secretion of Na^+ from secretory cells; thus, these results suggest that the functions of the secretory tubules/ducts of the salt gland are likely quite different from function of the ducts of the harderian gland. Among the *Nerodia*, two glands – the anterior and posterior sublingual glands – are populated by a single cell type expressing basolateral NKA and NKCC (Fig 3-5,3-6,3-8,3-9). Interestingly, the ducts of several additional glands (premaxillary, nasal, and infralabial) also have this biochemical phenotype; thus, as compared with the duct of the harderian gland, which lacks NKA, these glands might actually be better representatives of the ancestral gland from which the salt gland was co-opted. While these observations of the shape of the sublingual glands and the localization of NKA and NKCC in the basolateral membranes of the cells populating their epithelia hold true for *N. fasciata*, which is known to be highly intolerant of salt water, it is notable that the abundance of NKA and NKCC in the posterior sublingual gland of *N. fasciata* appear to be lower than that of *N. c. clarkii* (compare Fig 3-5H with Fig 3-6H and Fig 3-8H with Fig 3-9H). Though true quantitative estimates of protein abundance cannot be made from immunohistochemical analyses, I suspect that quantitative analyses of the abundance of NKA in the posterior sublingual gland of *N. c. clarkii* and *N. fasciata* will support these findings.

Surprisingly, despite the use of a variety of anti-CFTR antibodies, I was unable to detect CFTR in any of the glands examined in this study. Considering that some of

these antibodies shared a high identity with the predicted amino acid sequence for lsCFTR (Fig 3-11), I think further investigations into the identity of the putative apical Cl^- channel are warranted in these species, especially *L. semifasciata*. Interestingly, I was able to demonstrate that CFTR is transcribed in both the salt gland and the harderian gland, as are NKA and NKCC1 (Fig 3-10). NKA, NKCC1, and CFTR are also transcribed together in the esophagus, kidney, and lung (Fig 3-10), tissues known to secrete watery solution. Though these results might reflect that CFTR is transcribed but not translated in these two glands, I, conservatively, suggest that CFTR is likely the apical Cl^- channel in reptilian salt glands, as it in the salt glands of elasmobranchs and birds (Lowy et al., 1989; Riordan et al., 1994).

AQP3 clearly populates the basolateral membranes of the duct cells in the harderian gland of *L. semifasciata* (Fig 3-14), as well as the duct cells in the premaxillary, nasal, and harderian glands of *Nerodia* and all cell types in the infralabial, anterior sublingual, and posterior sublingual glands of these species (Figs 3-15,3-16). Basolateral localization of AQP3 has also been identified in the mucous glands of amphibian integument (Akabane et al., 2007), lending support to the idea that the presence of this protein relates to secretion of mucus by these tissues. Since AQP3 has been proposed to be a key regulator of the water transport involved in mucus secretion (Lignot et al., 2002), I hypothesize that a reduction in the mucus-secretory function of the cells populating the salt gland may have been a key step in the evolution of specialization for ion secretion. Additionally, while neutral mucins are present in the secretory cells of the salt gland and the ducts of the harderian gland, the secretory acini of the harderian gland completely lack neutral mucins (Fig 3-12). These results may

suggest that the secretory cells (ducts and tubules) of the salt gland and the duct cells of the harderian gland share a similar function in the secretion of neutral mucins. While early hypotheses about the evolution of salt glands suggested that they arose by elongation of the ducts of acinar glands (with loss of the cells populating the acini; Peaker and Linzell, 1975) and the PAS results presented here may provide initial support for this idea, I have also identified several important differences between the secretory tubules of the salt glands and the ducts of non salt secreting glands (including the harderian gland), above.

Considering I did not detect *significant* differences in the abundance or localization of NKA, NKCC, CFTR, or AQP3 following salinity acclimation (Fig 3-17), the functional differences between specialized salt glands and unspecialized glands may derive primarily from the presence/absence or standing abundance of key ion and water regulatory proteins, rather than their plasticity in response to environmental conditions. In this light, a critical next step in this line of research is to collect and analyze the secretion from the sublingual gland of each species to determine if they vary in the concentration of NaCl that they can secrete. In particular, though neither *N. c. clarkii* nor *N. fasciata* is known to have a salt gland, it is possible that *N. c. clarkii* can secrete a NaCl solution that is more concentrated than that of *N. fasciata*. In combination with quantitative analyses of protein abundance in the sublingual glands of these species would allow me to further test the hypothesized evolutionary trajectory detailed below. Another important experiment to do would involve characterization of the mechanism by which reptilian salt gland cells become stimulated to secrete. Among birds and elasmobranchs, VIP and ACh are known to regulate NaCl secretion through

phosphorylation of NKA and CFTR (Ernst et al., 1967; Hildebrandt, 1997). Thus, in order to more fully describe the potential mechanism by which functional salt glands evolved, it is imperative to understand how the phosphorylation state of these proteins and their respective enzymatic activities varies following salinity acclimation. Specifically, it would be interesting to compare the phosphorylation response of CFTR in both the salt gland and harderian gland of *L. semifasciata* following acclimation to know if the different functional nature of the salt and harderian glands is also associated with different stimulatory agents (e.g., endocrine or neurotransmitter) or if similar agents simply have different down-stream (intracellular) effects in these two tissues.

The combined results of these comparisons between the salt gland and the harderian gland in *L. semifasciata* and the survey of cephalic gland morphology and biochemistry in marine and freshwater watersnakes enable me to make several hypotheses about the steps involved in the evolution of salt glands in reptiles (summarized in Fig 3-18). (i) Evolution of compound tubular shape appears to be a critical step in the evolution of a salt gland. In support of this, all known salt glands are compound tubular, and, in the watersnakes, there are three glands that exhibit this shape (nasal, anterior sublingual, and posterior sublingual) but lack various other features of the salt gland. (ii) The evolution of cells specialized for the secretion of NaCl likely involved an increase in the abundance of the basolaterally located NKA and NKCC. Two pieces of evidence support this as another critical step in the evolution of salt glands: first, NKA and NKCC are absent or in extremely low abundance in the duct cells of the harderian gland in the sea snake and, second the abundance of both NKA and NKCC is qualitatively higher in the posterior sublingual gland of *N. c. clarkii* (the

marine species) than *N. fasciata* (the freshwater species). While the posterior sublingual gland of *N. c. clarkii* is not known to be a salt gland, I think this correlation between habitat use and gland biochemistry suggests that the sublingual gland in *N. c. clarkii* may have a different function that than of *N. fasciata*. (iii) Considering that intracellular mucin and basolateral AQP3 are absent from the salt gland of *L. semifasciata*, I proposed that the presence of these proteins in the sublingual glands of both species of *Nerodia* suggests that these cells have functions that were either lost in the evolution of the salt gland or that the salt gland evolved from cells that already lacked this function. Specifically, I suggest that the sublingual glands in the two species of Nerodia play a role in the production of oral mucus and that this function is absent from the sublingual gland of *L. semifasciata.*

Several additional studies of gland form and function from additional snake taxa are necessary to evaluate the hypothesized trajectory laid out above. First, studies aimed at examining the distribution of NKA, NKCC, CFTR, AQP3, and mucin, in the sublingual glands of additional marine taxa are critical. In particular, studies employing comparative studies of marine taxa and closely related freshwater taxa would be very informative. Second, quantitative analysis of the abundance of NKA and NKCC in the sublingual glands of these various species in concert with a biochemical analysis of the secretion produced by the sublingual gland in each species is critical. With these data in hand it will be possible to relate the physiology of these animals to the morphological and biochemical observations I've made in this study. Finally, a thorough understanding of the conditions responsible for stimulating sublingual gland secretion and the mechanism by which this signal is transduced from the environment to the epithelium of

the gland is imperative. With these data in hand it will be possible to evaluate the importance of the signaling mechanism underlying gland secretion and the evolution of the specialized salt-secreting function.

Table 3-1. A sample of the anti-CFTR antibodies (Ab) used in this study. The epitope sequence and location (in amino acids) are indicated for the taxon of origin.

Ab	epitope	location	origin	Reference
MM13-4	RKGYRQRLELSD	aa: 25-36	*H. sapiens*	Millipore
L12B4	NLTTTEVVMENVTAFWEEGFGELFEKA	aa: 386-412	*H. sapiens*	Millipore
13-1	DEPLERRL	aa: 729-736	*H. sapiens*	R&D Systems
M3A7	DEPSAHLDPVT	aa: 1370-1380	*H. sapiens*	Bilan et al 2004
60	LQEEAEEDLQETRL	aa: 1479-1492	*S. acanthias*	Jack Riordan
24-1	DTRL	aa: 1477-1480	*H. sapiens*	R&D Systems

Table 3-2. Primers used for PCR/cloning, qRT-PCR, RACE, and duplexing PCR.

Primer	Application	Oligonucleotide sequence (5' → 3')
NKCC1 F1	Initial PCR	AAGGGGGTGCTAGTACGGTGYATGYTNAAYA
NKCC1 R2	Initial PCR	ATCAGTGCGTAGGATGCCARRAARAARTT
CFTR F1	Initial PCR	TCTGGCGATGGCTCATTTYRTNTGGAT
CFTR R2	Initial PCR	GAACGGAGCGTCCATTAGGTATARRTCNGCRTC
EF1a1 F2	Initial PCR	CTCCTGGACATCGAGACTTTATAAARAAYATGAT
EF1a1 R2	Initial PCR	CGCAAATTTACAAGCTATATGAGCAGTRTGRCARTC
NKCC1 F	qRT-PCR	AGGCATCTCGTTAGCAGGAA
NKCC1 R	qRT-PCR	GCCTCTGAAATCTGGTCCAA
CFTR F2	qRT-PCR	GGATCTACTGGAGCAGGCAAGA
CFTR R2	qRT-PCR	CCAGGCATAATCCATGACACTT
EF1a1 F1	qRT-PCR	TGCTGTCCTTATCGTTGCTG
EF1a1 R1	qRT-PCR	CCCCAACAATGAGCTGTTTT
CFTR F4	3'RACE	TCTGAACAAGGGGAGGCAATTCTGC
CFTR F7	3'RACE	CCCTCAACAAACTCAAAGCAGGTGGA
CFTR R1	5'RACE	ACTGCCCAAGGGAACTGTCTAGT
CFTR R2	5'RACE	CCTGCTCGCTGATCTCTGTATTTC
NKA F1	Duplex PCR	GGAAGTGAAGGGAGGGGACA
NKA R1	Duplex PCR	CCTCAGGGACATTGGCAACA
NKCC1 F2	Duplex PCR	GGGTCCAGAATTTGGTGGTG
NKCC1 R2	Duplex PCR	ATCCGCAAGATCACCTGAGA
CFTR F1	Duplex PCR	TTTTTGGGATGAGGGAAGTG
CFTR R1	Duplex PCR	GAAATTCTGGCTCGTTGACC

Abbreviations: F – forward/sense, R – reverse/antisense

Table 3-3. NCBI accession numbers and %identities for CFTR sequences from the indicated taxa.

Taxon	aa accession #	% identity / % positive	nu accession #	% identity
G. gallus	NP_001099136.1	80/90	NM_001105666.1	77
H. sapiens	NP_000483.3	79/89	NM_000492.3	76
S. acanthias	AAA49616.1	69/83	M83785.1	74

Abbreviations: aa – amino acid; nu - nucleotide

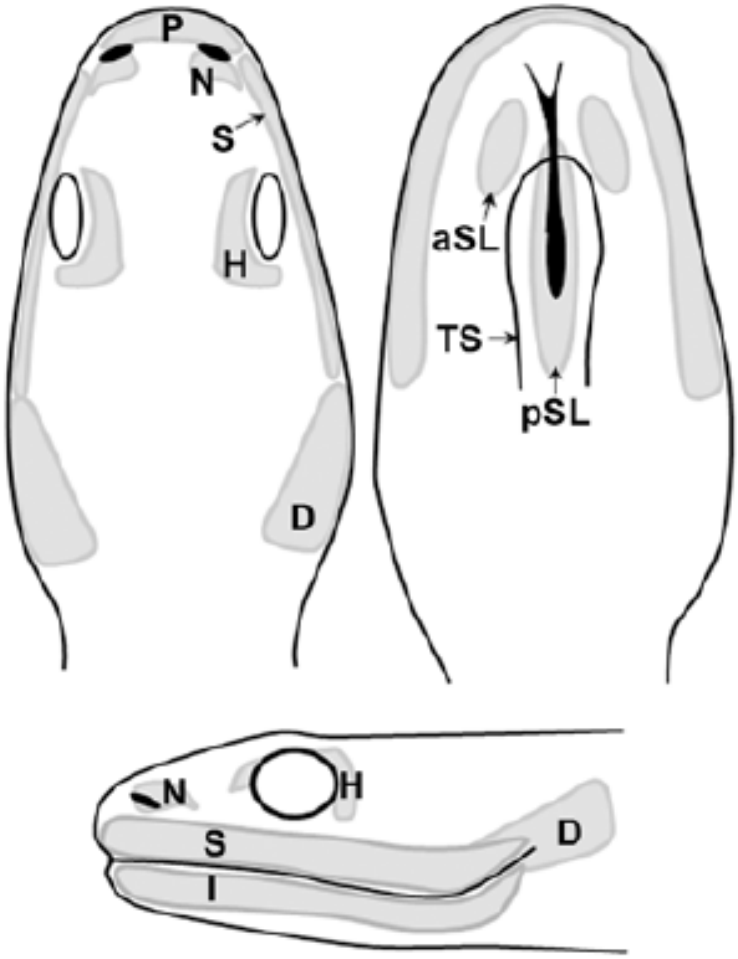

Figure 3-1. Diagram of the approximate locations of the cephalic glands in *Nerodia*. Abbreviations: aSL – anterior sublingual, D – duvernoy's, H – harderian, I – infralabial, N – nasal, P – premaxillary, pSL – posterior sublingual, S – supralabial, TS – tongue sheath. Adapted from: Burns and Pickwell (1972), and http://www.flmnh.ufl.edu/herpetology/fl-guide/Nerodiaffasciata.htm.

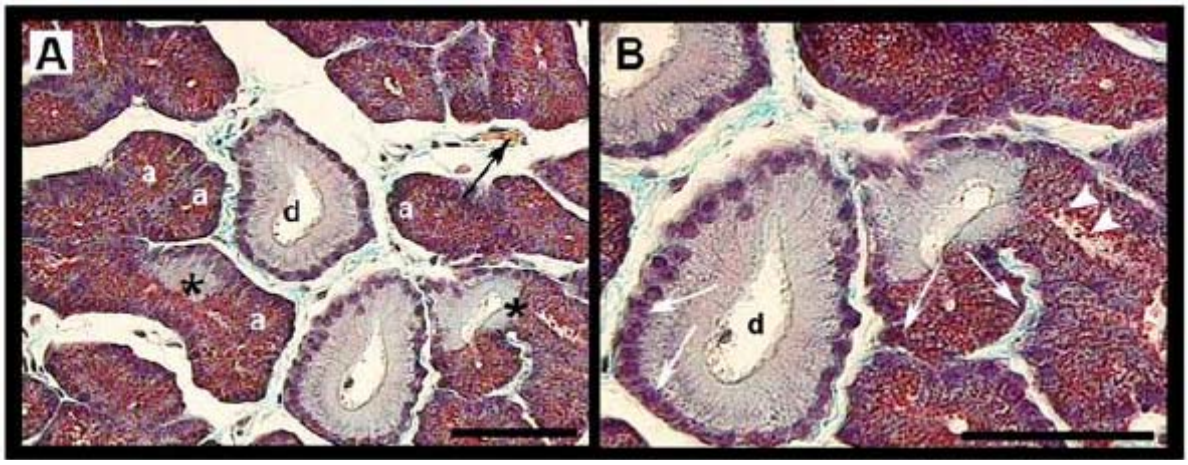

Figure 3-2. Morphology of the harderian gland in *L. semifasciata*. (A) The cytoplasm of the ducts (d) appears clear/light green using Masson Trichrome. By contrast, the cytoplasm of the secretory acini (a) is filled with basophilic secretory granules (white arrowheads). Nuclei are positioned basally in both ducts and acini (white arrows) and connective tissue fibers (green) can be seen surrounding and separating both ducts and acini. Red blood cells (black arrow) can be seen in the interstitial space around/between acini. Areas where secretory acini join ducts are indicated by *. Images produced via light microscopy. Scale bars = 50μm.

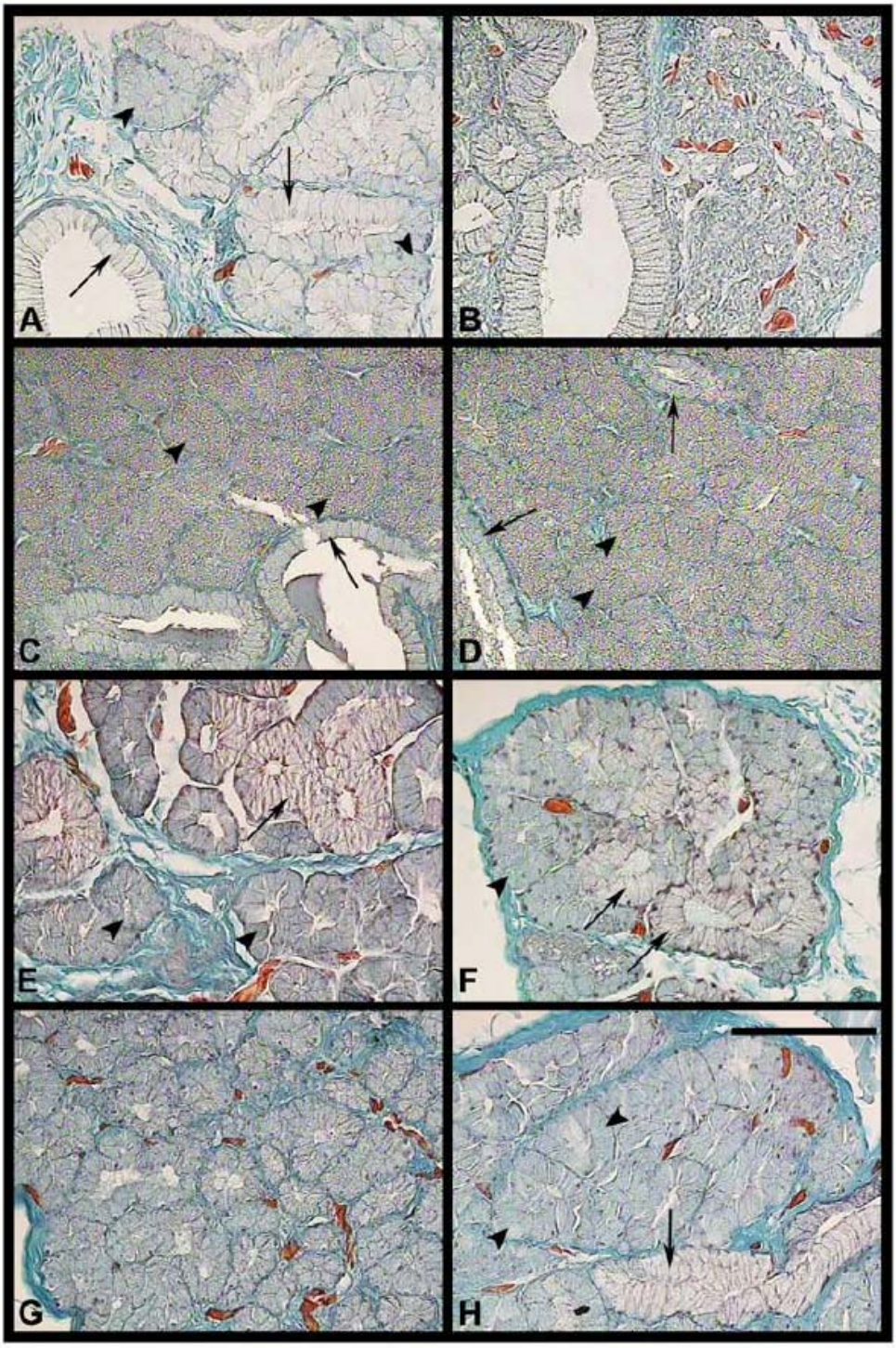

Figure 3-3. Morphology of the cephalic glands in *N. c. clarkii*. (A) Premaxillary, (B) nasal, (C) harderian, (D) duvernoy's, (E) supralabial, (F) infralabial, (G) anterior sublingual, and (H) posterior sublingual. In each image, mucus cells/ducts are indicated by arrows and serous cells/acini are indicated by arrowheads. Images produced via light microscopy using Masson Trichrome. Scale bars = 50μm.

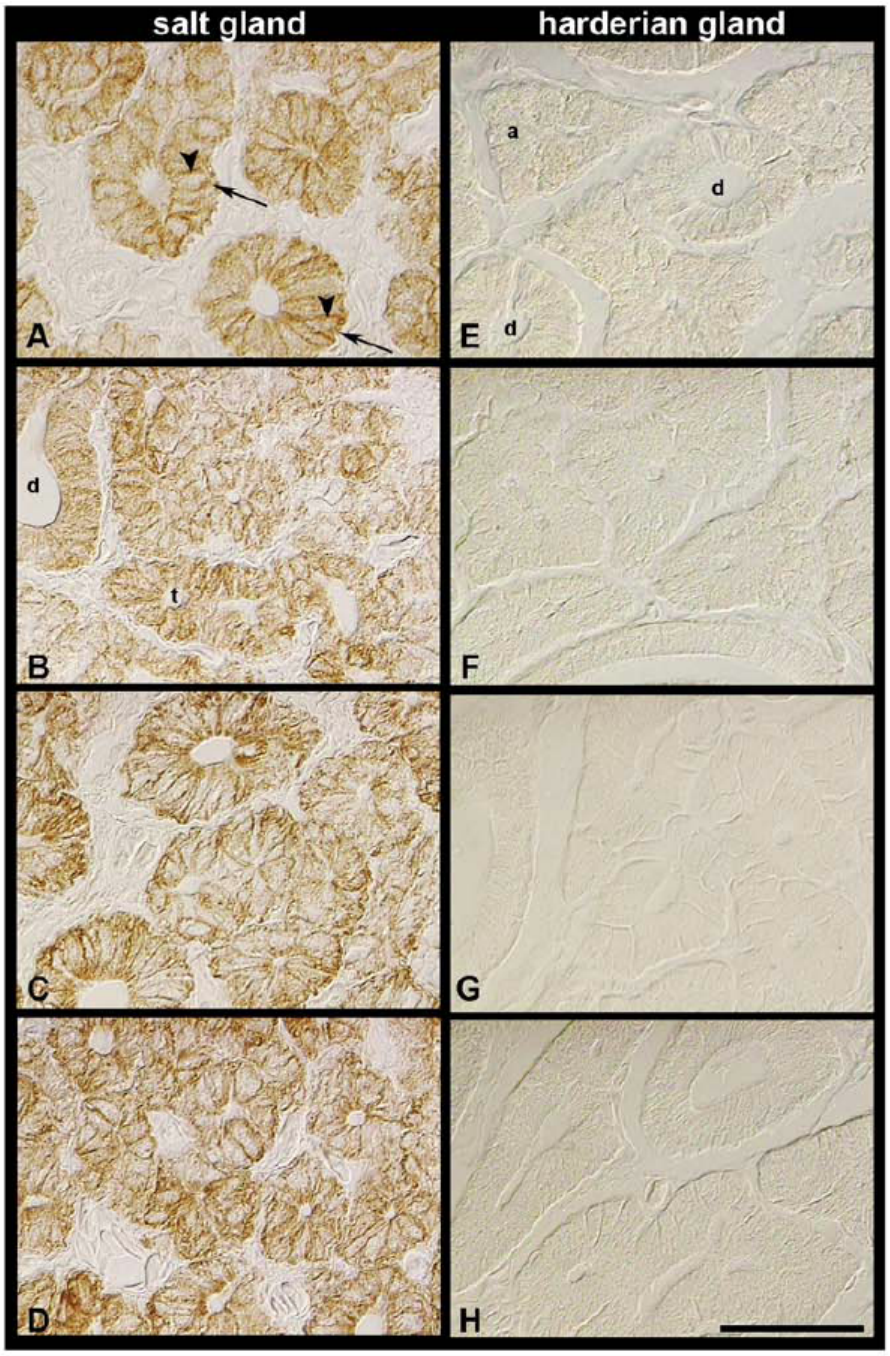

Figure 3-4. Immunolocalization of NKA in the salt gland (A-D) and harderian gland (E-H) of *L. semifasciata.* (A) NKA is present in the basal (arrows) and lateral (arrowheads) membranes of the cells in the secretory ducts (d) and tubules (t) of the salt gland from control animals and there was no effect of treatment on localization (compare B-D). (E) NKA is not detectable in either the ducts (d) or the secretory acini (a) of the harderian gland by immunolocalization; this also does not change with treatment (compare F-H). Treatments: A,E – control; B,F – 0% SW; C,G – 50% SW; and D,H – 100% SW. Images produced via differential interference contrast microscopy. Scale bar = 50µm.

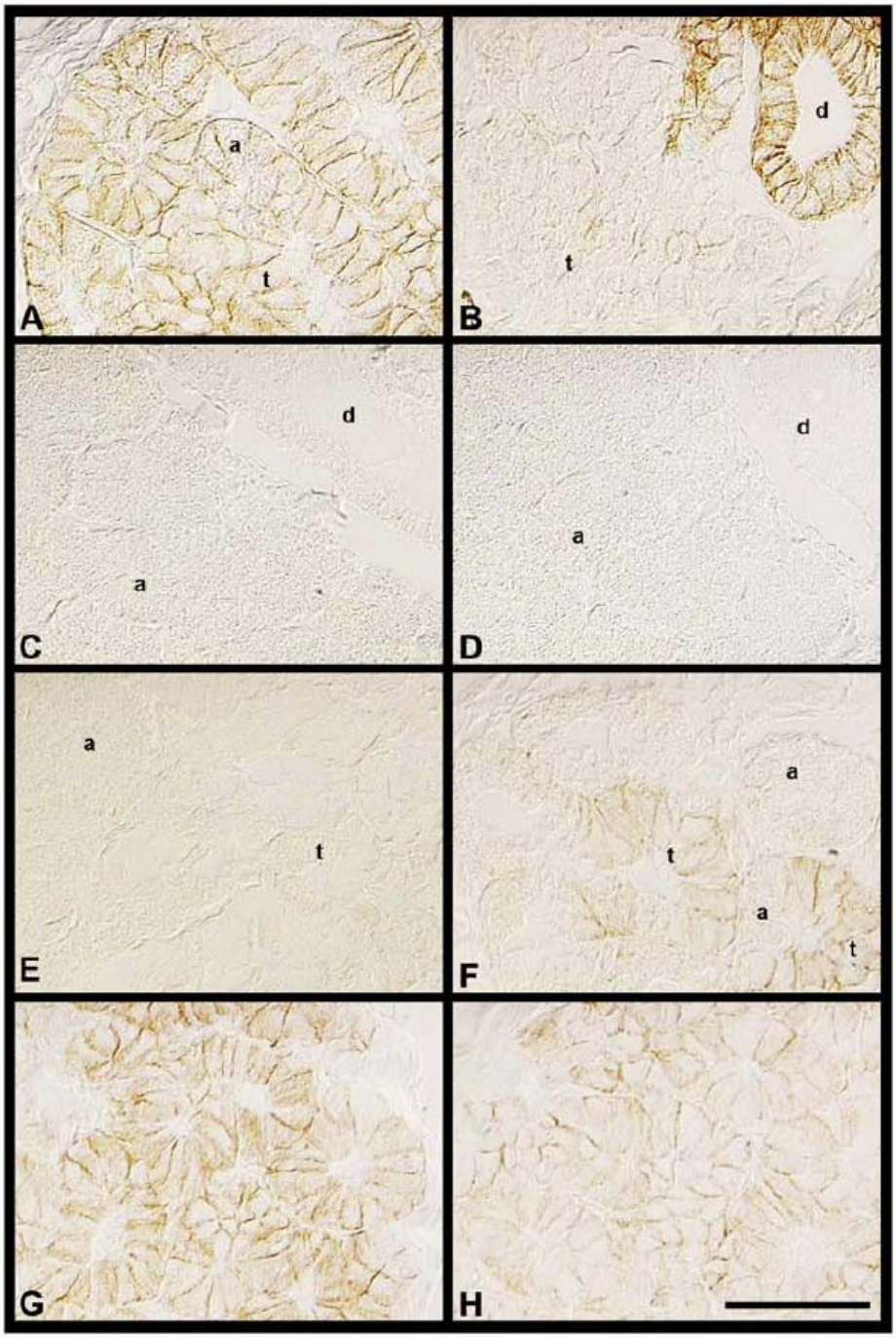

Figure 3-5. Immunolocalization of NKA in the cephalic glands of *N. c. clarkii*. NKA is basolateral in both the secretory acini (a) and ducts (d) of the premaxillary gland (A) and basolateral in the ducts (d) but absent from the tubules (t) of the nasal gland (B). NKA was not detected in the harderian (C), duvernoy's (D), or supralabial (E) glands, but was basolateral in the ducts of the infralabial glands (F). Both the anterior (G) and posterior (H) sublingual glands were populated entirely by cells expressing basolateral NKA. Images produced via differential interference contrast microscopy. Scale bar = 50µm.

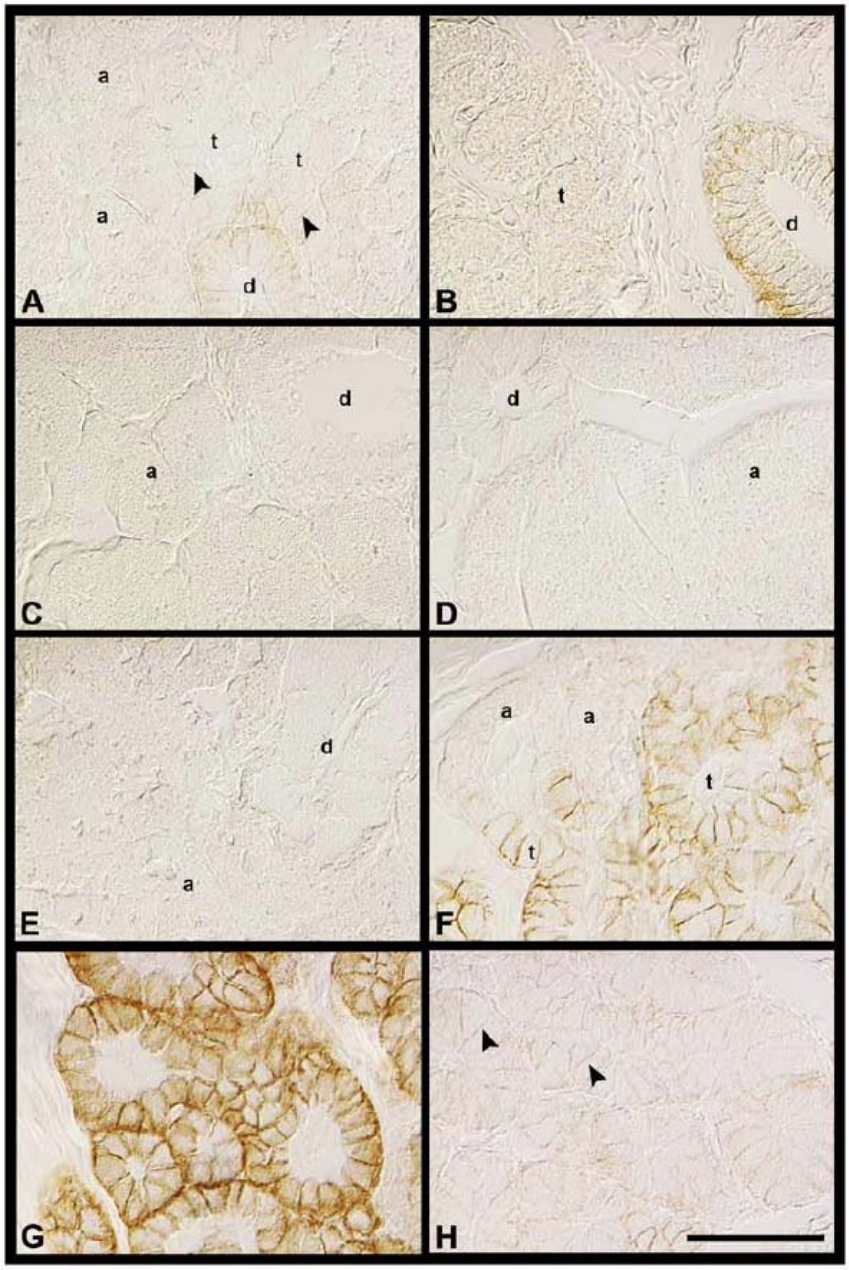

Figure 3-6. Immunolocalization of NKA in the cephalic glands of *N. fasciata*. NKA is only weakly expressed in the ducts (d) but not the acini (a) of the premaxillary (A) and nasal (B) glands. NKA was not detected in the harderian (C), the duvernoy's (D), or the supralabial (E) gland in this species. In the infralabial gland (F), NKA is restricted to the basolateral membranes of the duct cells (d). The anterior sublingual gland (G) is populated entirely by NKA-expressing cells. NKA can also be seen in the basolateral membranes (arrowheads) of the posterior sublingual gland, though expression in this tissue is weak. Images produced via differential interference contrast microscopy. Scale bar = 50μm.

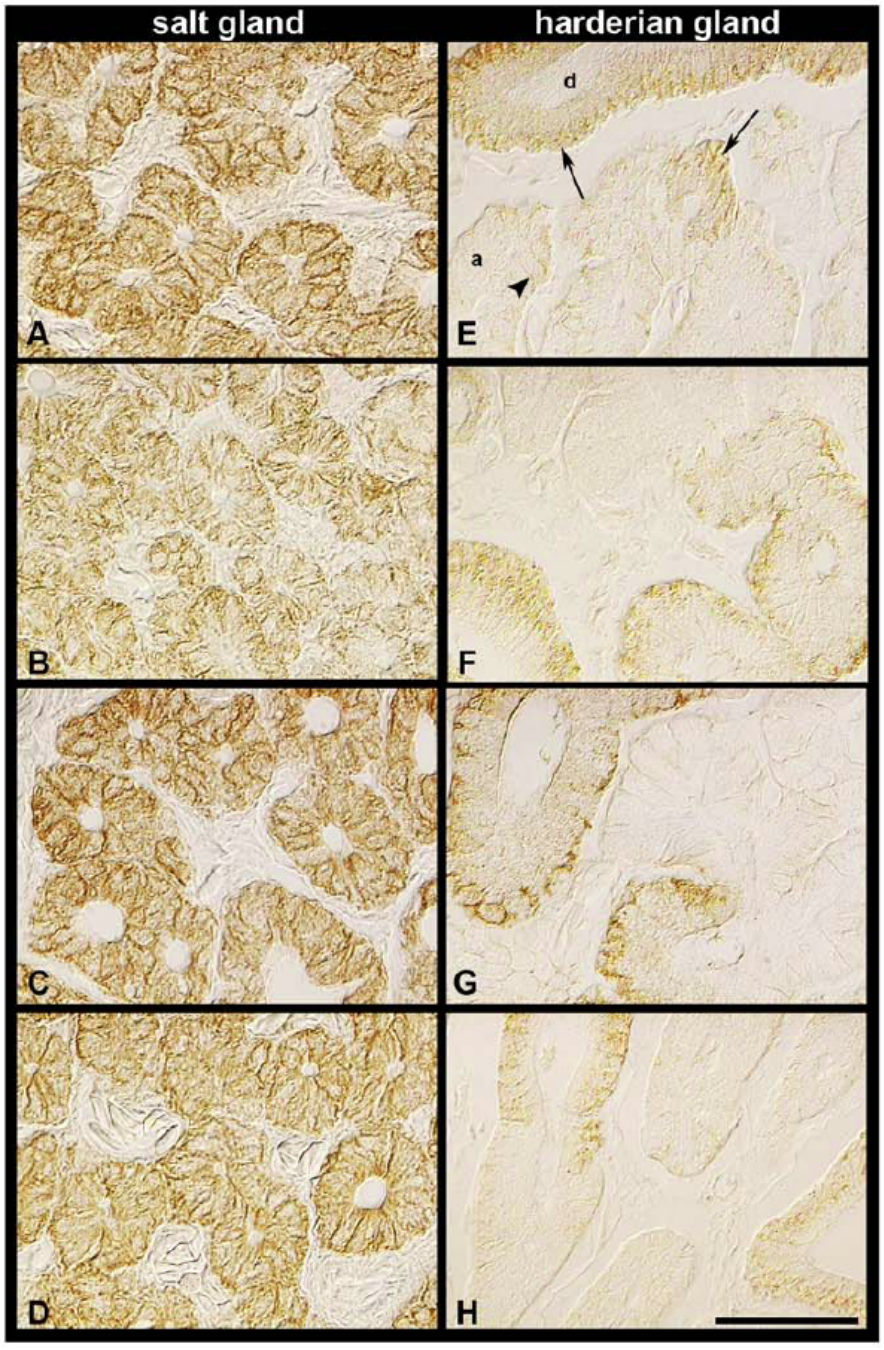

Figure 3-7. Immunolocalization of NKCC in the salt gland (A-D) and harderian gland (E-H) of *L. semifasciata.* (A) NKCC is basolateral in the secretory ducts and tubules of the salt gland and this localization was unaffected by salinity (compare B-D). (E) NKCC is basolateral in both the ducts (d) and acini (a) of the harderian gland, though expression seems to be relatively greater in the ducts (see arrows) than the acini. There was no effect of salinity on the localization of NKCC in the harderian gland (compare F-H). Treatments: A,E – control; B,F – 0% SW; C,G – 50% SW; and D,H – 100% SW. Images produced via differential interference contrast microscopy. Scale bar = 50µm.

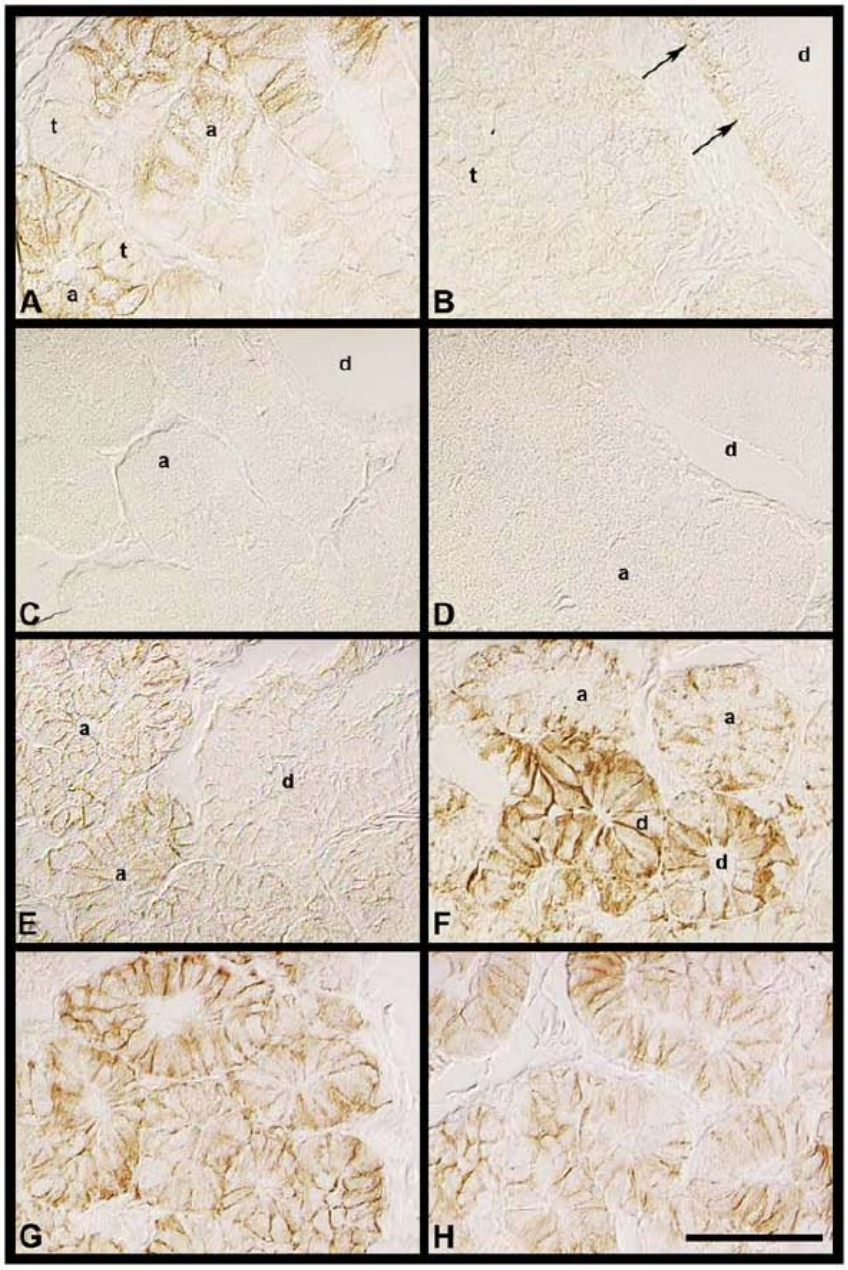

Figure 3-8. Immunolocalization of NKCC in the cephalic glands of *N. c. clarkii*. NKCC is expressed in the premaxillary gland (A) in the basolateral membranes of the acinar cells (a), which also express secretory granules; it is very weak but basolateral (arrows) in the ducts (d) of the nasal gland but absent from the tubules (t) in this tissue. NKCC was not detected in the ducts (d) or acini (a) of the harderian (C) or duvernoy's (D) glands. Expression is basolateral in both the duct (d) and acinar cells (a) of the supralabial (E) and infralabial (F) glands, though both tissues appear to be heterogeneous. All cells in both the anterior (G) and posterior (H) sublingual glands express basolateral NKCC. Images produced via differential interference contrast microscopy. Scale bar = 50μm.

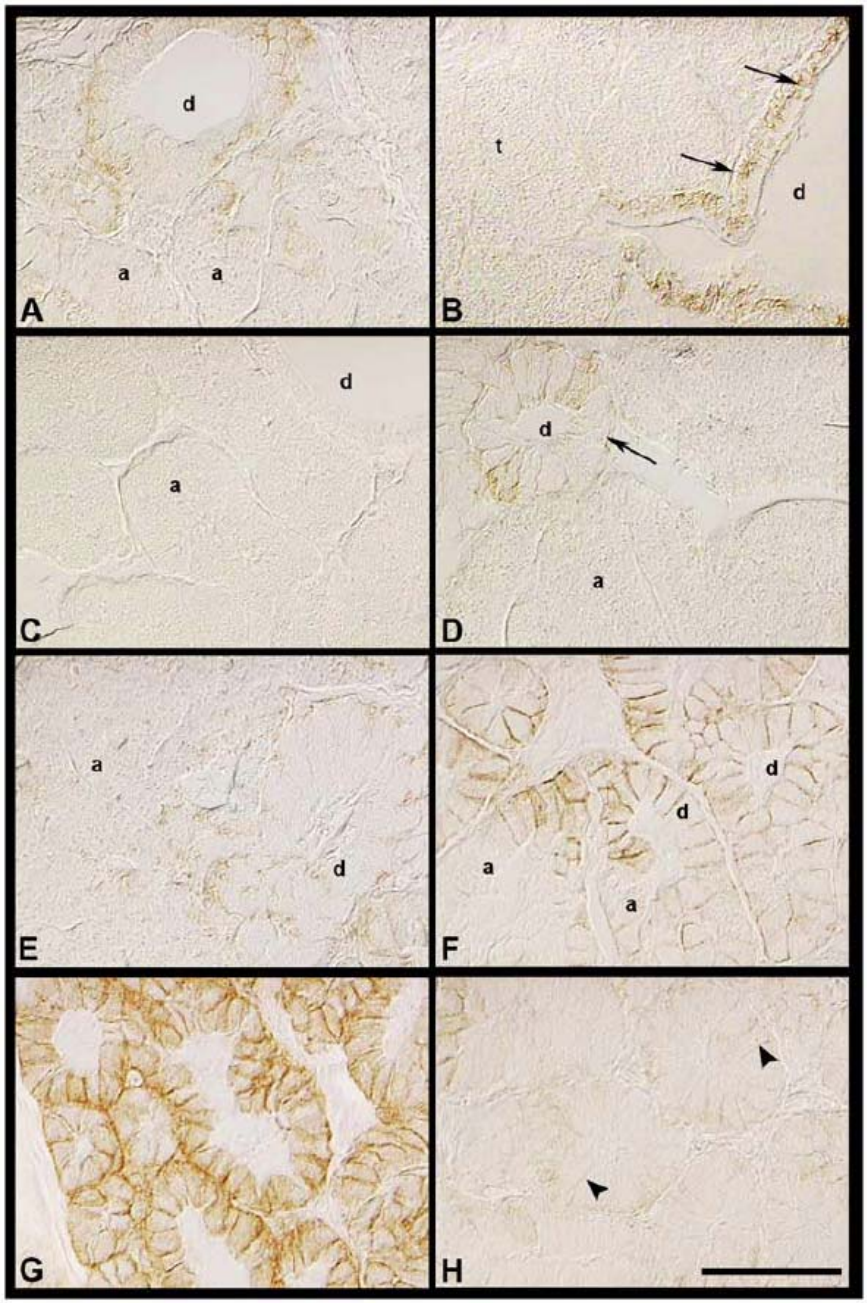

Figure 3-9. Immunolocalization of NKCC in the cephalic glands of *N. fasciata.* NKCC is restricted to the basolateral membranes of the duct cells (d) in the premaxillary (A) and nasal (B) glands, and is absent from the harderian gland (C). Duct cells (d) are also positive in the duvernoy's (D), supralabial (E) and infralabial (F) glands. All cells of the anterior (G) and posterior (H) sublingual glands are basolaterally positive for NKCC, though expression in the posterior sublingual gland is very weak (arrowheads point to weak positive staining). Images produced via differential interference contrast microscopy. Scale bar = 50μm.

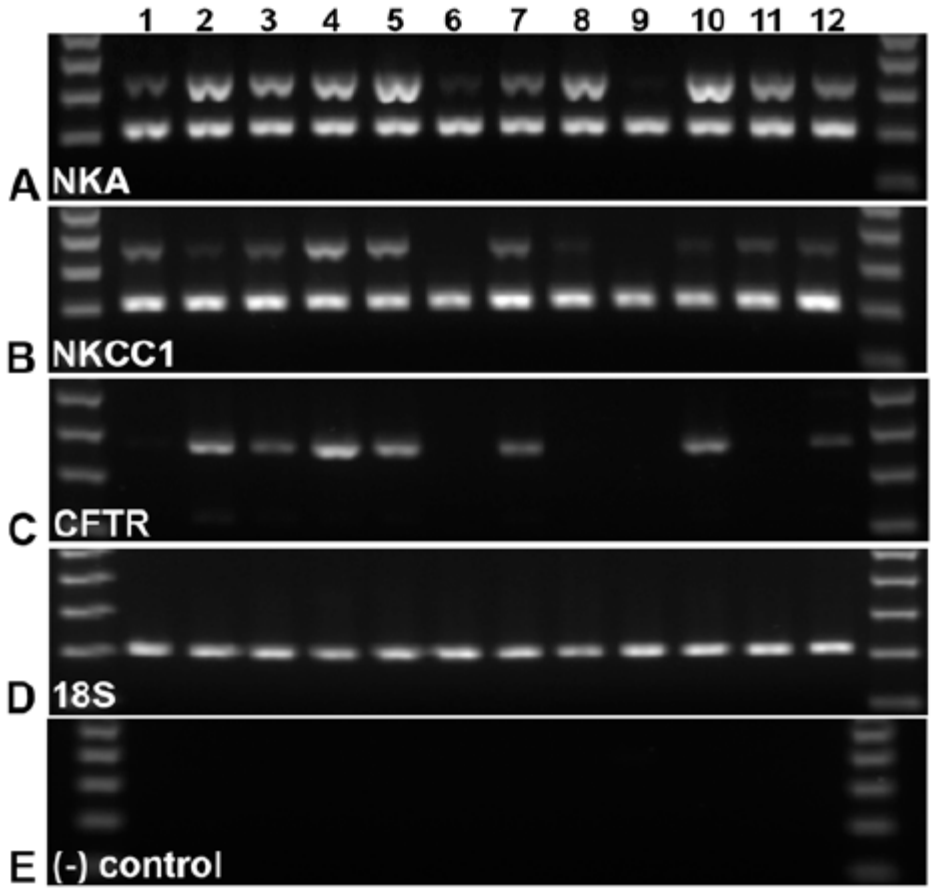

Figure 3-10. Tissue distribution of (A) NKA, (B) NKCC1, and (C) CFTR in *L. semifasciata*. Expression of NKA and NKCC1 is shown relative to the expression of 18S amplified from the same samples at the same time (bands of lower molecular mass in the same panel). Due to interference between the CFTR and 18S primers, CFTR expression is shown relative to (D) the expression of 18S in separate samples amplified at the same time. (E) A representative negative control; no expression was detected when CFTR RNA was used as a template. Lanes: (1) brain, (2) duodenum, (3) esophagus, (4) harderian gland, (5) kidney, (6) liver, (7) lung, (8) skeletal muscle, (9) pancreas, (10) salt gland, (11) stomach, (12) testis.

Figure 3-11. The predicted amino acid sequence for lsCFTR. Areas highlighted in grey represent the sequence recognized by the antibody indicated above the grey box. The % identity shared between lsCFTR and the sequence against which the antibody was constructed is indicated above the box in bold. See Table 3-2 for epitope sequences from their taxa of origin. The lsCFTR amino acid sequence was predicted from the full-length mRNA using the Translate Tool on the Swiss Institute of Bioinformatics proteomics server.

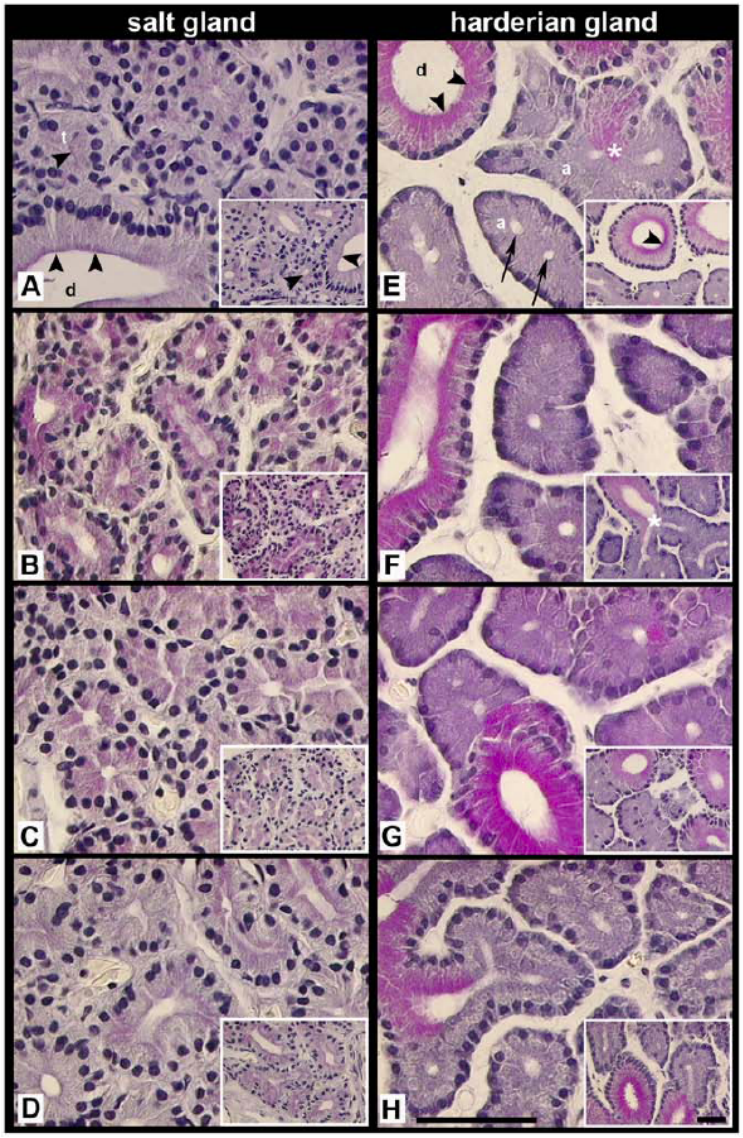

Figure 3-12. Representative sections of salt gland (A-D) and harderian gland (E-H) from *L. semifasciata* showing the presence of PAS^+ secretion. (A) PAS^+ material is restricted to the apical-most cytoplasm of the cells (arrowheads), particularly the ducts. Inset: Pre-digestion with α-amylase does not reduce the area of expression of PAS^+ material. There was no effect of treatment on the domain of expression of PAS^+ material in salt glands (compare B-D). (E) PAS^+ material appears to be secreted in abundance from the ducts of the harderian glands, as the domain of expression extends from the apical membrane (arrowheads) down to at least the midpoint of the cell. Secretory acini are PAS^- (arrows). Inset: Pre-digestion also did not affect the domain of expression of PAS^+ material in the harderian gland. There was also no effect of salinity treatment on expression of PAS^+ material in the harderian gland (compare F-H). Treatments: A,E – control; B,F – 0% SW; C,G – 50% SW; and D,H – 100% SW. Areas where secretory acini join ducts are indicated by *. Images produced via light microscopy. Scale bars = 50μm.

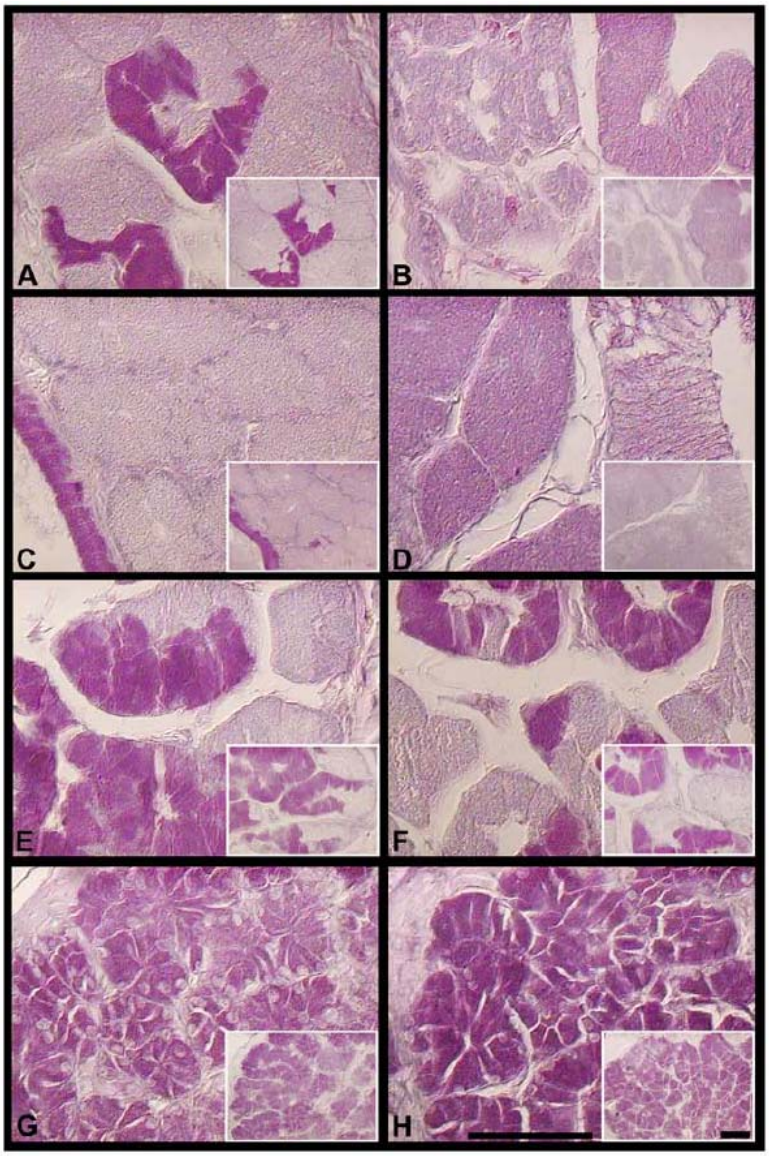

Figure 3-13. PAS reaction in the cephalic glands of *N. c. clarkii*. PAS^+ material is restricted to the ducts of the premaxillary gland (A) and is absent from all cell types in the nasal gland (B). The ducts of the harderian gland are PAS^+. The duvernoy's gland (D) is slightly PAS^+ but this slight staining appears to uniformly decrease following digestion with α-amylase (inset; see Materials and Methods). The acini of the supra- (E) and infralabial (F) glands are PAS^- while the tubule cells are PAS^+. All cells in the anterior (G) and posterior (H) sublingual glands are PAS^+. Insets: Pre-digestion with α-amylase does not reduce the area of expression of PAS^+ material in any of the glands pictured, though the duvernoy's gland appears to lose magenta coloration uniformly throughout the tissue. Images produced via light microscopy. Scale bars = 50μm.

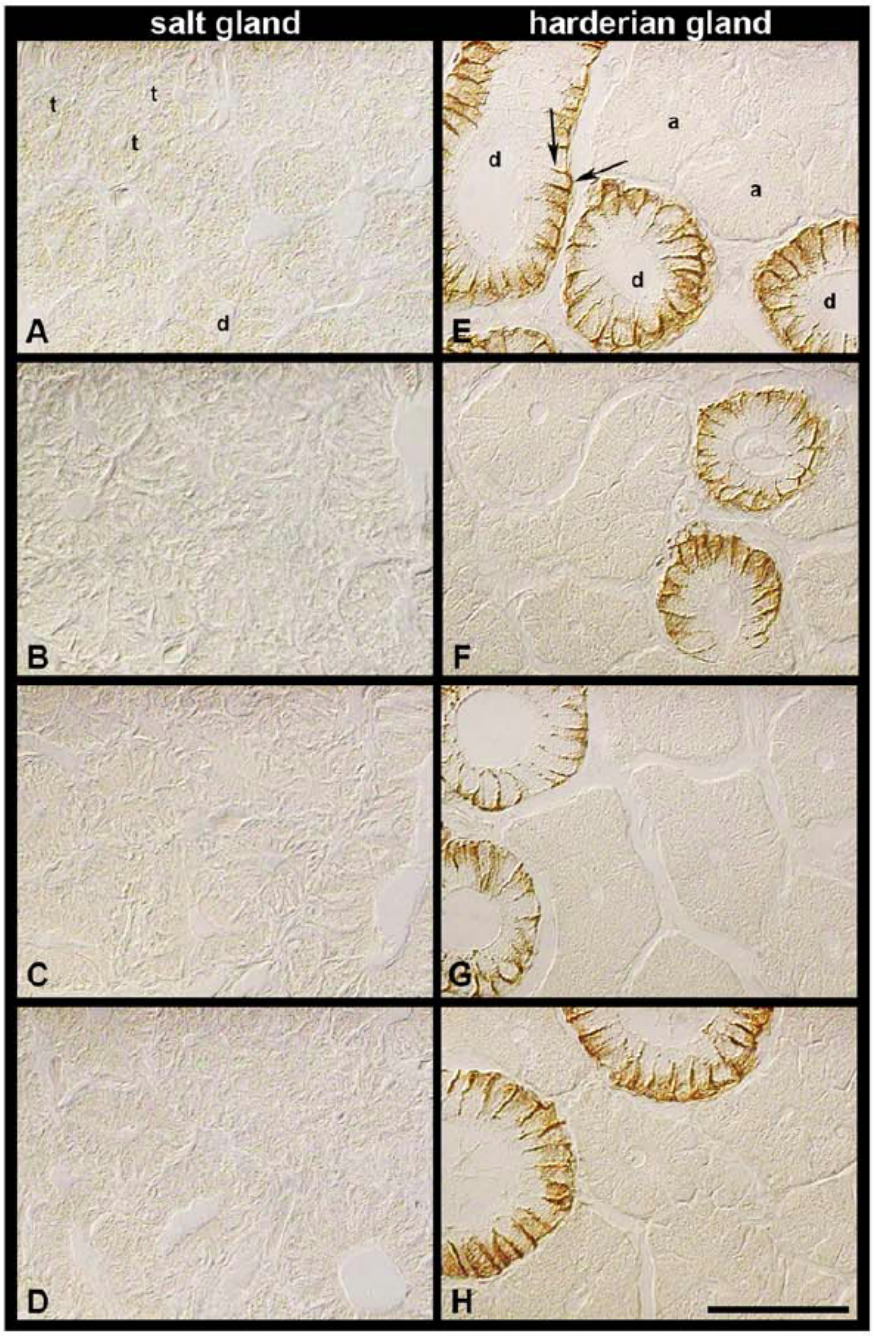

Figure 3-14. Immunolocalization of AQP3 in the salt gland (A-D) and harderian gland (E-H) of *L. semifasciata*. (A) AQP3 is absent from the ducts (d) and secretory tubules (t) of the salt gland and this did not change with treatment (compare B-D). (E) AQP3 is detected in the basolateral (arrows) membranes of the harderian gland ducts (d) but is absent from the secretory acini (a). The localization of AQP3 was not affected by treatment in the harderian gland either (compare F-H). Treatments: A,E – control; B,F – 0% SW; C,G – 50% SW; and D,H – 100% SW. Images produced via differential interference contrast microscopy. Scale bar = 50µm.

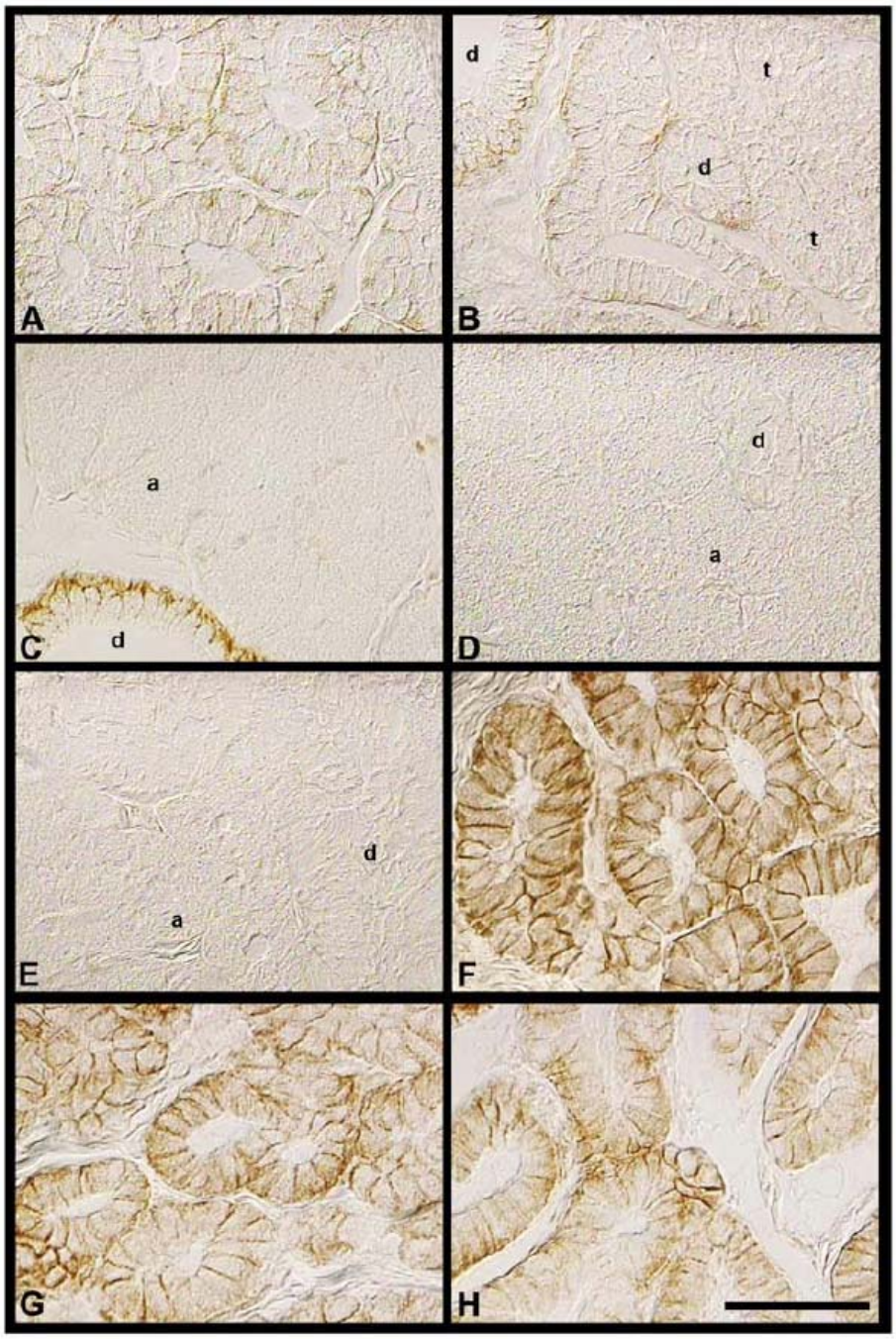

Figure 3-15. Immunolocalization of AQP3 in the cephalic glands of *N. c. clarkii*. AQP3 is expressed in the basolateral membranes of the duct (d) and acinar (a) cells in the premaxillary gland (A) and in the ducts cells (d) but not the tubule (t) or acinar (a) cells of the nasal (B) and harderian (C) glands. The duvernoy's (D) and supralabial (E) glands completely lack AQP3, while it is expressed throughout the cells of the infralabial (F), anterior sublingual (G) and posterior sublingual (H) glands. Images produced via differential interference contrast microscopy. Scale bar = 50μm.

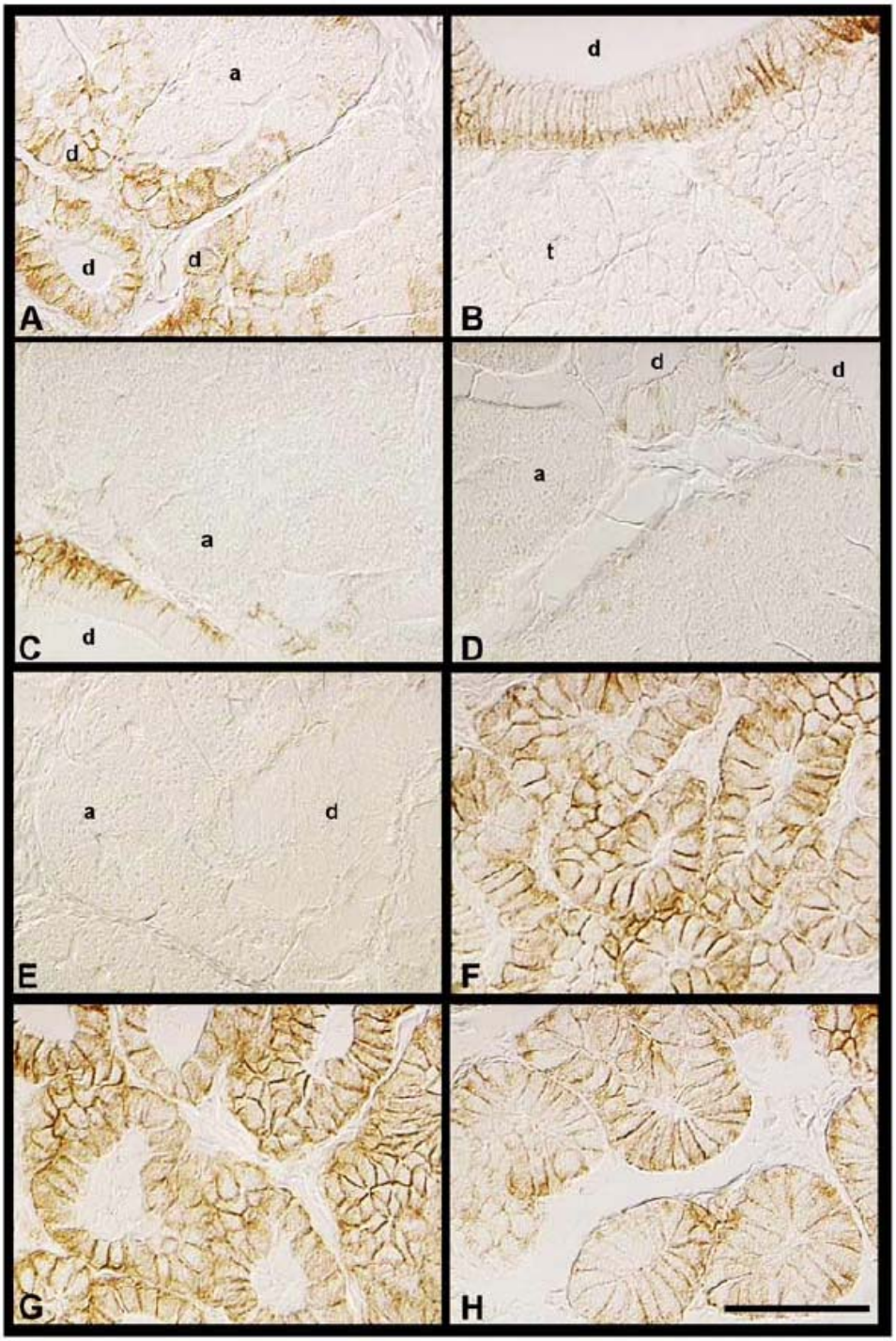

Figure 3-16. Immunolocalization of AQP3 in the cephalic glands of *N. fasciata.* AQP3 is basolateral in the ducts (d) of the premaxillary (A), nasal (B), harderian (C), and duvernoy's (D) glands and is absent from the acini (a)/tubules (t) of these glands and all cell types in the supralabial (E) glands. The infralabial (F), anterior sublingual (G), and posterior sublingual (H) glands are populated entirely by AQP3-expressing cells. Images produced via differential interference contrast microscopy. Scale bar = 50μm.

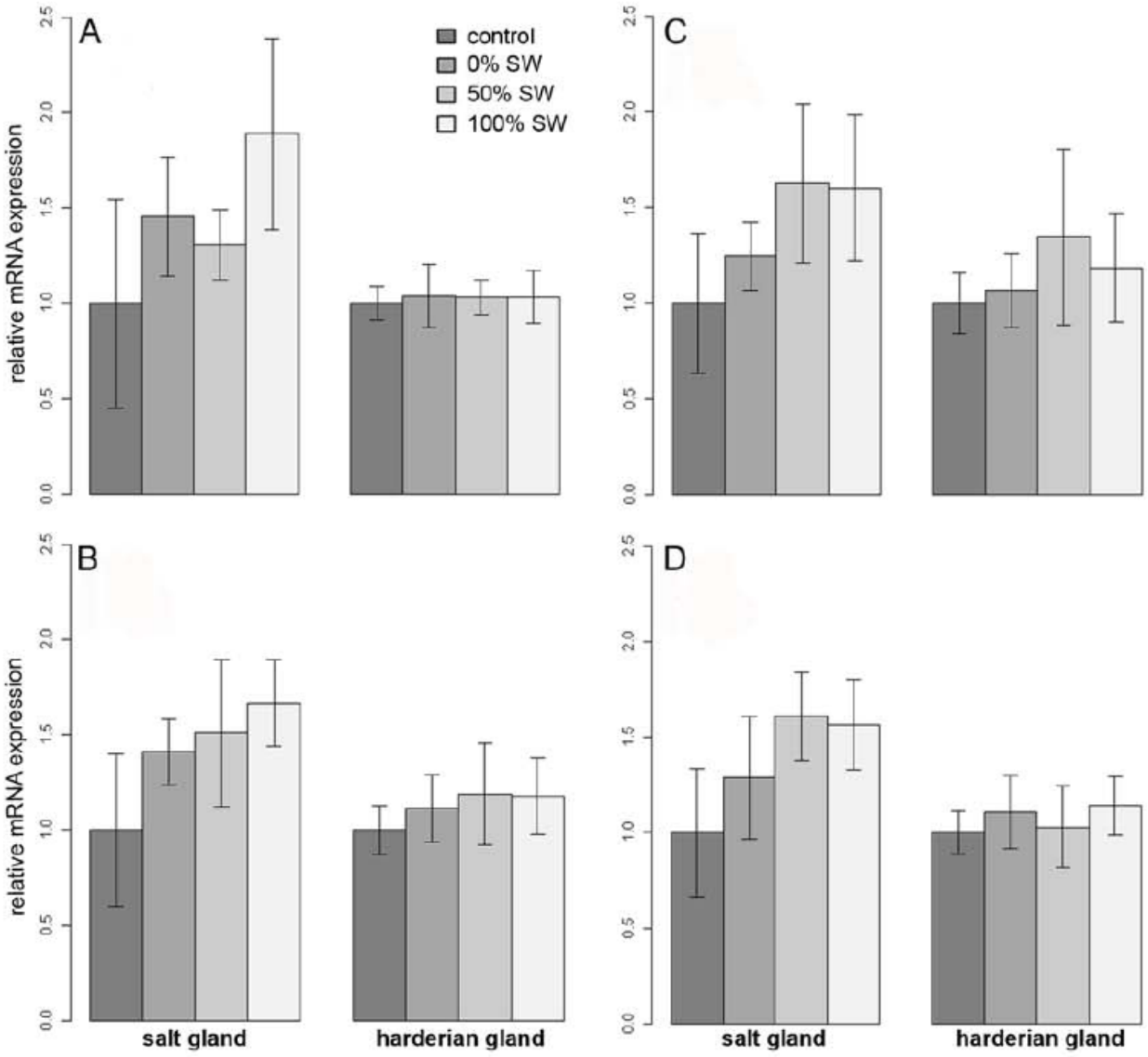

Figure 3-17. mRNA expression for (A) NKA, (B) NKCC1, (C) CFTR, and (D) AQP3 did not differ significantly across treatments in either the salt gland or the harderian gland of *L. semifasciata*. Log_{10} transformed expression values were normalized to log_{10}(EF1a1) and standardized to the control for each species/gene (see Materials and Methods for details). Data are presented as standardized mean ± scaled s.e.m.

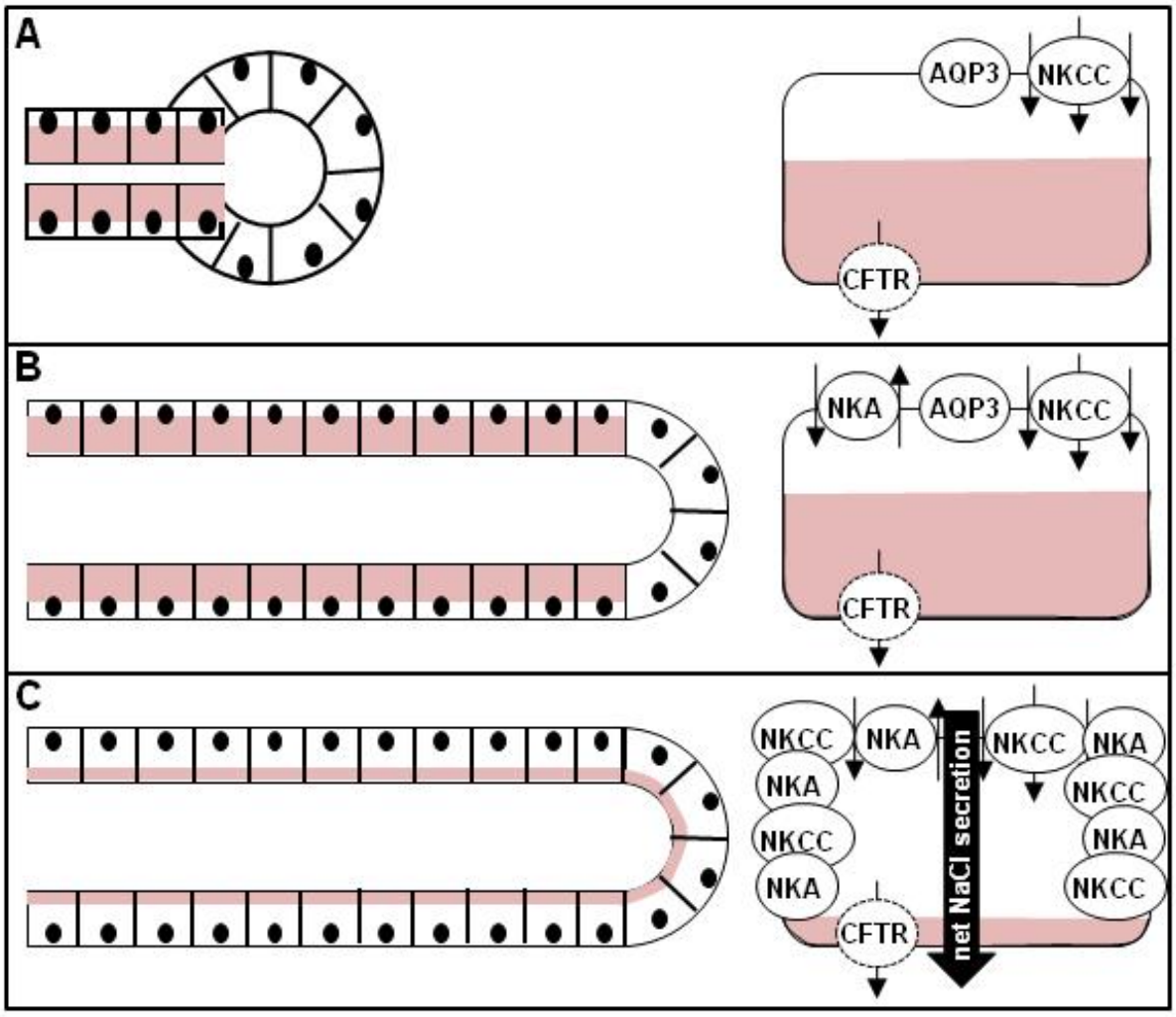

Figure 3-18. Schematic representation of the hypothesized steps in the co-option of a salt gland from an unspecialized precursor. (A) Beginning with an ancestral gland that was acinar or tubuloacinar and populated by cells with phenotype similar to those cells in the harderian gland of *L. semifasciata*, the earliest modifications (B) may have included elongation of the duct/tubule portion of the gland and an increase in the abundance of NKA in the basolateral membranes of these duct cells. (C) In the final stages of co-option, heterogeneity in cell type was lost or reduced as was the ability to secrete large amounts of neutral mucins (indicated by the portion of the cell shaded pink). This final stage was likely associated with loss of basolateral AQP3 from the secretory cells and further increases in abundance of NKA and NKCC. The hypothesized localization of CFTR in the apical membranes of the secretory cells is indicated by a dotted line.

CHAPTER 4
RENAL RESPONSES TO SALINITY CHANGE IN SNAKES WITH AND WITHOUT SALT GLANDS[1]

Renal Osmoregulation in Reptiles

The reptilian kidney has long been known to be incapable of eliciting urine hyperosmotic to the blood plasma (Dantzler, 1976; but, see: Yokota et al., 1985); purely renal regulation of NaCl, therefore, is thought to be insufficient for maintaining ion balance in reptiles inhabiting desiccating (e.g., marine/desert) environments. Despite this, both marine and desert environments are rich in reptile diversity, suggesting that reptiles integrate renal and various extra-renal osmoregulatory systems effectively. Notably, many marine and desert species possess salt glands for enhanced excretion of excess ions; yet, only few studies of reptiles have attempted to analyze renal function in species with and without salt glands, and clear correlations between possession of salt glands and kidney structure/function in reptiles remain to be examined. Though reptile kidney physiology has been studied for many decades, a recent review of reptile renal function (Dantzler and Bradshaw, 2009) reveals just how much remains to be discovered in the field of renal ion regulation.

Although reptilian kidneys are incapable of excreting urine significantly hypertonic to the blood plasma, many species are capable of modifying urine composition in response to environmental pressures (e.g., water diuresis). The ability of the reptilian kidney to modify urine composition likely derives from at least three important features of this tissue: (i) rate of filtration at the glomerulus, (ii) the heterogeneity of cell types

[1] Reprinted with permission from: Babonis LS, Miller SN, Evans DH. *In press*. Renal responses to salinity change in snakes with and without salt glands. J Exp Biol

populating the various segments of the nephron, and (iii) variation in the number of functioning nephrons (Dantzler and Bradshaw, 2009). Much like the nephron of mammalian kidneys, the reptilian kidney is comprised of several segments: the proximal tubule is connected to the distal tubule through a short intermediate segment and the distal tubule connects to the collecting duct through a connecting segment. Among snakes (and other squamates), the connecting segment is a sexually dimorphic structure (sometimes called the renal sex segment) thought to be involved in the seasonal production/modification of the seminal fluid (Cuellar et al., 1972). Results from studies of garter snakes (*Thamnophis sirtalis*) suggest that Na^+ and Cl^- are reabsorbed in both the proximal and distal segments of the snake nephron, a process that is thought to require active Na^+ and passive Cl^- transepithelial transport (Dantzler and Bradshaw, 2009). Among mammals, apical Na^+ uptake is modulated by the apical Na^+/H^+ exchanger (NHE) in the proximal tubule, a combination of NHE and the absorptive isoform of the $Na^+/K^+/2Cl^-$ cotransporter (NKCC2) in the loop of Henle, the Na^+/Cl^- symporter (NCC) in the distal tubule, and the epithelial Na^+ channel (ENaC) in the connecting tubules and collecting ducts. By contrast, the basal extrusion of Na^+ is facilitated by Na^+/K^+-ATPase (NKA) in all segments of the mammalian kidney (Kinne and Zeidel, 2009). Although early studies of renal function in snakes provide indirect evidence that some of the same ion transporters may regulate NaCl balance in reptiles as well (Beyenbach and Dantzler, 1978; Dantzler et al., 1991), to my knowledge, no studies have directly examined the distribution/abundance of these ion transporters in the kidneys of any reptile species. Further, the relationship between the

distribution/abundance of these transporters and environmental salinity has yet to be determined in any reptile species.

In concert with reabsorption of NaCl, modification of urine can be achieved through reabsorption of water from the filtrate. In many vertebrates, this process is stimulated primarily through the action of aquaporin (AQP) 1, in the proximal tubules, and AQP2, 3, and 4 in the distal tubules, connecting segments, and collecting ducts (Borgnia et al., 1999). Both AQP2 and AQP3 are known to be hormonally-regulated (via vasopressin) in mammals (Terris et al., 1996; Kinne and Zeidel, 2009), and a similar mechanism of regulation has been proposed for avian AQP2 (Lau et al., 2009) and amphibian AQP2 (Ogushi et al., 2007). Upon stimulation by vasopressin (or AVT, in birds and amphibians), AQP2 is mobilized from the cytoplasmic vesicles, where it is stored, to the apical membrane of the collecting duct cells, facilitating luminal passage of water into the cell (Nielsen et al., 1995). Water then exits the cell via the basolaterally located AQP3 (Sugiura et al., 2008; Kinne and Zeidel, 2009). While renal expression of AQP3 is restricted to the basolateral membranes of collecting duct cells in mammals and birds, its distribution among amphibians appears to extend into the distal tubules (Akabane et al., 2007; Mochida et al., 2008) and among fishes the localization of AQP3 remains equivocal (Cutler and Cramb, 2002). As reviewed by Dantzler (1976), the permeability of the distal tubule to water is quite variable among reptiles (and can also vary considerably with hydration status within a given species). Though some evidence suggests that the basolateral membrane of the distal tubule in snakes may in fact be quite permeable to water (Beyenbach, 1984), the potential role of AQP3 in regulating basolateral renal water transport in any reptile has yet to be studied.

Animals with an extra-renal means for secreting a concentrated NaCl solution might be expected to drink salt water and absorb NaCl across the gut, cloaca, and nephron epithelia (even when experiencing high environmental salinity) because they can effectively excrete the salt and retain the water. Those animals without such means, however, might be expected to minimize drinking and salt reabsorption across these epithelia since they are unable to excrete the excess salt. Furthermore, within a species, regulation of the renal mechanisms for NaCl absorption may be expected to vary with the salinity of the environment; the ways in which renal water economy is affected by aquaporins is entirely unknown among reptiles. Thus, the objectives of this study were to examine changes in the structure/function of snake kidneys, including changes in the localization and abundance of NKA, NKCC(2), and AQP3, after acclimation to 0% seawater (SW), 50% SW, and 100% SW (32 ppt). To determine if the structural/functional responses of the kidneys were related to the presence of an extra-renal site for salt excretion, I compared one marine species with a salt gland (*Laticauda semifasciata*; Reinwardt, 1837) to one marine species without a salt gland (*Nerodia clarkii clarkii*; Baird and Girard, 1853). To determine if kidney structure/function was related to habitat use, I compared two congeneric species lacking salt glands: one which inhabits marine environments (*N. c. clarkii*) and one which inhabits freshwater environments (*Nerodia fasciata*; Cope, 1895).

Methods

Animal Collection and Maintenance

Adult banded sea kraits (*L. semifasciata*; 497.4 ± 121.2 g initial mass) were collected by hand from Orchid Island, Taiwan, and housed individually in plastic aquaria in 100% seawater (SW; 32 ppt) prior to the beginning of the experiment. Aquarium

water was mixed fresh daily using Instant Ocean (Spectrum Brands, Inc., Madison, WI, USA) and tapwater from National Taiwan Normal University (Taipei, Taiwan) and changed daily. For the first five days in the lab, all animals were acclimated in 100% SW at room temperature (RT; 29.67 ± 0.62˚C). At the end of this five-day period, control animals (N = 6) were selected randomly and sacrificed. The remaining animals were assigned to one of three treatments: 0, 50, or 100% SW (N = 6, per treatment). To assess the response of kidney structure/function to these defined salinity treatments and to avoid the response to salinity shock (from direct transfer), I reduced the salinity of the cage water in small increments over a period of seven days until animals reached their final treatment salinity. Animals from all three treatments were then held in their final salinities for one week before being sacrificed by rapid decapitation, as outlined in the American Veterinary Medical Association's Guidelines on Euthanasia. Throughout the experiment, animals were fasted and maintained in enough water such that they could rest, submersed, on the bottom of the cage while still being able to reach the surface easily for respiration. In accordance with the guidelines of the University of Florida's Institutional Animal Care and Use Committee, animals were blotted dry and weighed (± 0.1 g) daily throughout the duration of the experiment, and cage water salinity was checked daily using either an Atago S/Mill refractometer (Tokyo, Japan) or a YSI 85 salinity meter (Yellow Springs, OH, USA). As in previous studies (Pettus, 1963; Dunson, 1980; Winne et al., 2001), rate of "dehydration" was determined as the percent loss of initial body mass per day for each individual.

Adult salt marsh snakes (*N. c. clarkii*; 118.8 ± 79.7 g) were collected from Seahorse Key, FL (Levy Co.; permit #05-012) and adult banded watersnakes (*N.*

fasciata; 136.3 ± 95.2 g) were collected from public roadways near Paynes Prairie, FL (Alachua Co.). Because *N. fasciata* was expected to be highly intolerant of 100% SW, I modified the design outlined above such that the control animals for both species of *Nerodia* were held in 0% SW (Gainesville, FL tapwater) for the lab acclimation period (room temperature: 23.23 ± 0.65˚C). As above, control animals (N = 5, per species) were sacrificed after the lab acclimation period, and the remaining animals were assigned to the indicated treatments (N = 5 per treatment, per species).

Tissue Preparation and Serum Analysis

Whole trunk blood was collected in unheparinized tubes within one minute of decapitation and centrifuged immediately to separate serum. Hematocrit was estimated as the percent of the total volume in the tube composed of red blood cells. Serum was then removed to a clean, unheparinized tube, snap frozen in liquid nitrogen, and stored at -80˚C prior to analysis. Total osmolality was measured on 10 µl triplicates of thawed serum using a Vapro 5520 vapor pressure osmometer (Wescor, Logan, UT, USA). Individual electrolytes were measured on 125 µl samples using a Stat Profile pHOx Plus C machine (Nova Biomedical, Waltham, MA, USA). The right kidney was also removed from each animal following sacrifice and immediately fixed in 4% paraformaldehyde for 24 h at 4˚C. Tissues were then washed three times (15 min each) in 10 mM phosphate buffered saline (PBS). Fixed/washed tissues were stored at room temperature in 75% ethanol before being embedded in paraffin wax, sectioned, and mounted on charged slides as previously described (Chapter 2).

Histology/Immunohistochemistry

To examine the morphology of the kidneys (organization of tubules, distribution of blood vessels, etc) I used the Lillie (1940) modification of the Masson Trichrome

technique (Humason, 1972). Additionally, because the secretion of acidic mucosubstances from the distal segments of the snake nephron is thought to protect the nephron epithelium from damage caused by the passage of colloids/organic osmolytes (More, 1977), I examined changes in the secretion of mucins and/or their precursors (glycogen), by pairing the Alcian blue (AB) technique with a modified Periodic Acid Schiff (PAS) technique. Sections stained with AB were counterstained by incubation for 30s in Nuclear Fast Red (Humason, 1972) and those stained with PAS were counterstained in hematoxylin, as previously described (Chapter 2).

To localize NKA, NKCC, and AQP3, I used the immunohistochemical techniques as described previously (Chapter 2). Briefly, after blocking endogenous peroxidases and non-specific proteins, I incubated tissue sections with anti-NKA (1/100), anti-NKCC (1/1000), or anti-AQP3 (1/500) overnight at 4˚C. All antibodies were diluted in Protein Block (BioGenex, San Ramon, CA, USA). Sections were rinsed of primary antibody and prepared for visualization using BioGenex's Supersensitive™ Link-Label universal secondary antibody kit with a DAB (3, 3'-diaminobenzidine tetrahydrochloride) chromagen. Negative controls were produced by incubating sections in BioGenex Protein Block rather than primary antibody, and positive controls were produced via Western blotting (for NKA and NKCC; see below) or by peptide preabsorption (AQP3). To preabsorb anti-AQP3, primary antibody was incubated in approximately 200-fold molar excess of peptide while shaking at 4˚C overnight (Pandey et al., 2010). Enough BioGenex Protein Block was then added to bring anti-AQP3 to a final concentration of 1/500 before use. A minimum of three individuals per treatment were examined for each species.

Primary Antibodies

Monoclonal anti-NKA (α5), developed by Dr. Douglas Fambrough, and monoclonal anti-NKCC (T4), developed by Drs. Christian Lytle and Bliss Forbush III, were obtained from the Developmental Studies Hybridoma Bank developed under the auspices of the National Institute of Child Health and Human Development and maintained by The University of Iowa, Department of Biological Sciences, Iowa City, IA 52242. While anti-NKA is directed against the α1 subunit of the NKA heterodimer (Takeyasu et al., 1988), anti-NKCC is directed against a conserved epitope in the carboxyl tail of NKCC1, NKCC2, and NCC (Lytle et al., 1995). Anti-AQP3 (Hc-3) and its blocking peptide were generous gifts from Dr. David Goldstein at Wright State University (see: Pandey et al., 2010 for epitope).

Western Blotting

Frozen kidneys were homogenized on ice and prepared for electrophoresis using the methods previously described (Chapter 2). I then electrophoresed 25 ug of total protein in 10% Tris-HCl polyacrylamide Redi-gels (Bio-Rad, Hercules, CA, USA) before transferring proteins to polyvinylidine fluoride membranes for blot analysis (Bio-Rad). Dry blots were rehydrated in 100% methanol and rinsed in de-ionized (DI) water before blocking in a solution of 5% non-fat dry milk in tris-buffered saline (TBS; 25 mmol/L tris, 150 mmol/L NaCl; pH 7.4) for 2 h at RT while shaking. Following the blocking step, blots were incubated in anti-NKA or anti-NKCC overnight at RT while shaking. Primary antibody was removed in three washes with TTBS (TBS with 0.1% Tween-20; pH 7.4) before blots were incubated in alkaline-phosphatase conjugated goat anti-mouse IgG (1/3000 diluted in blocking solution) while shaking for 1 h at RT. Secondary antibody was removed from the blots with three washes in TTBS before Immun-Star alkaline

phosphatase-conjugated chemiluminescent signal (Bio-Rad) was applied, following the manufacturer's protocol. Following analysis, each blot was stained with 0.02% Coomassie blue stain (diluted in 50% methanol, 40% water, and 10% acetic acid) to visualize total protein. All blot images were scanned and digitized for analysis and brightened using Photoshop CS3 (Adobe, San Jose, CA, USA).

RNA Preparation, Cloning, and Sequencing

I followed the protocol of Choe et al. (2005) for the molecular techniques. In short, total RNA was extracted from RNA*later* (Ambion, Woodward Austin, TX, USA) fixed tissues using Tri-Reagent (Sigma, St. Louis, MO, USA), quantified and checked for purity using a micro-volume spectrophotometer (Nanodrop ND-1000, Thermo Scientific, Wilmington, DE, USA), and cDNA was synthesized from mRNA using oligo-dT primers and the Superscript III reverse-transcription kit (Invitrogen, Carlsbad, CA, USA). Degenerate primers were designed to amplify NKA, NKCC2, and AQP3 in all three taxa using the CODEHOP online primer design software (Rose et al., 2003). Amplification was accomplished using standard PCR cycles for 0.5 µl oligo-dT cDNA and Ex-taq Hot Start DNA Polymerase (Takara Bio, Madison, WI, USA) in an Express thermocycler (ThermoHybaid, Franklin, MA, USA). Amplicons were then transfected into PCR®-4 TOPO vectors and transformed into TOP10 chemically competent cells using the TOPO-TA cloning kit for sequencing (Invitrogen). Plasmids were sequenced in both directions by the Marine DNA sequencing facility at the Mount Desert Island Biological Laboratory (Salisbury Cove, ME, USA) and the resulting species-specific sequences were used to design primers for all other applications (see Table 4-1 below). Quantitative real-time PCR (qRT-PCR) primers were designed to amplify an amplicon of ~100-150 bp and tissue distribution primers amplified an amplicon of ~450 bp using the

Primer-3 Plus online primer design software (Untergasser et al., 2007). All specific sequences were deposited in GenBank (see Table 4-2 for accession numbers.)

Quantitative Real-time PCR and RACE PCR

To examine changes in the abundance of NKA, NKCC2 and AQP3 mRNA across treatments, I performed qRT-PCR, as has previously been described (Choe et al., 2005). In brief, I loaded 24 µl triplicates of reaction mixture (1 µl of 1/10 diluted cDNA, 7.4 pmol specific primers, and SYBR® Green Mastermix; Applied Biosystems, Foster City, CA, USA) into 96-well optical plates (BioRad) and PCR-amplified using an I-cycler IQ thermocycler (Bio-Rad) and the following cycling protocol: step 1 - 95˚C for 10 min (initial denaturing step), step 2 - 95˚C for 35 s, 60˚C for 30 s, 72˚C for 30 s (repeat for a total of 40 cycles), step 3 - melting curve analysis (to ensure amplification of only a single product) . Each plate also contained 24 µl triplicates of a 5-point dilution series, which was mixed fresh for each use from a mixed sample of species-specific, undiluted cDNA. No-template control reactions, lacking cDNA, and negative control reactions, made with pre-reverse transcription RNA rather than cDNA, were amplified using the preceding procedure to ensure amplification was either absent or occurred at >10 cycles later than the latest cycle of amplification for target DNA. To ensure specificity of amplified products, a random selection of samples from each plate were extracted, sequenced, and identity-searched using BLAST (NCBI, Bethesda, MD, USA).

To determine the sequence of a full-length mRNA for AQP3, I amplified both the 5' and 3' ends of the AQP3 transcript, from *Laticauda semifasciata* (lsAQP3), following the manufacturer's protocol for the GeneRacer kit (Invitrogen). Specific RACE primers were designed using Primer-3 Plus.

AQP3 Sequence Analysis

Nucleotide comparisons were made using the coding sequence only for lsAQP3 and the blastn algorithm. Predicted amino acid sequences were compared using the tblastn algorithm. For comparisons of *Laticauda* and *Anolis*, I used NCBI's bl2seq function with the blastn (nucleotide) or blastp (amino acid) algorithm. Accession numbers: *Anolis carolinensis* (ENSACAT00000012739), *Gallus gallus* (XM_424500.2), *Homo sapiens* (NM_004925.3), and *Hyla chrysoscelis* (DQ364245.1).

Semi-quantitative Duplexing PCR

To examine the distribution and relative abundance of AQP3 across snake tissues, I extracted RNA as described above from the brain, duodenum, esophagus, harderian gland, kidney, liver, lung, muscle (skeletal), pancreas, salt gland, stomach, and testis of *L. semifasciata*. cDNA was then reverse transcribed from total RNA using random hexamer primers (Superscript III kit, Invitrogen). Specific primers were designed to amplify a 450 bp long amplicon of AQP3 and duplexing PCR was then performed by amplifying cDNA in the presence of both AQP3 specific primers and control primers (Quantum RNA™ 18S internal standard primer kit; Ambion, Woodward Austin, TX, USA). To ensure accurate representations of relative cDNA abundance, reactions were terminated in the exponential phase of the PCR protocol. Consistency in 18S amplification across tissues indicates low variability in cDNA quality and quantity across tissues. To visualize amplicons, PCR products were electrophoresed at 60 V in a 2% agarose gel, stained with ethidium bromide, and digitized using the Gel Doc™ XR system (Bio-Rad). Negative control reactions were prepared with RNA rather than cDNA for each tissue.

Statistical Analysis

Average rates of daily mass loss, serum electrolytes (including total osmolality), hematocrit, and mRNA expression values were compared among species and treatments using ANOVA with the Tukey HSD post-hoc test. For qRT-PCR analysis, cycle threshold values were compared at the arbitrary threshold position of 100 using the MyIQ Optical System software version 1.0 (BioRad). Expression values for samples loaded onto each plate were adjusted to the standard curve run on the same plate and log-transformed to homogenize variance. Transformed expression values were then normalized to the expression value for the reference gene: ribosomal protein L8, chosen because it was invariant across treatments (L. S. Babonis, unpublished). These normalized gene expression values were then standardized to the control treatment for each species (thus, mRNA expression values for the control treatment will always appear as 1.0). Error estimates were calculated from the log transformed data and rescaled to the standardized mean. All analyses were performed in the R statistical environment (R Development Core Team, 2008).

Results

Body Mass and Survival

There was no effect of treatment on rate of mass loss in any of the three species examined (Table 4-3). Furthermore, mass loss in *N. c. clarkii* (the marine watersnake) did not differ from mass loss in *N. fasciata* (the freshwater watersnake) in any treatment, though total mass loss (calculated as a percentage of initial body mass) was considerably more variable (see standard deviations in Table 4-3) in these two species in all treatments than in *L. semifasciata* in any treatment. Both *N. c. clarkii* and *N. fasciata* lost more mass per day in 100% seawater than did *L. semifasciata* (the sea

snake) in 0% SW but perhaps more interestingly, *N. fasciata* lost mass at a greater rate in 0% SW than did *L. semifasciata* in all treatments. Because rates of mass loss were not different in the freshwater and saltwater treatments for any species, I consider these rates to reflect merely the effect of fasting rather than dehydration.

Survival differed among treatments for *N. fasciata* only. Whereas *L. semifasciata* and *N. c. clarkii* were found to have 100% survival in all three treatments, among *N. fasciata* survival decreased from 100% in 0% SW to 80% in 50% SW and 60% in 100% SW.

Serum Electrolytes and Hematocrit

For each species, treatment means were compared to the mean value for the species-specific control group to determine if there was an effect of salinity on serum. Total osmolality was not affected by treatment in *L. semifasciata*. For *N. c. clarkii*, total osmolality decreased in the 0% SW group ($p = 0.026$, relative to control) and in *N. fasciata* it increased in the 50% SW group ($p = 0.014$, relative to control) (Fig 4-1A). Conversely, *L. semifasciata* experienced a decrease in both Na^+ ($p = 0.028$) and in K^+ ($p = 0.019$) in the 0% SW treatment, while Na^+ and K^+ levels in *N. c. clarkii* and *N. fasciata* did not differ significantly among treatments (Fig 4-1B,C). Cl^- levels were not affected by treatment in *L. semifasciata* or *N. c. clarkii* but exhibited an increase in both the 50% SW ($p = 0.003$) and the 100% SW ($p = 0.041$) treatments among *N. fasciata* (Fig 4-1D). Though hematocrit levels (not measured in *L. semifasciata*) did not differ among treatments for either *N. c. clarkii* or *N. fasciata* (Fig 4-2), the values I obtained for both *N. c. clarkii* and *N. fasciata* through this experiment were similar to published values for these species and their marine and freshwater congeners (Pough, 1979; Dunson, 1980).

Anatomy/Histochemistry

Using histology, I examined the cell types populating each segment of the snake nephron (Fig 4-3). Originating at the glomerulus, the neck segment is characterized by low cuboidal cells with very little cytoplasm. Filtrate passes through the neck segment to the proximal tubule, which is characterized by relatively large cells, with centrally positioned nuclei, surrounding a lumen that can vary in size from essentially collapsed (Pc in Fig 4-3A) to quite open (Po in Fig 4-3B). Following the proximal tubule is the relatively short intermediate segment, typified by low cuboidal cells, organized around a relatively small lumen (Fig 4-3A). The distal tubule follows the intermediate segment and is comprised of two sub-segments. The early distal tubule (De) is comprised of cells that are intermediate in size between those of the intermediate segment and those of the proximal tubule, and has nuclei that are positioned basally and often appear flattened against the basal membrane (Fig 4-3A). Cells in this sub-segment appear to have more cytoplasm than those of the intermediate segment and the shape of the cell appears more rounded at the apical margin than cells from other segments. By contrast, the cells of the late distal tubule (Dl) are much more regular in shape and have basally-positioned round nuclei (Fig 4-3B).

The connecting tubule (hereafter referred to as the renal sex segment) is sexually dimorphic, appearing engorged with secretory granules in the males (so much so that the lumen is often not visible; Fig 4-3B,C). In females, this segment often resembles that of the proximal tubule but with flatter and more basally positioned nuclei. This segment is also relatively short in females, being confined only to the outer margins of the kidney (near the collecting ducts). Though many hypotheses about the function of the renal sex segment have been proposed (Cuellar et al., 1972, and references

therein), this segment does not appear to contribute to water or ion balance and will not be considered further in this study. At the distal end of the renal sex segment is a short (often <20 cells in length) segment connecting the renal sex segment to the primary collecting duct (Fig 4-3C). This connecting segment is similar in appearance to the primary collecting duct (columnar cells with basal, flattened nuclei) and, often, can be distinguished from primary collecting ducts only by their smaller diameter (Fig 4-3D). Primary collecting ducts from each nephron eventually join with other primary collecting ducts to become secondary collecting ducts (Fig 4-3D), which merge to form the ureter (Fig 4-3E,F). The primary and secondary collecting ducts and the ureter are distinguishable only by the diameter of their lumena.

There was no effect of salinity on the secretion of mucus/glycogen in the kidneys of any of the three species examined (Fig 4-4). In *L. semifasciata*, AB^+ material was detected only at the apical margin of the cells comprising the distal tubules (early and late), the connecting segments, and the collecting ducts (Fig 4-4A-E). This pattern was consistent in both *N. c. clarkii* (Fig 4-4F-J) and *N. fasciata* (Fig 4-4K-O), however, unlike *L. semifasciata*, the distribution of AB^+ material in the early distal tubules of the *Nerodia* was diffuse, extending all the way through the basal cytoplasm of the cell. Similarly, I detected PAS^+ material in the apical margins of the distal tubules, connecting segments, and collecting ducts of all three species yet no effect of treatment in any of them (Fig 4-5). The basement membranes of the nephrons (especially around the renal sex segment) and the apical membrane of the proximal tubule were also PAS^+ in all three species.

Immunolocalization and Primary Antibody Specificity

NKA localized to the basolateral membranes of the distal tubules (early and late), the connecting segments, and the collecting ducts of all three species (Fig 4-6). Early distal tubules often exhibited strong staining in the basal membrane and only faint staining of the lateral membranes whereas late distal tubules exhibited prominent staining in both basal and lateral membranes (compare De and Dl in Fig 4-6J). There was no effect of treatment on the localization of NKA in any of the three species examined (Fig 4-6C-E, H-J, and M-O). NKCC was undetectable in the kidney from any of the three species studied (Fig 4-7). AQP3 localized to the basolateral membranes of the connecting segments and collecting ducts of all three species (Fig 4-8B, G, L); this protein was also detected in the apical membrane and subapical cytoplasm of the late distal tubules in *L. semifasciata* (Fig 4-8A) but was absent from these tubules in *N. c. clarkii* (Fig 4-8F) and *N. fasciata* (Fig 4-8K). The localization of AQP3 did not vary with treatment in any of the three species examined (Fig 4-8C-E, H-J, and M-O).

The specificity of anti-NKA (α5) and anti-NKCC (T4) for their target proteins has already been verified via Western blotting for *L. semifasciata* (Chapter 2). Here, I further demonstrate specificity of α5 for a protein of approximately 110 kDa in both *N. c. clarkii* and *N. fasciata* (Fig 4-9). When kidney homogenates were probed with T4, no proteins were detected in any of the three species (data not shown). Whether this suggests an affinity of T4 for NKCC1 (which is far less abundant than the absorptive isoform, NKCC2, in the vertebrate kidney; Russell, 2000) or extremely low abundance of NKCC1/NKCC2/NCC in the kidney of these three species cannot be evaluated at this time. Though I was unable to confirm specificity of the AQP3 antibody (Hc-3) through Western blot analysis, peptide pre-absorption of Hc-3 completely abolished staining

from the distal tubules of *L. semifasciata* (Fig 4-10A) and the connecting segments/collecting ducts of all three species (Fig 4-10B-D).

mRNA Abundance

I found only minor effects of treatment on mRNA expression (Fig 4-11). mRNA expression for NKA was variable but not statistically different among treatments in any of the three species examined. In *L. semifasciata*, AQP3 abundance was approximately twice as high in the 0% SW treatment as in the 50% or 100% SW treatments ($p = 0.013$; Fig 4-11A). There was no effect of salinity on AQP3 in either *N. c. clarkii* or *N. fasciata*. NKCC2 expression was higher in the 50% SW treatment than in the 0% SW treatment for *N. c. clarkii* only ($p = 0.048$; Fig 4-11B). There was no effect of salinity on mRNA expression for NKA, NKCC2, or AQP3 in *N. fasciata* (Fig 4-11C).

Sequence Analysis of lsAQP3

I sequenced the full-length mRNA transcript from *L. semifasciata* and compared both the predicted amino acid and nucleotide sequences of lsAQP3 with that of *Hyla chrysoscelis* (the species against which the Hc-3 antibody was made) as well as *Anolis carolinensis*, *Gallus gallus*, and *Homo sapiens* (Table 4-4). When comparing amino acid sequences, lsAQP3 shared the highest percent identity with AQP3 from *Anolis* (85% identical); percent identities between lsAQP3 and AQP3 from *Gallus*, *Hyla*, and *Homo* were all very similar (81-82%). Nucleotide sequences showed slightly lower congruence but lsAQP3 still shared the highest similarity with AQP3 from *Anolis*. Importantly, lsAQP3 was determined to have both NPA motifs (a defining characteristic of aquaporins) as well as the conserved Lysine (D) residue ~50 amino acids upstream of the second NPA motif (Fig 4-12), confirming it is a member of the glycerol transporter subgroup of aquaporins (Zardoya and Villalba, 2001).

Duplexing PCR/Tissue Distribution of lsAQP3

lsAQP3 was detected in all tissues examined, though expression was notably low in brain, liver, and pancreas (Fig 4-13A). Intermediate expression was detected in the kidney, skeletal muscle, and testis, and relatively high expression was detected in the duodenum, esophagus, harderian gland, lung, salt gland, and stomach. No amplification occurred in the negative control (Fig 5-4-13B).

Discussion

The ability of some species of snake to inhabit marine environments without the aid of a specialized salt gland has been well-documented; however, the mechanisms by which these animals carry out water/ion regulation are unknown. Both of the marine species studied herein (*L. semifasciata*, the sea snake, and *N. c. clarkii*, the marine watersnake) appear to have been largely unaffected by changes in environmental salinity. Survival was 100% in all treatments for each of these species and three metrics of plasma ion homeostasis (total osmolality, K^+, and Cl^-) were robust to increases in salinity in these species as well (Fig 4-1). Together, these observations suggests either of two things: (i) the acclimation period was not long enough to induce salinity stress/elicit an osmoregulatory response in the two marine species, or (ii) these animals utilized some mechanism to keep plasma ion levels low while experiencing increases in environmental salinity. By contrast, survival among *N. fasciata* (the freshwater watersnake) decreased with an increase in salinity and both total osmolality and Cl^- ion concentration increased with salinity. Though total osmolality in 100% SW was not significantly different from the 0%SW treatment, this likely reflects the reduction in sample size due to death of two of the animals in this treatment. Because Cl^- ion concentration was also significantly elevated in both the 50% SW and 100% SW groups

and there was a trend toward increased Na^+ in these groups as well (though these groups were not statistically different from the 0% treatment) the increase in total osmolality in *N. fasciata* seems to be a result of inadequate NaCl regulation. These results suggest that further investigation into the specific mechanisms by which *N. c. clarkii* maintains low serum Na^+ and Cl^- concentrations may reveal the functional differences underlying variation in salinity tolerance among marine and freshwater watersnakes.

To determine if elevated Na^+ and Cl^- levels in *N. fasciata* from the 50% and100% SW groups were a result of increased ion intake or a reduction in plasma water (indicating dehydration), I examined both rates of mass loss and changes in hematocrit across treatments. Average rates of mass loss in *L. semifasciata* and *N. fasciata* were similar to those previously reported for these species (Dunson, 1978; Lillywhite et al., 2009), whereas estimates in *N. c. clarkii* were slightly higher than previously reported (Pettus, 1963; Dunson, 1980). Among-individual variation in average daily mass loss was very high in both species of *Nerodia*, likely reflecting the large overall range in body mass in these two species, and mass loss did not differ among treatments in any of the species examined. Furthermore, hematocrit neither differed across treatments in either species, nor differed between *N. c. clarkii* and *N. fasciata* in any treatment (Fig 4-2). Because rate of mass loss did not differ with the salinity of the environment, these results are likely a result of fasting during the experiment rather than dehydration. It is important to note that previous studies of salinity acclimation in marine snakes have suggested that these animals cannot maintain water balance while fasting (Dunson and Robinson, 1976). Because some amount of both water and salt are likely taken up orally

(indeed, in all species examined - marine, estuarine, and freshwater – the majority of Na^+ influx occurs orally; Dunson and Robinson, 1976), the osmoregulatory stress experienced by wild animals may not be easily extrapolated from these results. Future tests of the effects of salinity on water and ion balance in these and other species should make explicit comparisons of fasted and fed animals to determine, for example, the effect of access to prey on survival times of *N. fasciata* in salt water.

Early studies of water and ion balance in reptiles suggest that the transport properties of the integument may vary with habitat type (Dunson and Robinson, 1976; Stokes and Dunson, 1982). Specifically, *N. fasciata* and other freshwater species are known to experience greater Na^+ influx than efflux and greater water efflux than influx but this pattern is reversed in *N. c. clarkii* and other marine species (Dunson, 1978). Thus, the increases in serum osmolality among *N. fasciata* may also be explained by the relatively greater influx of ions across the skin. It was surprising, however, to find that rates of mass loss observed in this study were not higher in *N. fasciata* than either *N. c. clarkii* or *L. semifasciata*. One possible explanation for the lack of differences among rates of mass loss is that the freshwater watersnakes used in this study in fact did undergo relatively higher rates of mass loss (similar to those observed by Dunson, 1978) but that this loss was balanced by water intake via drinking. If true, this scenario could also explain the relative increases in the concentration of Na^+ and Cl^- ions in the blood of *N. fasciata* without dramatic reductions in body mass.

Among fishes, kidney morphology has been shown to vary with habitat use, extreme examples of which include nephrons that completely lack glomeruli, proximal tubules, or distal tubules (see references in: Evans and Claiborne, 2009). Although

limited examples of aglomerular nephrons have been reported among squamates as well (Dantzler and Bradshaw, 2009), I find no evidence for a correlation between nephron morphology and habitat use among the species examined in this study. In fact, the only morphological variation evident among individuals in these experiments was the previously described sexual dimorphism in the renal sex segment. These observations suggest that differences in the osmoregulatory ability of the kidney across species are likely reflected in the physiology (and perhaps the microanatomy) of the kidney, rather than in the gross differences seen among the Osteichthyes.

As a first indication of the effect of salinity on kidney function, I examined the kidneys of all three species for changes in the production/secretion of mucosubstances. I find no evidence for increased secretion of mucus (no change in the expression domain of AB^+ material across treatments in any of the species; Fig 4-4) and no evidence for the upregulation of the muco-synthesis pathway (no change in the domain of expression of PAS^+ material across treatments; Fig 4-5). These results suggest that either these animals do not secrete increased amounts of mucus in concert with increased osmolyte excretion or that these animals did not undergo increases in osmolyte excretion coincident with these treatments. It is interesting to note, however, the general observation that AB^+ material appeared to be more abundant in the distal tubules of *N. fasciata* from all treatments than in *L. semifasciata* from any treatment. Functional studies of changes in the organic components of urine composition as well as studies aimed at understanding the integration of renal and post-renal mechanisms of urine modification in species from marine and freshwater environments would be very interesting in this context.

Using a combination of histology and immunohistochemistry, I demonstrate a basolateral localization of NKA in the distal tubules, connecting segments, and collecting ducts of all three species (Fig 4-6). Previous studies demonstrating ouabain-inhibited Na^+ reabsorption in the distal tubules of snake kidneys (Beyenbach and Dantzler, 1978) support this finding. Though I was unable to detect NKA in the proximal tubule using immunohistochemistry, previous studies of proximal tubule membrane transport in snakes suggest that NKA may be present in the basolateral membrane of this tubule as well (Dantzler, 1972; Benyajati and Dantzler, 1988). Given that Na^+ reabsorption from filtrate is likely facilitated in the proximal tubule by the presence of an apical Na^+/H^+ exchanger (Dantzler et al., 1991), and that K^+-activated p-nitrophenylphosphatase (the enzyme responsible for the dephosphorylation of NKA) has been localized to the basolateral membrane of this tubule (Benyajati and Dantzler, 1988), these results likely reflect low abundance of NKA in the proximal tubules of these species (relative to other renal tubules in these species), rather than absence. In contrast with what is known about Na^+ transport in snake distal tubules, ouabain has been shown to be ineffective at inhibiting fluid reabsorption in the proximal tubule (Dantzler and Bentley, 1978), suggesting that Na^+-independent fluid absorption may be occurring in this tubule as well. Finally, the localization of NKA did not change with treatment in any of the three species examined but this was not surprising since previous studies of the effects of diuresis on renal function in watersnakes have suggested that changes in total solute secretion are a result of changes in the number of functioning nephrons rather than changes in nephron membrane physiology (Lebrie and Sutherland, 1962).

Early studies of AVT-induced anti-diuresis in watersnakes demonstrated increased tubular reabsorption of Na^+ and K^+ upon stimulation by AVT (Dantzler, 1967a), a process which, in mammals, is mediated by apical NKCC2 in the proximal tubules (Giménez and Forbush, 2003). Further studies by Beyenbach and Dantzler (1978) identified a transepithelial K^+ flux in the distal tubule of *Thamnophis* (the garter snake) that was inhibited by ethacrynic acid (a known NKCC2 inhibitor). Considering that NKCC2 is also expressed in the apical membranes of the proximal tubules in birds (Nishimura and Fan, 2002) and in the apical membranes of the distal tubules in both fishes (Katoh et al., 2008) and amphibians (Guggino et al., 1988), it was surprising that NKCC was not detectable in the kidneys of any individuals in this experiment (Fig 4-7). Because anti-NKCC (antibody T4) has been demonstrated previously to react with the NKCC1 isoform in the salt gland of *L. semifasciata* (Chapter 2), it is unlikely that these negative results represent a methodological anomaly. Thus, studies aimed at assessing the effects of furosemide (another known inhibitor of NKCC2) on ion reabsorption as well as those aimed at understanding the distribution of putative AVT receptors in reptilian kidneys would be very informative in unraveling the mechanisms by which K^+ ion reabsorption is regulated in reptiles.

I demonstrate the first localization of any aquaporin in the tissues of a reptile. AQP3 was detected in the basolateral membranes of the cells comprising the connecting segments and collecting ducts of all three species examined herein (Fig 4-8). This localization is consistent with the localization of this protein in other vertebrate taxa and supports earlier observations of transepithelial water flux in the distal portion the snake nephron (Dantzler, 1967b; Beyenbach, 1984). Further, I demonstrate an

apparent apical/subapical localization of this protein in the cells comprising the distal tubule epithelium in *L. semifasciata* (Fig 4-8A). This localization of AQP3 in the distal tubule of sea snakes is reminiscent of the localization of AQP2 in the apical membranes and subapical vesicles of the collecting duct in mammals (Kinne and Zeidel, 2009); whether this apical AQP3 has a function in snakes similar to that of AQP2 in mammals remains to be determined. Although there was no effect of treatment on the localization of AQP3 in any of the three species examined (suggesting in may not be regulated in the same way as mammalian AQP2), the putative novel localization of this protein in the distal tubules in *L. semifasciata* may suggest that AQP3 plays a role in water balance in marine snakes that has yet to be identified among other vertebrate taxa.

The localization of lsAQP3 to the apical/subapical cytoplasm of the distal tubules is both novel and surprising. It is possible that the antibody Hc-3 cross-reacted with another protein (e.g., putative lsAQP2), however, I find this to be unlikely for several reasons. First, peptide preabsorption of Hc-3 completely abolishes all staining in the kidney of all three species examined (Fig 4-10), suggesting that the immunoreactivity was a specific result of the interaction of antibody Hc-3 with its antigen. Additionally, a BLAST search for the Hc-3 antibody sequence returns an overwhelming number of records for other vertebrate AQP3 homologs and only two other vertebrate proteins: a recombination activating gene in the bull shark (*Carcharhinus leucas*, AAB17267.1) and a protein of unknown function in the zebrafish (*Danio rerio*, XP_002667244.1). Finally, no significant similarity is found when the Hc-3 antibody sequence is BLASTed against AQP2 from *Anolis* (ENSACAP00000008275), *Gallus* (ENSGALP00000016674), or

Homo (NP_000477.1). Taken together, I think these results support a novel localization for the AQP3 ortholog in *L. semifasciata*.

Animals without an extra-renal means to excrete excess salts (i.e., those species lacking salt glands) may be expected to alter the composition of the urine (in as much as reptiles have this capacity) to excrete a maximally concentrated urine when experiencing dehydration. Thus, the kidneys of *N. c. clarkii* and *N. fasciata* (the two species used in this study that lack salt glands) were expected to exhibit decreases in NKA and NKCC2 abundance (to minimize reabsorption of NaCl) and increases in AQP3 abundance (to facilitate reabsorption of water) under these conditions. Despite these predictions but in support of my findings that the localization of NKA, NKCC, and AQP3 did not differ across treatments, I found only minor differences in the mRNA expression across treatments. NKA expression values were variable but statistically indifferent among treatments for all three species. Since changes in the function of NKA are often associated with post-translational modification (e.g., phosphorylation/dephosphorylation; Bertorello et al., 1991), the finding that transcription of this molecule did not decrease significantly does not rule out the possibility that the activity of this enzyme changed with treatment. Furthermore, because NKA is likely found in the basolateral membranes of all parts of the nephron (which vary in function), the relationship between the abundance of this ion transporter and environmental salinity may vary along the length of the nephron. Further investigations into the activity and abundance of NKA should examine isolated segments of the nephron to resolve these issues.

NKCC2 mRNA, though also highly variable, was found to be significantly higher for *N. c. clarkii* in 50% SW than in 0% SW. At the present time, I cannot determine whether

NKCC2 is transcribed in the kidney but not translated or the abundance of the protein is simply too low to detect (via immunohistochemistry or Western blot) in this tissue. Furthermore, the high variability in NKCC2 expression within a treatment for these species suggests that more data are necessary to interpret the potential role of NKCC2 in regulating renal ion balance among snakes.

In *L. semifasciata*, I found significantly higher expression of AQP3 in the freshwater treatment; whether this unexpected pattern is coincident with the novel localization of the AQP3 protein or whether it reflects a role in facilitating the production of dilute urine in low salinity environments cannot be determined at this time. Previous studies of AQP3 expression in the kidneys of chicken demonstrated increases in AQP3 only with water deprivation, not with salt loading (Sugiura et al., 2008). Since I demonstrated no difference in the dehydration rate across species and, further, no difference in hematocrit between *N. c. clarkii* and *N. fasciata*, it is not surprising that I detected no difference in the expression of AQP3 across treatments in *N. c. clarkii* or *N. fasciata*; however, the large overall variation in mRNA expression seen among individuals in the same treatment suggests that the response of snake kidneys to salinity acclimation may be very complex.

I found that the predicted amino acid sequence for lsAQP3 shares a high percent identity with AQP3 from *A. carolinensis*, *G. gallus*, *H. chrysoscelis*, and *H. sapiens* (Table 4-4), lending support to the hypothesis that lsAQP3 is, in fact, an ortholog of AQP3 from these other taxa. Importantly, lsAQP3 exhibits the two NPA motifs characteristic of all aquaporins as well as two aspartic acid (D) residues at positions 163 and 219 (Fig 4-12), characteristics of the aquaglyceroporin subgroup (Borgnia et al.,

1999). While I cannot confirm that the protein detected by the Hc-3 antibody was the same protein encoded by the lsAQP3 mRNA that was extracted from these kidneys, I think these results warrant further investigations into the localization and potential functions of the putative distal tubule form of AQP3 identified from a marine snake.

Similar to the results of AQP3 distribution studies in fishes, amphibians, and mammals (Mobasheri et al., 2005; Pandey et al., 2010; Tipsmark et al., 2010), lsAQP3 mRNA was detected in a wide range of tissues (Fig 4-13). Those tissues with the highest relative expression are also those that are comprised of mucous epithelia, supporting the hypothesis that AQP3 may play a role in the water transport associated with epithelial mucus secretion (Lignot et al., 2002). Interestingly, lsAQP3 was also expressed in both the harderian gland (a cephalic seromucous gland) and the salt gland (a specialized serous gland). Given its potential role in facilitating production of mucus, the expression of lsAQP3 in the harderian gland is not surprising. Although mucus-secretion is an unlikely role for AQP3 in the salt gland, my evidence of AQP3 in this tissue combined with recent evidence of AQP3 from the rectal gland of the dogfish (Cutler, 2007) and evidence of AQP1 and AQP5 from the salt glands of marine birds (Muller et al., 2006), suggests that much remains to be learned about the concerted roles of the various AQP isoforms in vertebrate salt gland physiology.

In summary, though I largely found no renal effects of salinity acclimation in any of the three species examined in this study, I was able to contribute to a general understanding of the regulation of water and ion balance at various locations along the snake nephron. These results regarding the distribution of NKA and AQP3 in the snake nephron combined with previous studies of *Thamnophis* (the garter snake) are

summarized in Fig 4-14. Since neither the localization nor the abundance of NKA, NKCC2, or AQP3 changed with treatment, these results are consistent with the hypothesis that changes in kidney function are not the result of changes in the physiology of the functioning nephrons but are, potentially, a result of changes in the number of functioning nephrons (as suggested by: Lebrie and Sutherland, 1962). Further studies of long-term salinity acclimation and variation in the number of functioning nephrons are required to evaluate this hypothesis fully. I also report the first localization of an aquaporin in any reptile tissue. IsAQP3 mRNA is expressed in a variety of tissues but, importantly, the localization of the protein to the apical membrane of the distal tubules suggests that AQP3 may play additional roles among marine snakes that have not yet been demonstrated from other taxa. Furhter, I find no differences in either the structure or the function of the kidneys when comparing *N. c. clarkii* to *N. fasciata* (sister species which use very different habitats). The mechanism by which *N. c. clarkii* is able to regulate osmotic and ionic balance in the marine environment, therefore, remains elusive.

Table 4-1. Primers used for PCR/cloning, qRT-PCR, RACE, and duplexing PCR.

Primer	Application	Oligonucleotide sequence (5' → 3')
NKA F1	Initial PCR	TGAAGAAAGAGGTAGATATGGACGAYCAYAARYT
NKA R2	Initial PCR	TCCGATTCTGGGTTAGAGTTCCNGTYTTRTC
AQP3 F2	Initial PCR	GCCATCTAAACCCGGCAGTNACNTTYGC
AQP3 R1	Initial PCR	CAACGTGCCAGCCGAYCATNARYTG
L8 LsF1	qRT-PCR	GGCAGTTCGTTTATTGTGGCAA
L8 LsR1	qRT-PCR	TCCACGATCTCCAGGTTTCTCT
L8 NF1	qRT-PCR	AACTGTTCATTGCAGCGGAGG
L8 NR1	qRT-PCR	TGAGCTGAGCTTTCTTGCCAC
NKA LsF1	qRT-PCR	GCTGCAACAGGAGAAGAACCCA
NKA LsR1	qRT-PCR	ACAGCAGCCAGCACAACACCTA
NKA NcF1	qRT-PCR	CTGGCTGCTGTTGTCATCATAA
NKA NcR1	qRT-PCR	CACCATGTTTTTGAAGGACTCC
NKA NfF1	qRT-PCR	GAGTCCTTCAAAAACATGGTGC
NKA NfR1	qRT-PCR	TCTCCTCCCTTCACCTCCACTA
NKCC2 LsF2	qRT-PCR	GGAAAAATAACGAACCCATCCG
NKCC2 LsR2	qRT-PCR	GGTATTCAGCTTGGCAATCAGA
NKCC2 NcF2	qRT-PCR	GTTTTTCAGGCCCTCTGCA
NKCC2 NcR2	qRT-PCR	GCCAGAGCAATGATGAACGTC
NKCC2 NfF1	qRT-PCR	TCAGTGGCTGGTATGGAATGG
NKCC2 NfR1	qRT-PCR	GCCCTCTTCTCTGCATTGCTA
AQP3 LsF1	qRT-PCR	CATCTTTGCCACCTATCCTTCA
AQP3 LsR1	qRT-PCR	AAACGATCAACGCCGCAGT
AQP3 NcF1	qRT-PCR	ACCGTTGGAGCATTTCTCGGA
AQP3 NcR1	qRT-PCR	TTGCACCGAATGCCCAGAT
AQP3 NfF1	qRT-PCR	AACCGTGGATCAAACTTCCG
AQP3 NfR1	qRT-PCR	TTCGTTTGCACCGAATGC
AQP3 F3	3'RACE	CAGTTTATGCCCTCGCGCAAACCAT
AQP3 F4	3'RACE	TTGGGACCTCCATGGGCTTCAACTC
AQP3 R2	5'RACE	CAATGGCCAGGACACAAACG
AQP3 R4	5'RACE	GGGTTGACGGCATAACCGGAGTTGA
AQP3 F2	Duplex PCR	CCAGGAAGGGAGCAACAATA
AQP3 R2	Duplex PCR	CGGGAACCTTGGATCAAACT

Symbols/Abbreviations: Ls – *Laticauda semifasciata*, Nc – *Nerodia clarkii clarkii*, Nf – *Nerodia fasciata*, N – primer sequence identical for *N. c. clarkii* and *N. fasciata*, F – forward/sense, R – reverse/antisense

Table 4-2. GenBank accession numbers for sequences.

Gene	*L. semifasciata*	*N. c. clarkii*	*N. fasciata*
NKA	HQ377187	HQ377188	HQ377189
NKCC2	HQ377184	HQ377185	HQ377186
AQP3	HQ377190	HQ377191	HQ377192
L8	HQ386009	HQ386010	HQ386011

Table 4-3. Average daily rate of mass loss for each species in each treatment. Rates are calculated as percent initial body mass lost per day (mean ± s.d.).

Species	Mass (g)	0% SW	50% SW	100% SW
L. semifasciata (n = 6)	497.4 ± 121.2	0.35 ± 0.13	0.39 ± 0.08	0.54 ± 0.13
N. c. clarkii (n = 5)	118.8 ± 79.7	0.97 ± 0.28	0.99 ± 0.51	1.17 ± 0.31†‡
N. fasciata (n = 5)	136.3 ± 95.2	1. 33 ± 0.48 †‡*	0.85 ± 0.55	1.31 ± 0.66 †

†, ‡, and * indicate significant differences from LS in 0%, 50%, and 100%, respectively.

Table 4-4. BLAST results for the comparison of lsAQP3 with other vertebrate AQP3 orthologs.

Taxon	Amino acid % identity / % positive	Nucleotide % identity
Anolis carolinensis	85 / 93	80
Gallus gallus	82 / 91	76
Hyla chrysocelis	81/ 91	73
Homo sapiens	81 / 90	76

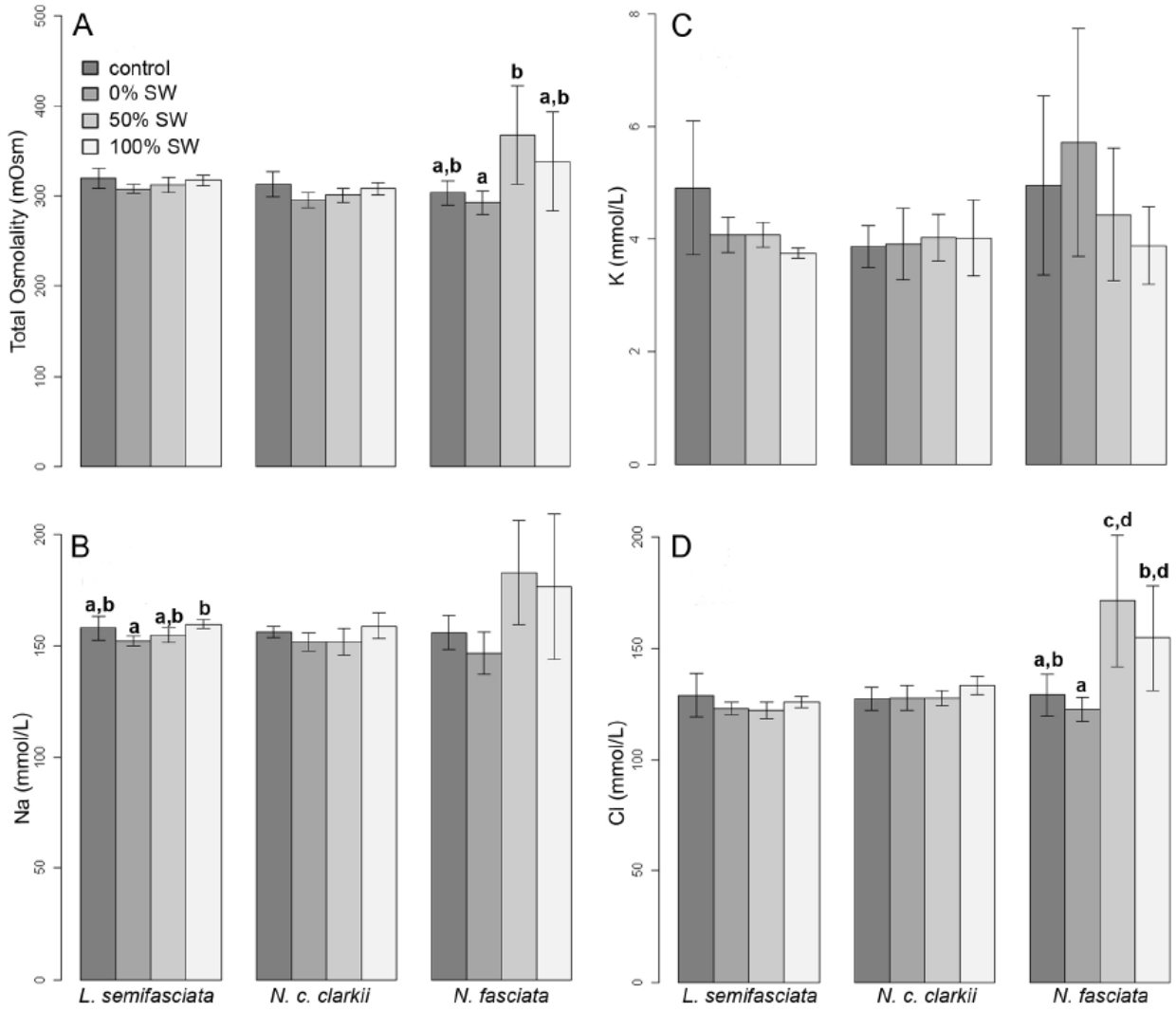

Figure 4-1. Effects of environmental salinity (%SW) on serum ion concentrations. Ion values are compared for each species to the control value for that species only; groups that were significantly different are indicated by different letters. Sample sizes, per treatment: *L. semifasciata* (N=6), *N. c. clarkii* (N=5), *N. fasciata* (N = 5, 5, 3, 3 for: control, 0%, 50%, and 100% SW, respectively). Data are plotted as mean ± s.e.m.

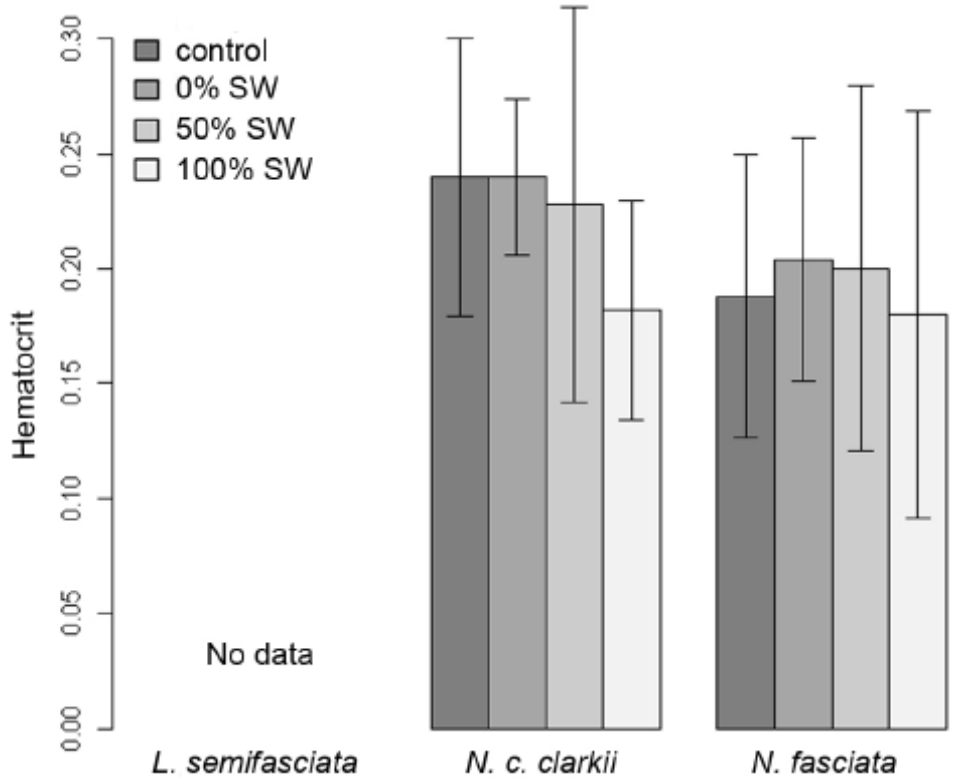

Figure 4-2. Hematocrit does not vary with treatment in either *N. c. clarkii* or *N. fasciata*. No data are available for *L. semifasciata*. Sample sizes, per treatment: *L. semifasciata* (N=6), *N. c. clarkii* (N=5), *N. fasciata* (N = 5, 5, 4, 3 for: control, 0%, 50%, and 100% SW, respectively). Data are plotted as mean ± s.e.m.

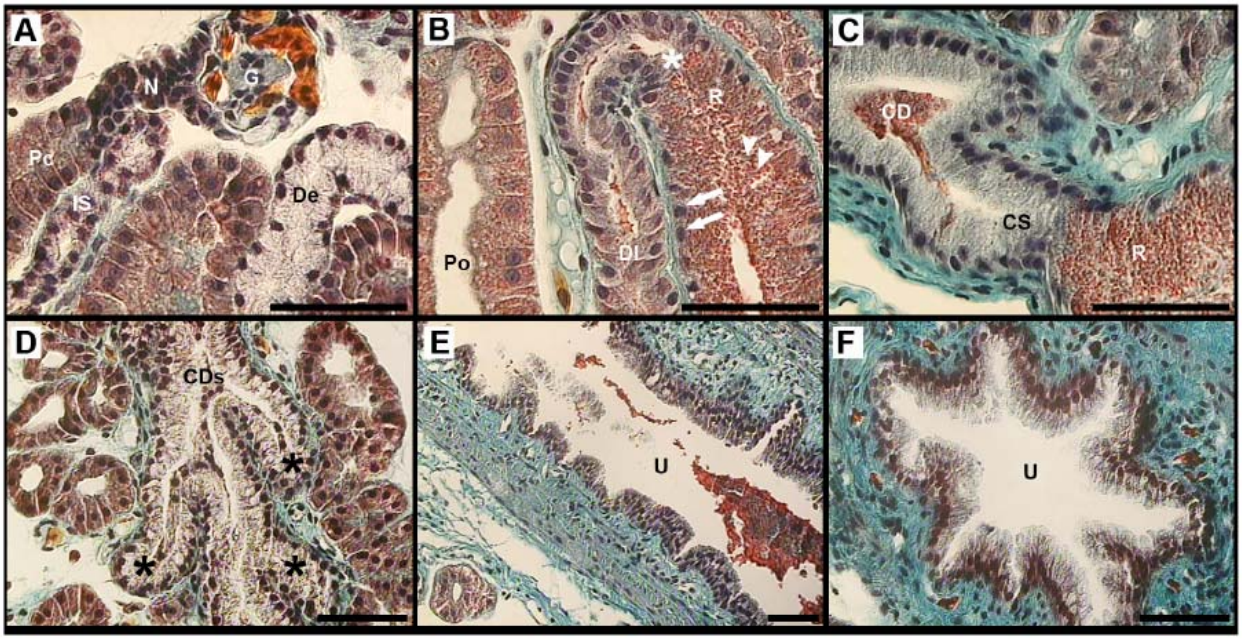

Figure 4-3. Histological structure of the kidney of *Nerodia clarkii*. (A) The glomerulus (G) is connected to the proximal tubule (P) by the short, narrow neck segment (N). Both closed-type (Pc) and open-type (Po) proximal tubules can be seen (A,B). The proximal tubule is connected to the early distal tubule (De) by the intermediate segment (IS). (B) The late distal tubule (Dl) connects (*) to the renal sex segment (R), which can be distinguished from the proximal tubule by the abundance of secretory granules in the cytoplasm (arrowheads) and the basal position of the nuclei (arrows). (C) The renal sex segment connects to the primary collecting duct (CD) via a short connecting segment (CS). (D) Primary collecting ducts (black *s) empty into secondary collecting ducts (CDs) which eventually join to form the ureter (U in panels E,F). Masson Trichrome technique; differential interference contrast microscopy. Scale bars = 50 um.

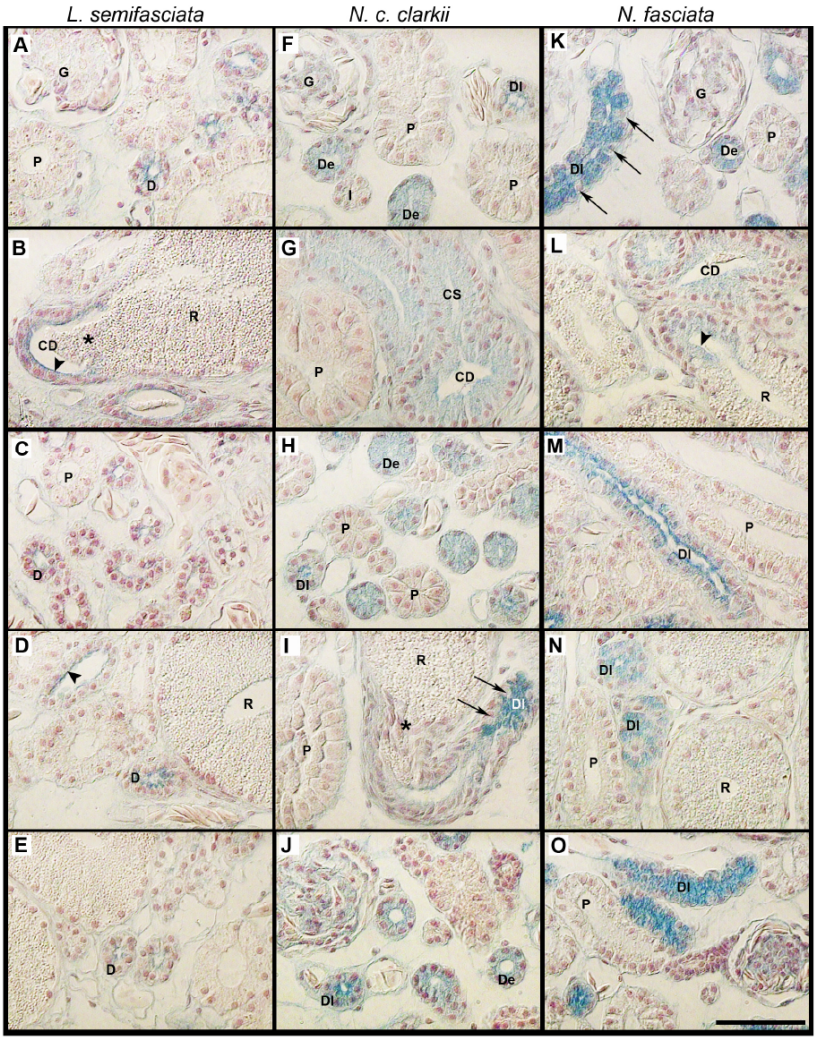

Figure 4-4. Alcian blue^{+} (AB^{+}) material is secreted in the distal tubules and collecting ducts of all species. Sections from control animals for *L. semifasciata* (A,B), *N. c. clarkii* (F,G), and *N. fasciata* (K,L), respectively. The proximal tubules (P) and intermediate segments (I) are negative but the glomerulus (G), distal tubules (D), connecting segments (CS), and collecting ducts (CD) are positive in all species. Distal tubules vary from being only apically positive to expressing AB^{+} material throughout the cytoplasm (*). The localization of AB^{+} material in *L. semifasciata* is restricted to the apical most margins of the distal tubule (D) and connecting segment/collecting duct (black arrowheads). At least two different staining patterns are present in the distal tubules of *N. c. clarkii* and *N. fasciata*; the early distal tubules (De) tend to express AB^{+} material throughout the cytoplasm whereas the late distal tubules (Dl) exhibit AB^{+} material either only at the apical margin or throughout the cytoplasm in alternating cells (alternating AB^{-} cells marked by black arrows). Positive reaction for AB material did not vary with treatment in any of the three species (0% SW: C,H,M; 50% SW D,I,N; 100% SW: E,J,O). Images produced by differential interference contrast microscopy. Scale bar = 50 um.

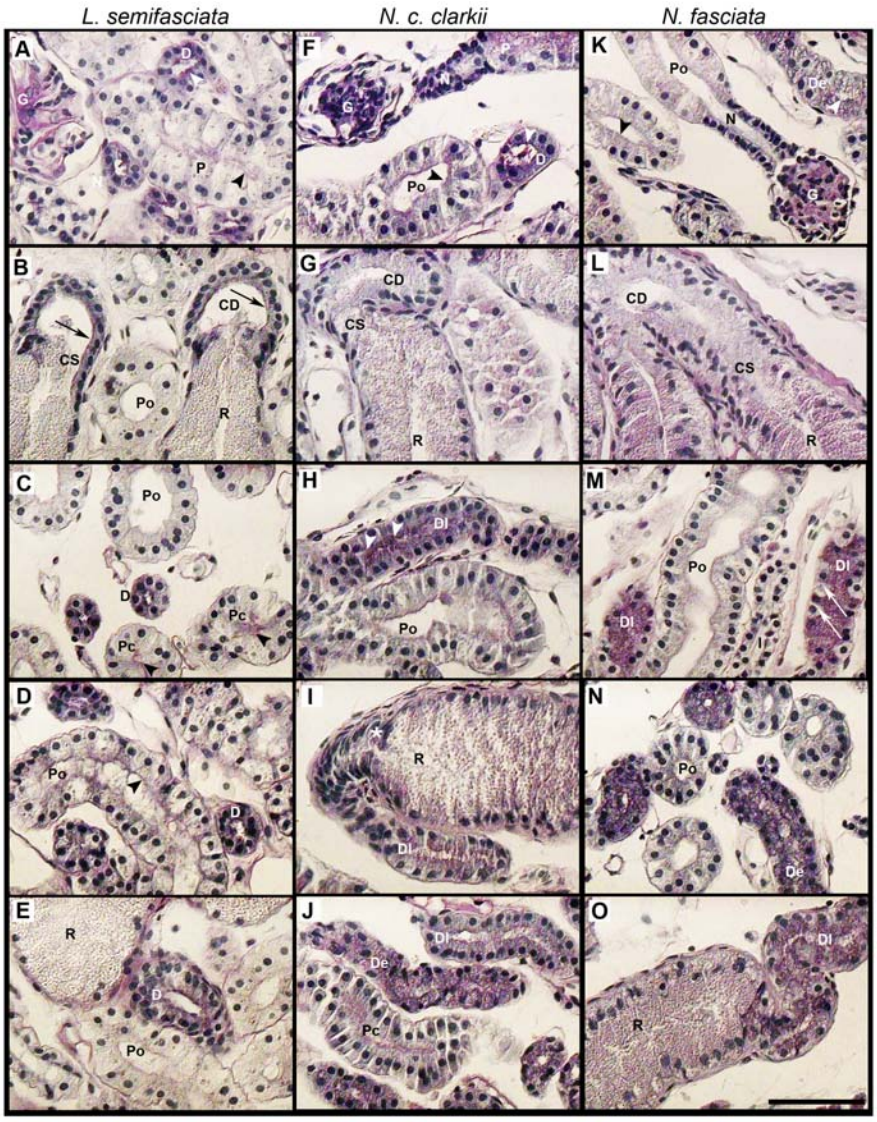

Figure 4-5. Periodic acid Schiff positive (PAS^+) material is secreted in the proximal and distal tubules of all species. Sections from control animals for *L. semifasciata* (A,B), *N. c. clarkii* (F,G), and *N. fasciata* (K,L). The glomerulus (G) and proximal tubules (P and black arrowheads) are PAS^+ in each species while the neck segment (N) is negative. The distal tubules (D and white arrowheads), connecting segments (CS and black arrows), and collecting ducts (CD and black arrows) are apically positive in *L. semifasciata*, but only the proximal (P; black arrowheads) and distal (D; white arrowheads) tubules are PAS^+ in *N. c. clarkii* (F) and *N. fasciata* (K). Connecting segments and collecting ducts are PAS^- in *N. c. clarkii* (G) and *N. fasciata* (L). Both open type proximal tubules (Po) and closed-type proximal tubules (Pc) are evident in each species. The localization of PAS^+ material does not vary with treatment in any species (0% SW: C,H,M; 50% SW D,I,N; 100% SW: E,J,O). Images produced by differential interference contrast microscopy. Scale bar = 50 um.

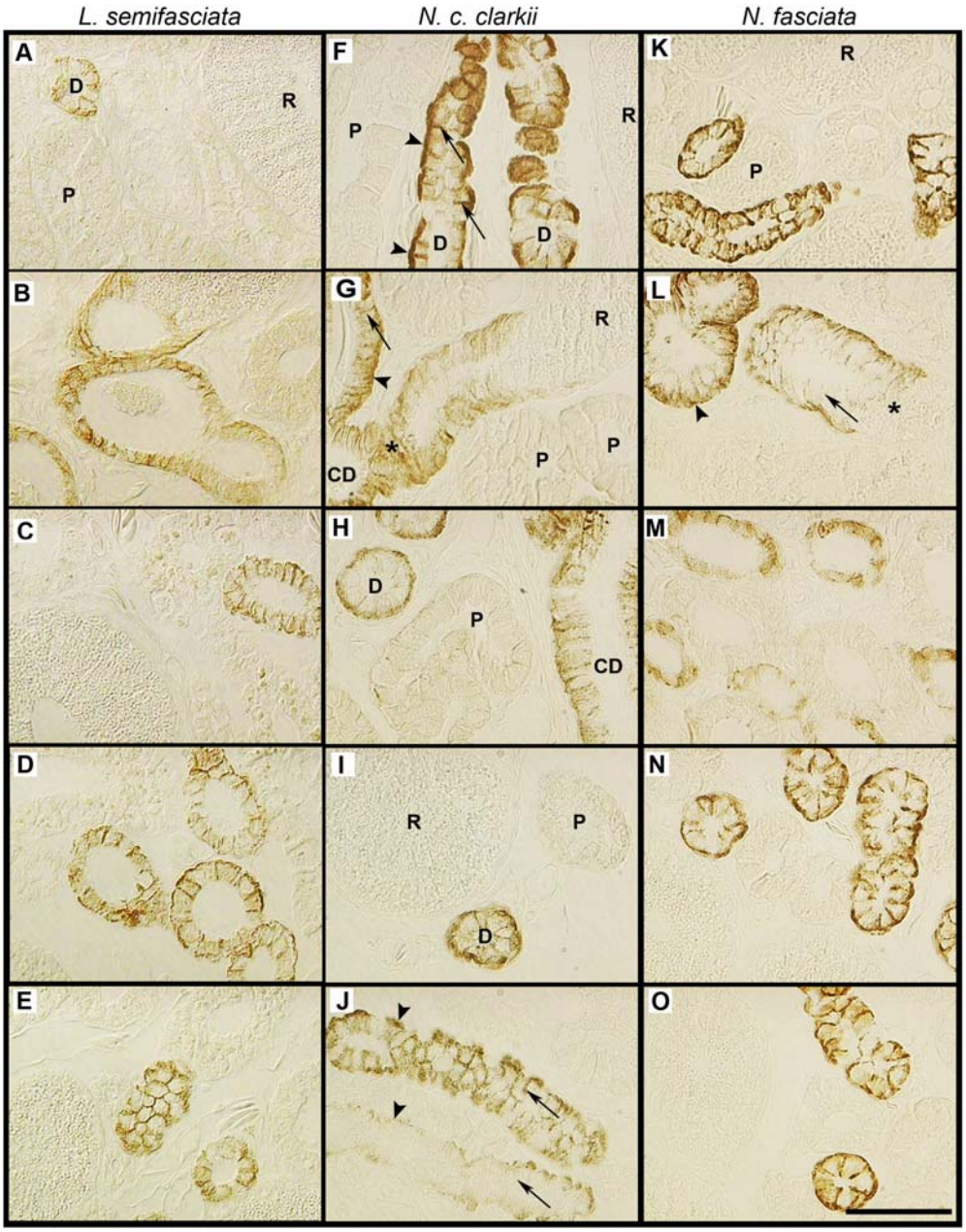

Figure 4-6. NKA localizes to the basolateral membranes of the distal tubules (D) and collecting ducts (CD) of all three species studied. (A,B; F,G; K,L) Sections from control animals for *L. semifasciata*, *N. c. clarkii*, and *N. fasciata*, respectively. Immunoreactivity for NKA in the distal tubule of *N. c. clarkii* is strongest in the basal membranes (F; arrowheads) though positive reaction was also detected in the lateral membranes of these tubules (arrows). In the collecting ducts, lateral reactivity was fainter than basal reactivity in (G) *N. c. clarkii* and (L) *N. fasciata*. There was no effect of treatment on localization of NKA and any of the three species examined (0% SW: C,H,M; 50% SW D,I,N; 100% SW: E,J,O). Images produced by differential interference contrast microscopy. Scale bar = 50 um.

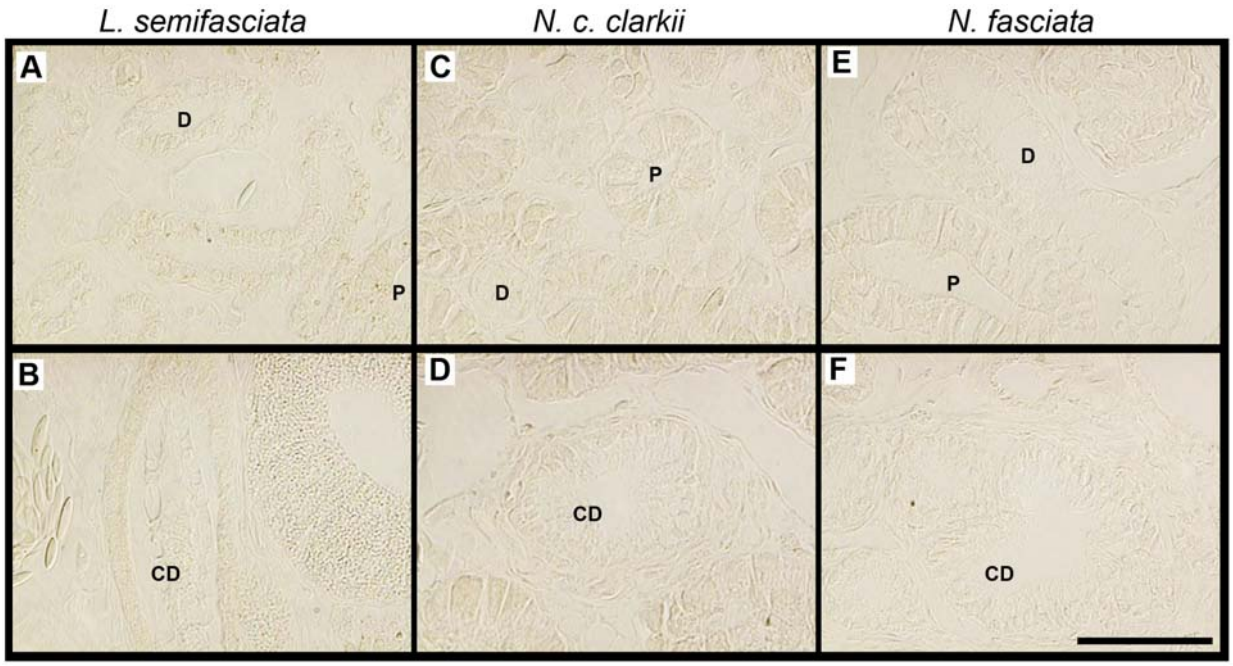

Figure 4-7. NKCC was undetectable in the kidneys of *L. semifasciata* (A,B), *N. c. clarkii* (C,D), and *N. fasciata* (E,F). Abbreviations: P – proximal tubule, D – distal tubule, CD – collecting duct. Images produced by differential interference contrast microscopy. Scale bar = 50 um.

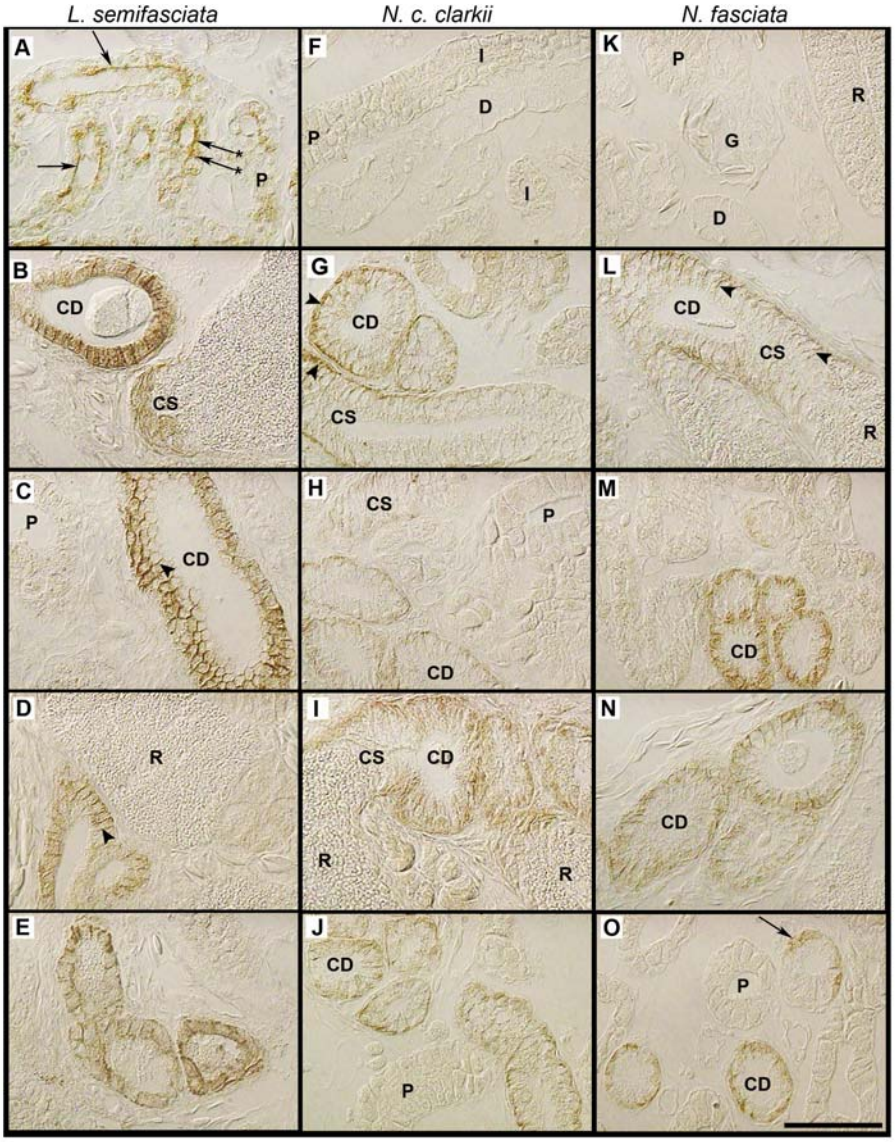

Figure 4-8. AQP3 localizes to the basolateral membrane of the connecting segments and collecting ducts in control animals of all three species (A,B; F,G; K,L). Glomeruli (G), proximal tubules (P), and intermediate segments (I) show no reactivity for AQP3. Apical (black arrow) and subapical/cytoplasmic (starred arrows) portions of the distal tubules (D) are positive for AQP3 in *L. semifasciata* (A) but show no reactivity for AQP3 in *N. c. clarkii* (F) or *N. fasciata* (K). AQP3 immunoreactivity was also detected in the connecting segments (CS) and collecting ducts (CD) of all three species (B, G, L), though in *N. c. clarkii* and *N. fasciata* expression appears to be restricted mostly to the basal membranes (arrowheads) while expression in *L. semifasciata* is dense and may include the cytoplasm of these cells. No changes in localization were observed across treatments in any of the three species (0% SW: C,H,M; 50% SW D,I,N; 100% SW: E,J,O). Images produced by differential interference contrast microscopy. Scale bar = 50 um.

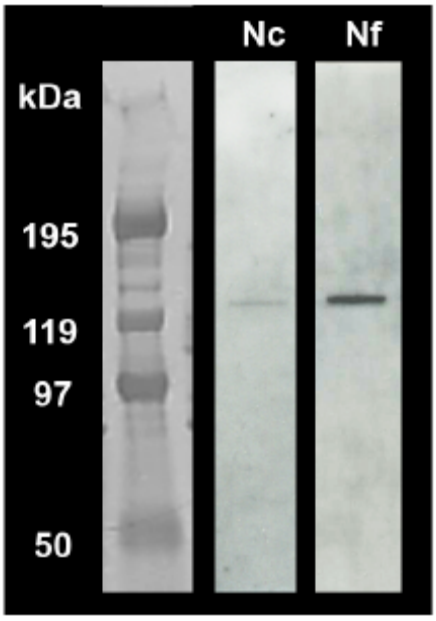

Figure 4-9. Representative Western blots for anti-NKA (α5) in *N. c. clarkii* (Nc) and *N. fasciata* (Nf). Protein sizes are indicated in kDa.

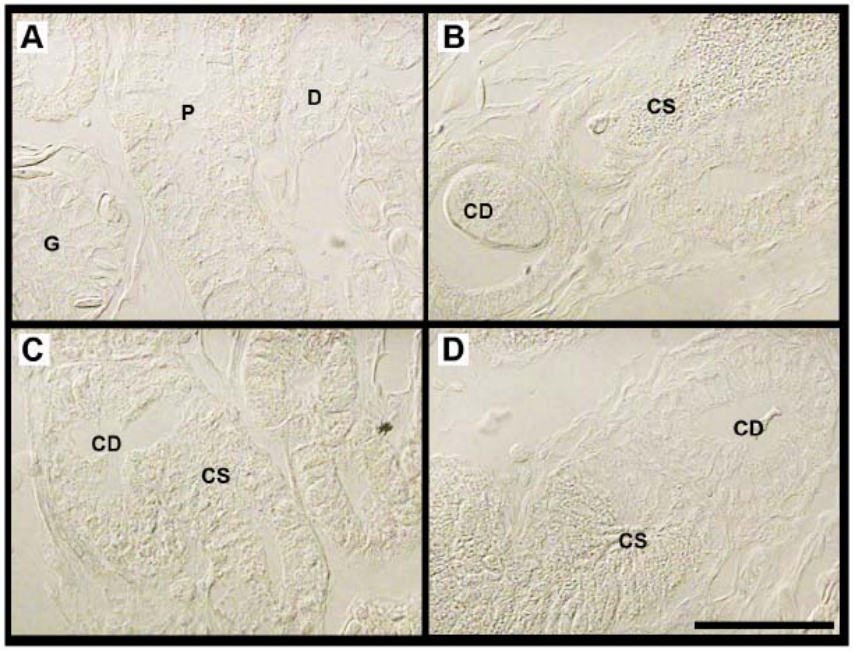

Figure 4-10. Peptide preabsorption completely abolished AQP3 staining in the distal tubules of *L. semifasciata* (A) and in the connecting segments/collecting ducts of *L. semifasciata* (B), *N. c. clarkii* (C), and *N. fasciata* (D). Scale bar = 50 um.

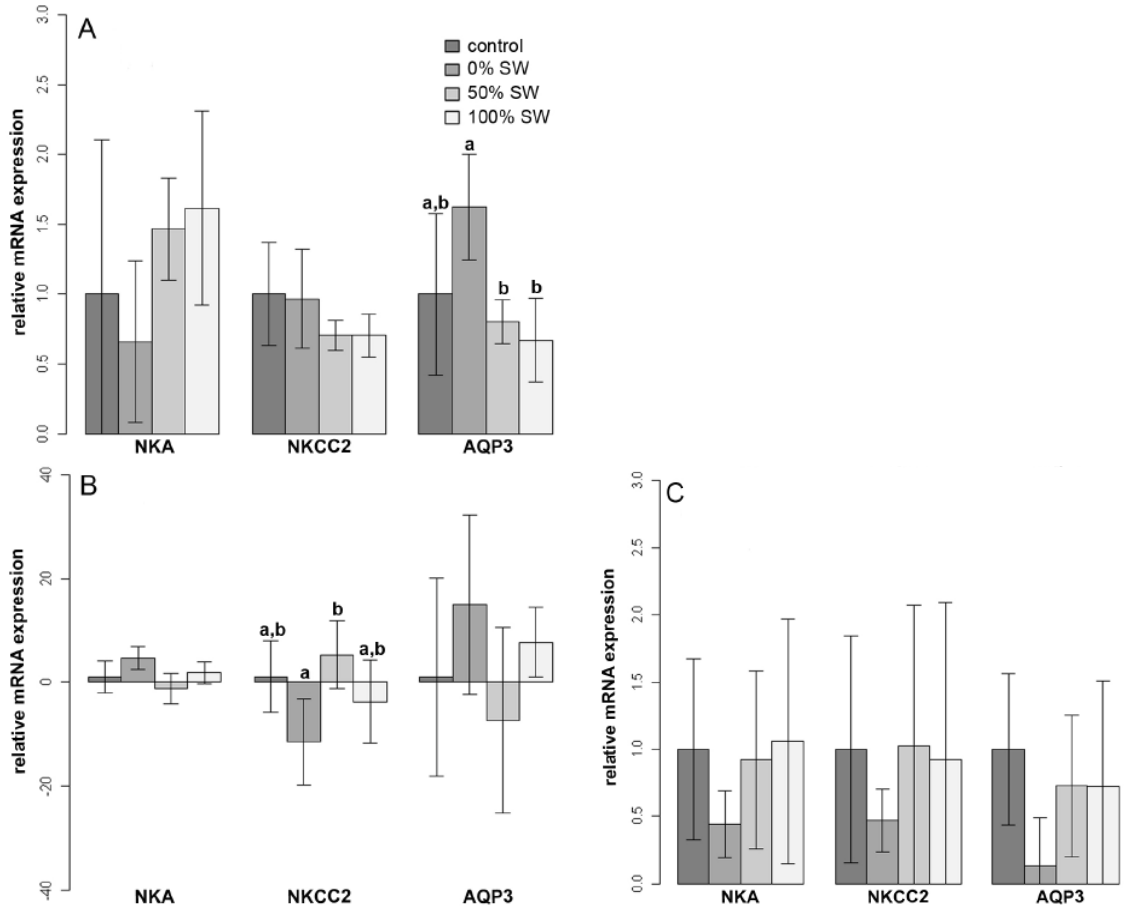

Figure 4-11. mRNA expression for NKA and NKCC2 was variable but not statistically different across treatments in *L. semifasciata* (A). AQP3 mRNA was higher ($p = 0.013$, Tukey HSD post-hoc) in 0% SW than in 50% SW in this species but neither of these treatments was statistically different from control or 100% SW. Expression of NKA and AQP3 mRNA did not differ significantly across treatments in either *N. c. clarkii* (B) or *N. fasciata* (C); however NKCC2 mRNA was found to be higher ($p = 0.048$, Tukey HSD) in the 50% SW treatment than in the 0% SW treatment for *N. c. clarkii*. There was no effect of salinity on NKCC2 expression in *N. fasciata*. Log_{10}-transformed expression values were normalized to log_{10}(L8) and standardized to the control for each species/gene (see Materials and Methods for details). Data are presented as standardized mean ± scaled s.e.m; letters indicate statistically different groups.

Figure 4-12. Comparison of the predicted amino acid sequence for lsAQP3 with AQP3 sequences from chicken (*Gallus gallus*), human (*Homo sapiens*), anole (*Anolis carolinensis*), and frog (*Hyla chrysoscelis*). Sections highlighted in grey denote conserved/aquaporin-specific NPA motifs and the boxed sequence at the C-terminus indicates the sequence recognized by the Hc-3 antibody. The underlined D residue is thought to be conserved among aquaglyceroporins only. The lsAQP3 amino acid sequence was predicted from the full-length mRNA using the Translate Tool on the Swiss Institute of Bioinformatics proteomics server and the alignment was produced in Clustal W2.

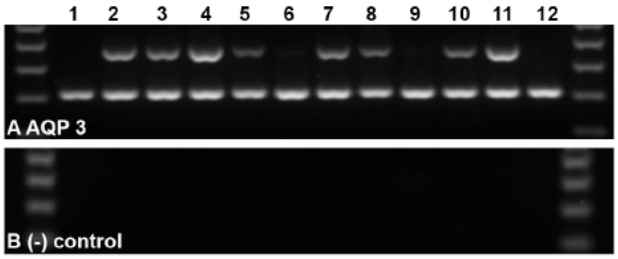

Figure 4-13. Tissue distribution of lsAQP3. (A) Semi-quantitative PCR showing expression of lsAQP3 relative to 18S. (B) No expression was detected when RNA was used as a template. Lanes: (1) brain, (2) duodenum, (3) esophagus, (4) harderian gland, (5) kidney, (6) liver, (7) lung, (8) skeletal muscle, (9) pancreas, (10) salt gland, (11) stomach, (12) testis.

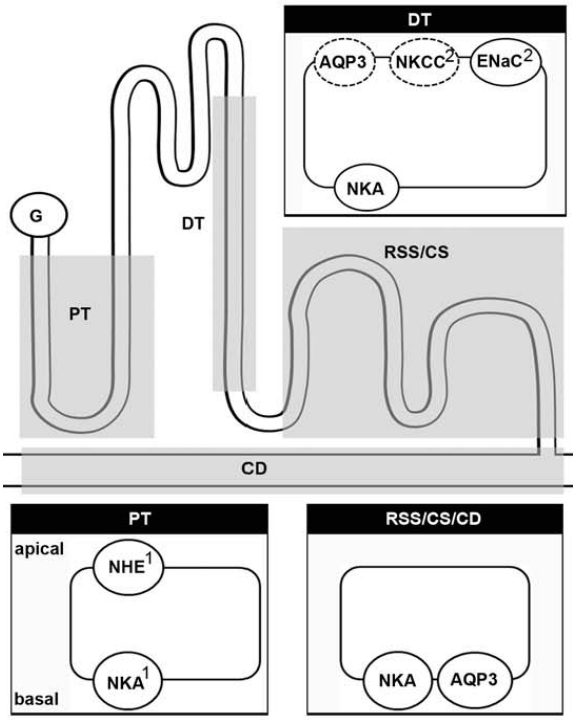

Figure 4-14. Summary of the distribution of known ion transporters in the apical and basolateral membranes of the epithelia comprising the indicated portions of the snake nephron. The putative apical localization of AQP3 in the DT is indicated by a dotted line. The localization of NKCC in the DT, though not supported by this study, was inferred from the presence of an ethacrynic acid inhibitable transepithelial K^+ flux in the indicated reference. Abbreviations: G – glomerulus, PT – proximal tubule, DT – distal tubule, RSS/CS – renal sex segment/connecting segment, CD – collecting duct, NHE – Na^+/H exchanger, NKA – Na^+/K^+-ATPase, AQP3 – aquaporin 3, ENaC – epithelial Na^+ channel. *Nephron diagram adapted from*: Beyenbach and Dantzler, 1978. *References:* 1. Dantzler et al., 1991; 2. Beyenbach and Dantzler, 1978.

CHAPTER 5
MORPHOLOGY AND PUTATIVE FUNCTION OF THE COLON AND CLOACA IN MARINE AND FRESHWATER SNAKES[1]

Post-renal Osmoregulation in Reptiles

The renal concentrating capacity of the reptilian kidney is known to be poor (Braun, 1998). Despite this, several groups of reptiles are capable of varying the concentration of their urinary waste through post-renal modification of the waste products in the bladder (turtles, tuataras, and some lizards) or, in bladderless reptiles (crocodiles, snakes, and some lizards), in the colon/cloaca (Dantzler and Bradshaw, 2009). Schmidt-Neilsen et al. (1963) hypothesized that animals possessing functional salt glands may increase reabsorption of salt from the distal digestive tract (intestine/cloaca) during times of salinity acclimation to gain water via solute-linked water reabsorption. Comparisons of cloacal urine composition following salinity acclimation in the saltwater crocodile (*Crocodylus porosus*; marine) and the American alligator (*Alligator mississippiensis*; freshwater) support of this hypothesis (Pidcock et al., 1997); however, studies of lizards (Bradshaw and Shoemaker, 1967) and tortoises (Nagy and Medica, 1986) reveal an alternative osmoregulatory strategy in desert environments. These latter studies suggest that even species without a salt gland may benefit from solute-linked reabsorption of water if they can tolerate the associated increase in plasma ion concentrations during intermittent times of drought. To my knowledge, only two previous studies have explicitly examined the morphology and putative osmoregulatory function of the colon/cloaca in snakes (Seshadri, 1959; Junqueira et al., 1966). Using histology and analysis of urine electrolytes, these studies

[1] This chapter is currently being considered for publication by the Journal of Morphology

suggest that the colon/cloaca play a role in post-renal modification of the urine through reabsorption of Na^+ (Junqueira et al., 1966) and water (Seshadri, 1959; Junqueira et al., 1966). Importantly, these previous studies examined only terrestrial species while the putative physiology of the gut/cloaca in aquatic snakes is unknown. Additionally, the distribution of ion transporters and water channels has never been examined in the gut/cloacal tissues of any snake species.

Although modification of the urine has been shown to occur in the coprodaeum (Schmidt-Nielsen and Skadhauge, 1967) and urodaeum (Kuchel and Franklin, 2000) of crocodilians, among lizards retrograde flow of the urine into the colon suggests that the intestinal epithelium may also be an important site of ion and water reclamation (Bentley and Bradshaw, 1972; Skadhauge and Duvdevani, 1977). Despite differences in habitat use and diet, many reptile species produce cloacal urine (i.e., urine collected after modification) that is low in Na^+ and high in K^+, relative to the ureteral urine (Bentley and Schmidt-Nielsen, 1965; Schmidt-Nielsen and Skadhauge, 1967; Minnich, 1970; Robinson and Dunson, 1976; Skadhauge and Duvdevani, 1977; Taplin, 1985). Additionally, the relative concentration of these ions is known to vary with dehydration and salt loading in some species (Bradshaw, 1972; 1975; Skadhauge and Duvdevani, 1977; Bradshaw and Rice, 1981; Kuchel and Franklin, 1998). The mechanisms by which this variation in ion secretion and water reabsorption might occur have received little attention in reptiles (but see:Bentley and Bradshaw, 1972, and references therein).

Here, I examine the morphology and biochemistry of the colon and cloacal chambers of marine and freshwater snakes to determine if evidence for secretion or reabsorption of Na^+ and water exists in aquatic species, and if the distribution of ion

transporters/water channels differs between freshwater and marine species. In a previous study I have shown that after acclimation to 0, 50, and 100% seawater (SW), plasma osmolality remains low in the gulf coast saltmarsh snake *Nerodia clarkii clarkii* and increases with salinity in the banded watersnake (freshwater) *Nerodia fasciata* (Chapter 4). *N. fasciata* has also been shown to have reduced survival in seawater (even over very short time periods) as compared with its marine congeners (Chapter 4; Pettus, 1963; Dunson, 1980). Thus, if the osmoregulatory capability of the cloaca is responsible for enabling *N. c. clarkii* to tolerate marine habitats, then, when acclimated to seawater, I expect *N. c. clarkii* to block the NaCl reabsorption pathway to prevent increased plasma ion concentrations. By contrast, *N. fasciata* is not expected to have this response to increasing salinity. To test this hypothesis, I examined the effect of salinity acclimation on the morphology of the colon/cloaca as well as the distribution of two ion transporters, Na^+/K^+-ATPase (NKA) and $Na^+/K^+/Cl^-$ cotransporter (NKCC), and one water channel, aquaporin 3 (AQP3), in these tissues. Though these three proteins are distributed widely in vertebrate tissues, the part of the cell to which they localize can be indicative of their function. Specifically, I expect to find a basolateral localization of NKA, consistent with the previous observation of active Na^+ reabsorption, in the coprodaeum and urodaeum of the cloaca. Additionally, if the cloacal water reabsorption hypothesized by Junqueira et al (1966) and Seshadri (1959) is partly facilitated by aquaporin-mediated transepithelial water flux (rather than solely via solute-linked flux), I expect to find a basolateral localization of AQP3 as well. Lastly, if Na^+ reabsorption is facilitated by NKCC (as it is in the proximal tubule of the mammalian kidney), I expect to find an apical localization of NKCC in the coprodaeum and urodaeum as well.

Furthermore, if differential regulation of cloacal water/ion transport is responsible for the ability of *N. c. clarkii* to survive in marine environments, I expect this arrangement of ion transporters to change following acclimation to 100% SW in this species only.

Materials and Methods

Animal Collection and Maintenance

Gulf coast salt marsh snakes (*N. c. clarkii*) and banded watersnakes (*N. fasciata*) were collected from Levy and Alachua counties (FL), respectively. Animals were housed individually in plastic aquaria containing enough freshwater (tapwater, Gainesville, FL) to completely cover their cutaneous surfaces as they rested on the bottom. All animals were acclimated to laboratory conditions for a period of five days in 0% SW. After the five-day acclimation period, control animals were selected randomly (N = 5 from each species of *Nerodia*) and sacrificed via rapid decapitation. Remaining animals were then randomly assigned to one of the following treatments (N = 5 per treatment, per species): 0%, 50%, or 100% SW and acclimated to their final salinity by incremental salinity increases over a period of seven days. Animals were then retained in their final salinity for an additional week while still receiving daily cage water changes (tapwater or salt water mixed from Instant Ocean and tapwater). At the end of this experimental period, all animals were sacrificed via rapid decapitation in accordance with the American Veterinary Medical Association's guidelines on euthanasia using methods approved by the University of Florida's Institutional Animal Care and Use committee.

Tissue Collection and Preservation

Tissues were removed from animals immediately following sacrifice, rinsed of excess blood and fecal/urinary waste using 10mM phosphate buffered saline (PBS), and fixed immediately in 4% paraformaldehyde (diluted in deionized water) at 4˚C for 24

h. Following fixation, tissues were rinsed in three washes of 10mM PBS (15 min each) and stored in 75% ethanol overnight at room temperature (RT). Tissues were then removed to a fresh aliquot of 75% ethanol where they were stored, at RT, until processing. Before embedding, tissues were dehydrated through a series of ethanol baths of increasing concentration, followed by two 1 h rinses in Citrisolv (Fisher Scientific, Pittsburgh, PA USA), and four changes of paraffin wax (Tissue Prep 2, Fisher Scientific) at 55˚C for 1 h each. Embedded tissues were sectioned at 7µm, mounted on charged glass slides (Superfrost Plus, Fisher Scientific), and dried overnight at 30˚C.

Histology and Immunohistochemistry

The basic structure of the epithelia and supporting tissues for the colon and cloacal chambers was viewed using the Lillie modification of the Masson Trichrome stain (Humason, 1972). Acid mucins were detected using Alcian blue (pH 2.5; Humason, 1972) and the presence of neutral mucins is inferred from the presence of periodic acid Schiff positive (PAS^+) reaction (Humason, 1972). To examine the distribution of NKA, NKCC, and AQP3 in the epithelia, rehydrated tissue sections were incubated overnight at 4˚C in anti-NKA (1/100), anti-NKCC (1/2000) or anti-AQP3 (1/100) following a 30 min peroxidase block and a 20 min protein block (BioGenex, San Ramon, CA, USA), both at RT. Protein localization was then visualized using the Super Sensitive™ Link-Label universal secondary antibody kit (BioGenex) and 3'3-diaminobenzidine chromagen (BioGenex). Images were produced using a Hitachi KP-D50 digital camera (Hitachi, Tokyo, Japan) mounted on an Olympus BX60 light microscope (Olympus, Center Valley, PA, USA), digitized using ImagePro Express software (Media Cybernetics, Bethesda, MD, USA) and brightened using Adobe Photoshop CS3 (San Jose, CA USA).

Primary Antibodies

Monoclonal anti-NKA (α5), developed by Dr. Douglas Fambrough, and monoclonal anti-NKCC (T4), developed by Drs. Christian Lytle and Bliss Forbush III, were obtained from the Developmental Studies Hybridoma Bank developed under the auspices of the National Institute of Child Health and Human Development and maintained by The University of Iowa, Department of Biological Sciences, Iowa City, IA 52242. Anti-NKA detects the α1 subunit of the NKA heterodimer (Takeyasu et al., 1988) and anti-NKCC detects a conserved epitope in the carboxyl tail of NKCC1, NKCC2, and NCC (Lytle et al., 1995). Anti-AQP3 (Hc-3) is directed against the following epitope in the c-terminus of treefrog AQP3: CQENVKLSNVKHKERI (Pandey et al., 2010). Hc-3 and its blocking peptide were generous gifts from Dr. David Goldstein at Wright State University.

Results

Morphology of the Colon and Cloaca

Here, I use the term colon synonymously with large intestine. Colon samples were collected from the portion of the intestine just posterior to the ileocecal valve, which separates the small and large intestine. This portion of the intestine was easy to identify in both species since it frequently held a bolus of semi-solid fecal waste in contrast with the posterior-most segment of the small intestine, which was always empty. The position of the colon relative to the cloaca and the rest of the urogenital organs is illustrated in Figure 1. The cloaca of watersnakes is composed of three main chambers: the coprodaeum is the posterior-most portion of the colon and can be distinguished from the colon by epithelial morphology (described below). The urodaeum is comprised of two short finger-like chambers projecting toward the anterior, hereafter referred to as the left and right (L/R) urodael chambers, and a common chamber into which the L/R

urodael chambers empty. The junction of the common urodael chamber and coprodaeum serves to define the anterior-most margin of the proctodaeum, which extends caudally from this junction to the vent (Fig 5-1).

The colonic epithelium of both species (Fig 5-2A-C) is a simple columnar epithelium dominated by cup-shaped goblet cells (Gc) interspersed with tall columnar enterocytes (Et). The basement membrane (bm) is supported by a highly vascularized (red blood cells marked by *) lamina propria (lp). Supporting the lamina propria is a loosely organized submucosa (sm), around which lies a layer of circular muscle (cm), a small amount of connective tissue (ct), and a transverse muscle (tm) layer. As the colon transitions into the coprodaeum the epithelium becomes more pseudostratified with dark-staining basal cytoplasm and elongate basally-to-centrally positioned nuclei (Fig 5-2D-F). The coprodael epithelium becomes pseudostratified and the clear-staining apical cytoplasm becomes reduced in size such that the cells nearest the colon are columnar in shape (Fig 5-2E) whereas those near the junction with the urodaeum are more cuboidal (Fig 5-2F). The frequency of goblet cells decreases as the coprodaeum progresses posteriorly toward the proctodaeum. The L/R urodael chambers are located dorsolaterally to the coprodaeum in both species. In females, the L/R urodael chambers junction with the posterior-most ends of the vaginal pouches; in males, the L/R urodael chambers are shorter (rostrocaudally) but otherwise similar in morphology. The epithelium of the L/R urodael chambers is simple or slightly pseudostratified with tall columnar cells that have clear-staining cytoplasm (Fig 5-2G). There is a brush border lining the mucosal membranes of these chambers, which becomes patchy in the posterior. Moving caudally, the L/R urodael chambers merge along their midline to form

the common urodael chamber (Fig 5-2H), which is typified by a low pseudostratified epithelium. The cells of the anterior-most portion of the common urodael chamber are very tall columnar cells, which decrease in height toward the posterior (Fig 5-2I). The low cuboidal urodaeum merges with the coprodaeum to form the anterior boundary of the proctodaeum (Fig 5-2J), a transition marked by a decrease in cell height such that the epithelium of the proctodael chamber transitions into non-keratinized stratified squamous epithelium, anteriorly (Fig 5-2K), and keratinized stratified squamous epithelium as this chamber approaches the vent (Fig 5-2L).

The ducts of the reproductive tract as well as the ureters can easily be seen in the supporting tissue around the cloaca in these species. In females, the posterior vagina (V) can be easily distinguished from other ducts in the urogenital region by the extremely thick circular muscle layer surrounding it (shown relative to the thickness of the ureter in Fig 5-3A). Inside the circular muscle layer is a thick submucosa and a lamina propria directly underlying the simple columnar epithelium of the vagina. A brush border (bb; Fig 5-3B) can be seen on the apical membrane of the vaginal epithelium. The left and right posterior vaginas transition, posteriorly, into the left and right urodael chambers (Fig 5-3C), a transition that is marked, most notably, by a decrease in the thickness of the circular muscle layer around the L/R urodael chambers (compare the thickness of the submucosa of the vagina and urodaeum in Fig 5-3C). This supporting tissue also stains lighter with Trichrome (Fig 5-3C) than does the supporting layer around the vagina (V). The epithelium of the L/R urodael chambers is very similar to that of the vaginal epithelium except that the urodael epithelium appears to be more pseudostratified (compare Fig 5-2H with Fig 5-3B), and the brush border is less obvious

than in the vagina. In males, the ductus deferens is situated laterally to the other urogenital organs until it meets the urodaeum (Fig 5-3D). The ductus deferens is supported by a thin submucosa and a transverse muscle layer (Fig 5-3E) and the epithelium is unlike that of any other urogenital organ in these species. The ductus deferens epithelium is columnar with a low pseudostratified/transitional layer (Fig 5-3F). The nuclei are positioned basally and the cytoplasm stains darkly with Trichrome except at the apical-most tips of the cells (Fig 5-3F). The apical membranes of these epithelial cells also appear to be convex, rather than flat as is seen in most other epithelia, and lack a brush border (arrowheads in Fig 5-3F). In both sexes, the ureters meet the cloaca at the common urodael chamber (Fig 5-3D), posterior to where the ducts of the reproductive tract meet this chamber. The ureters are supported by a thick submucosa but only a very thin circular muscle layer (Fig 5-3G); the epithelium of the ureter is simple cuboidal/short columnar with basally positioned nuclei, clear-staining apical cytoplasm (Fig 5-3H), but becomes low squamous epithelium where the ureter meets the common urodaeum (Fig 5-3I).

Evidence for Mucus Secretion in the Colon/Cloaca

Using the Alcian blue (pH 2.5) and Periodic Acid Schiff staining techniques, I have detected acid and neutral mucins, respectively, in many of the intestinal/cloacal and reproductive epithelia. Both acid and neutral mucins were detected in the goblet cells (*) and the apical cytoplasm (arrowheads) of the colon (Fig 5-4A,B) and coprodaeum (Fig 5-4C,D) and in the apical cytoplasm of the urodaeum (Fig 5-4E,F). The proctodael epithelium was negative for acid mucins (Fig 5-4G) but positive in the region of the basement membrane for neutral mucins (Fig 5-4H). Among the reproductive epithelia, the vaginas (Fig 5-5A,B) stain positively throughout the epithelium for acid and neutral

mucins, whereas only the apical-most margin of the cytoplasm from the ductus deferens was positive for mucins (Fig 5-5C,D). The ureter is positive for both acid and neutral mucins in both sexes (Fig 5-5E,F; ureters pictured are from a male).

Distribution of NKA, NKCC, and AQP3/ Effects of Salinity

NKA was not detectable in the colon (Fig 5-6A) or any of the cloacal chambers (Fig 5-6D,G,J) of either species. By contrast, NKCC was detected in the basal cytoplasm of the cells lining the colon (Fig 5-6B), coprodaeum (Fig 5-6E), and proctodaeum (Fig 5-6K) in both species. AQP3 was patchy in the epithelium of the colon and appears to be associated with the mucus-secreting columnar cells, rather than the goblet cells, in this tissue (Fig 5-6C). AQP3 was undetectable in the coprodaeum (Fig 5-6F), faint in the basal cytoplasm of the urodaeum (Fig 5-6I) and absent from the proctodaeum (Fig 5-6L). NKA was absent from the vaginas (Fig 5-7A) and ducti deferentia (Fig 5-7D) but was basolateral in the epithelium of the ureter (Fig 5-7G). NKCC was also absent from the vaginas (Fig 5-7B) but was detected in the apical cytoplasm of the ducti deferentia (Fig 5-7E). NKCC was absent from the ureteral epithelium (Fig 5-7H). The epithelia of the vaginas (Fig 5-7C) and the ducti deferentia (Fig 5-7F) were negative for AQP3; however, the sperm in the duct pictured in Fig 5-7F were AQP3 positive. The ureters of both species and both sexes stained positively for AQP3 in the basal cytoplasm. There was no effect of salinity on the general morphology of the epithelia, including the proportion of goblet cells in the colonic and coprodael epithelia (data not shown), or on the distribution of NKCC or AQP3 in the colon/cloaca (Fig 5-8). Finally, while salinity acclimation also did not affect the distribution of NKA or AQP3 in the ureters (Fig 5-9) of either species, slight variation in the abundance of both NKA and AQP3 (assessed via IHC) are apparent. In particular, NKA appears to be

lower in abundance in the 100%SW treatment (Fig 5-9C), relative to the 50 and 0%SW treatments, and AQP3 (Fig 5-9F) appears to have the opposite pattern (i.e., AQP3 appears to be slightly more abundant in 100%SW, relative to 50% and 0%SW). Quantitative analyses of ion transporter/water channel abundance are necessary to confirm these hypothesized patterns.

Discussion

Morphology of the Colon/Cloaca in Watersnakes

The morphology and putative membrane transport function of the cloaca in aquatic snakes has never been examined, despite suggestions that the cloaca may contribute to urine modification in these animals (Dunson and Robinson, 1976; Yokota et al., 1985). Thus, the objectives of this work were to describe the morphology of the colon/cloaca in closely related species of snakes occupying different habitats (marine vs. freshwater) and to use knowledge of the relationship between form and function to hypothesize about the putative physiology of these organs in the context of epithelial ion and water transport. Previous studies of membrane anatomy and physiology in the cloaca of snakes suggested that both the colon and cloaca are important sites of Na^+ and water reabsorption (Seshadri, 1959; Junqueira et al., 1966). These results suggest that the colon, coprodaeum, and ureter might be important sites of ion transport, and, that the colon and common urodael chamber may be important sites of solute-independent water reabsorption in aquatic snakes.

The colon and the coprodaeum of both species of watersnake were typified by extensive infoldings and, while the colon is a simple columnar epithelium with abundant mucus-secreting goblet cells, the coprodael epithelium is pseudostratified and becomes more cuboidal than columnar as it progresses toward the proctodaeum (Fig 5-2). This

posterior transition from colon to coprodaeum to proctodaeum, is also marked by a dramatic decrease in the proportion of goblet cells in the epithelium from >>2/3 in the colonic epithelium to <<1/3 in the posterior coprodaeum to complete absence in the proctodaeum. These morphological descriptions of the colonic and coprodael epithelia are similar to those reported for the epithelial morphology of the colon/coprodaeum in other snakes (Junqueira et al., 1966) as well as crocodiles (Kuchel and Franklin, 2000) and birds (Johnson and Skadhauge, 1975). The left and right urodael chambers (referred to as the genital sinuses by Seshadri, 1959) in both species of watersnake are typified by tall simple/pseudo-stratified columnar cells with clear-staining apical cytoplasm, as has been shown for crocodiles (Kuchel and Franklin, 2000) and birds (Johnson and Skadhauge, 1975) and are typified by long, thin rugae in both sexes. Thick rugae are also present in the common urodael chamber, suggesting that this portion of the cloaca undergoes dramatic expansion at times; the fact that these large rugae are present in both males and females suggest this expansion may be associated with the storage/modification of large amounts of urine (rather than reproductive function), as has been suggested among crocodiles (Kuchel and Franklin, 2000). Further examination of the distribution of urine in the various segments of the cloaca during times of dehydration and saline load will be necessary to test this hypothesis. The proctodaeum in both species was determined to be stratified squamous epithelium, as has been described among birds as well (Johnson and Skadhauge, 1975), with a keratinized layer only in the portion nearest the vent.

Although the vagina in these species exhibit long thin rugae, similar to those of the L/R urodael chambers, the epithelium of the vagina is surrounded by a very thick

circular muscle layer which stains darker with hematoxylin than does the circular muscle underlying the urodaeum. These results are similar to observation made on the uterus/vagina in other snake species (Uribe et al., 1998; Sever and Ryan, 1999). By contrast, the circular muscle layer surrounding the ureters is very thin, and this layer is absent from the supporting tissue around the ductus deferens. These differences likely reflect the role of the muscular uterine wall in contracting during parturition and suggest that that similar contractions are not used in the expulsion of the urinary and seminal fluid from the ureters and ducti deferentia, respectively.

Putative Osmoregulatory Function

Reabsorption of NaCl from the proximal tubule of the mammalian kidney is known to rely on the combined actions of an apical NaCl symporter (NKCC2) and basolateral NKA (Kinne and Zeidel, 2009). Because several reptilian taxa have been shown to reabsorb NaCl across the cloacal membranes (Schmidt-Nielsen and Skadhauge, 1967; Minnich, 1970; Skadhauge and Duvdevani, 1977), I expected to find apical NKCC and basolateral NKA in the urodaeum and coprodaeum. Surprisingly, these are not the results I observed (Fig 5-6); in fact, NKCC was found in the basolateral portion of the colonic, coprodael, and proctodael epithelia and NKA was undetectable in all three of these tissues as well as the urodaeum. NKCC is also basolateral in the ducts of the mucus-secreting cephalic glands in these two species of *Nerodia* (Chapter 3). Thus, it is possible that the basolateral localization of NKCC in the cloaca is suggestive of the ion secretion associated with mucus production in mucosal membranes and has little relevance for the potential of the cloaca to serve as a means to significantly modify the ionic composition of the urine (i.e., to add enough solute to make the urine hypertonic). Interestingly, several studies of reptile cloacal physiology suggest that K^+ is secreted

into the urine during storage in the cloaca (Skadhauge and Duvdevani, 1977; Lauren, 1985). Studies of exocrine glands suggest that a basolateral localization of NKCC is consistent with a role in K^+ secretion from this tissue (Haas and Forbush, 2000). Though I find initial support for a similar role for NKCC in the cloaca of watersnakes, studies aimed at examining the response of NKCC during times of high K^+ load are necessary to support this idea. Additionally, identification of an apical K^+ channel in these tissues would provide further support for this hypothesis.

The lack of NKA in these tissues was surprising. Considering that NKA is easily detectable using IHC in active salt-secreting tissues (e.g., the salt glands of sea snakes), these results provide initial support for the idea that the cloacal tissues of watersnakes are not involved in the active secretion of salt. Before these claims can be substantiated, further studies on the distribution of NKA mRNA and the putative apical Na^+ channels are warranted. It is possible that, like the epithelium of the bladder in mammals (Smith et al., 1998) and the hindgut of some lizards (Bentley and Bradshaw, 1972), the apical Na^+ channel in the coprodael and/or urodael epithelia is the apical epithelial Na^+ channel (ENaC) rather than NKCC. Alternatively, apical Na^+ transport might be mediated by one of the Na^+/H^+ exchangers, which are known to be important in apical Na^+ transport in the gastrointestinal tract of mammals (Zachos et al., 2005). Studies aimed at blocking apical Na^+ transport with ENaC and NHE inhibitors in addition to localizing ENaC and NHE in these tissues (using IHC and *in situ* hybridization) would confirm the identity of the apical Na^+ channel and further shed light on the role of the basolateral NKCC in the cloaca of watersnakes.

AQP3 was detected in the basolateral cytoplasm and membranes of the colon and coprodaeum, though no immunolocalization was detected in the goblet cells of these tissues. These results are consistent with the localization of AQP3 in the distal colon of the rat (Frigeri et al., 1995) and amphibians (Mochida et al., 2008; Pandey et al., 2010) and suggest a role for AQP3 in fecal dehydration in watersnakes, as has been shown in these other taxa (Ishibashi et al., 1994; Frigeri et al., 1995). Taplin (1985) has previously suggested that crocodiles reabsorb water from the feces when experiencing desiccating conditions, though I am the first to suggest that this process involves AQP3 in reptiles. AQP3 was also basolateral in the epithelium of the ureters (urothelium). Basolateral localization of AQP3 in the urothelium has also been demonstrated in rats, as has a relative increase in the abundance of this protein (suggested via changes in the intensity of immunohistochemical staining and western blot) following dehydration (Spector et al., 2002). Although I did not detect a difference in the abundance of ureteral AQP3 following salinity acclimation, its presence in this tissue suggests that AQP3 may facilitate reabsorption of water from the urine (though only to the point at which urine becomes isotonic with blood plasma). In combination with the observation that NKA was also basolateral in the urothelium of the watersnakes, I suggest that the ureters of snakes, like those of some mammals (Spector et al., 2002, and references therein) may be involved in post-renal/pre-cloacal modification of the urine. Previous studies suggest that the ureter of lizards is relatively inactive, with respect to urine modification (Roberts and Schmidt-Nielsen, 1966), making this finding somewhat surprising. Future studies quantifying changes in AQP3 protein and mRNA abundance (using western/dot blots

and quantitative real-time PCR, respectively) would be useful in attempting to understand the relationship between habitat salinity and ureteral ion/water transport.

Additional studies aimed at understanding the mode of regulation of water/ion permeability in the species examined here would contribute much to a more thorough understanding of cloacal osmoregulation. Since arginine vasotocin (AVT) is known to increase Na^+ reabsorption (and also, likely, increase the cloacal permeability to water) in the monitor lizard, *Varanus gouldii* (Braysher and Green, 1970), and the abundance of AQP3 is known to be regulated by anti-diuretic hormone (ADH) in mammals, it is likely that cloacal Na^+ (and possibly water) transport is under hormonal control in watersnakes as well. If true, animals treated with AVT would be expected to increase the reabsorption of both Na+ and water from the cloaca. To test this hypothesis, identification of the other Na+ channels/transporters present in the cloacal epithelia and quantification of their response to AVT are necessary.

Though a description of the putative ion/water transport properties in the reproductive tract of watersnakes was not a main objective of this study, I report several observations regarding the distribution of NKA, NKCC, and AQP3 in the vagina and ductus deferens of watersnakes. NKA was not detected in any of these reproductive ducts and NKCC was in the basolateral portion of the epithelium of the ductus deferens. AQP3 was detected in the basolateral membranes of the vaginal epithelium. These results are similar to the basolateral localization in the oviduct of amphibians observed by Mochida et al. (2008). Finally, while sperm in the ductus deferens were positive for AQP3, no part of the epithelium of this duct exhibited localization of AQP3.

In summary, while the physiology and morphology of the avian cloaca has been studied in great detail, comparatively little is known about the role of the cloaca in regulating osmotic/ionic balance in reptiles, particularly snakes. Here, I provide initial analysis of the morphology of the colon, cloaca, and posterior reproductive structures of two species of watersnakes – one from a marine habitat and one from a freshwater habitat. The general lack of differences in the morphology/putative function of these epithelia suggests that these tissues do not contribute much, if at all, to the ability of *N. c. clarkii* to survive in marine habitats. Further studies aimed at examining the transport properties of the cloaca of sea snakes, which have a salt gland, would make an interesting comparison with the results presented here and with the results of similar studies from other vertebrates that also have a salt gland.

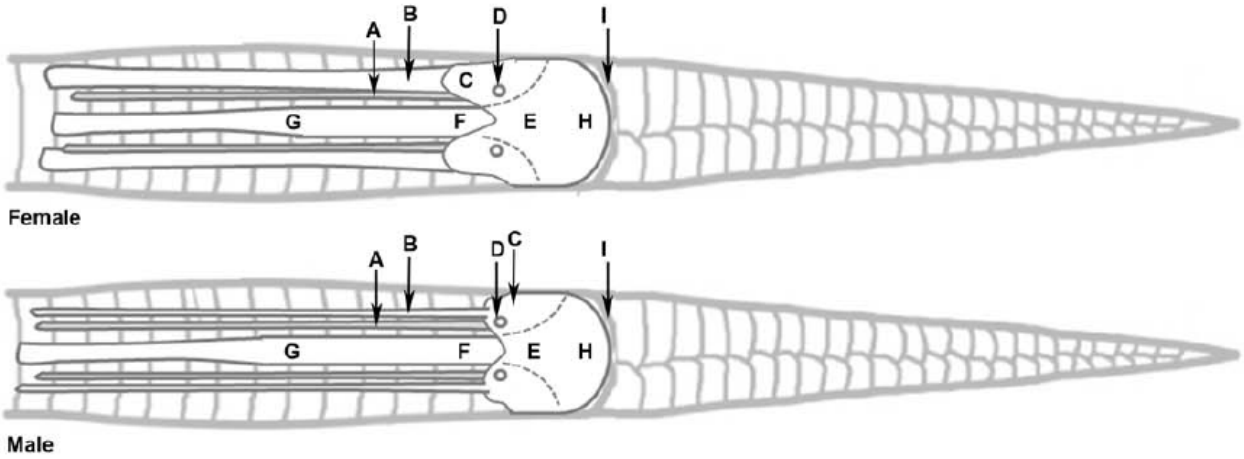

Figure 5-1. Line drawing of snake indicating relative positions of cloacal chambers in female (upper) and male (lower) watersnakes. The anterior of the animal is to the left in this figure. Key: A – ureter, B – posterior vagina (female)/ductus deferens (male), C – L/R urodael chambers, D – junction of ureter and common urodael chamber, E – common urodael chamber, F – coprodaeum (dotted lines indicate coprodeal/urodael junction), G – colon, H – proctodaeum, I – vent. Snake body outline adapted from: http://www.reptilesdownunder.com/arod/scale/.

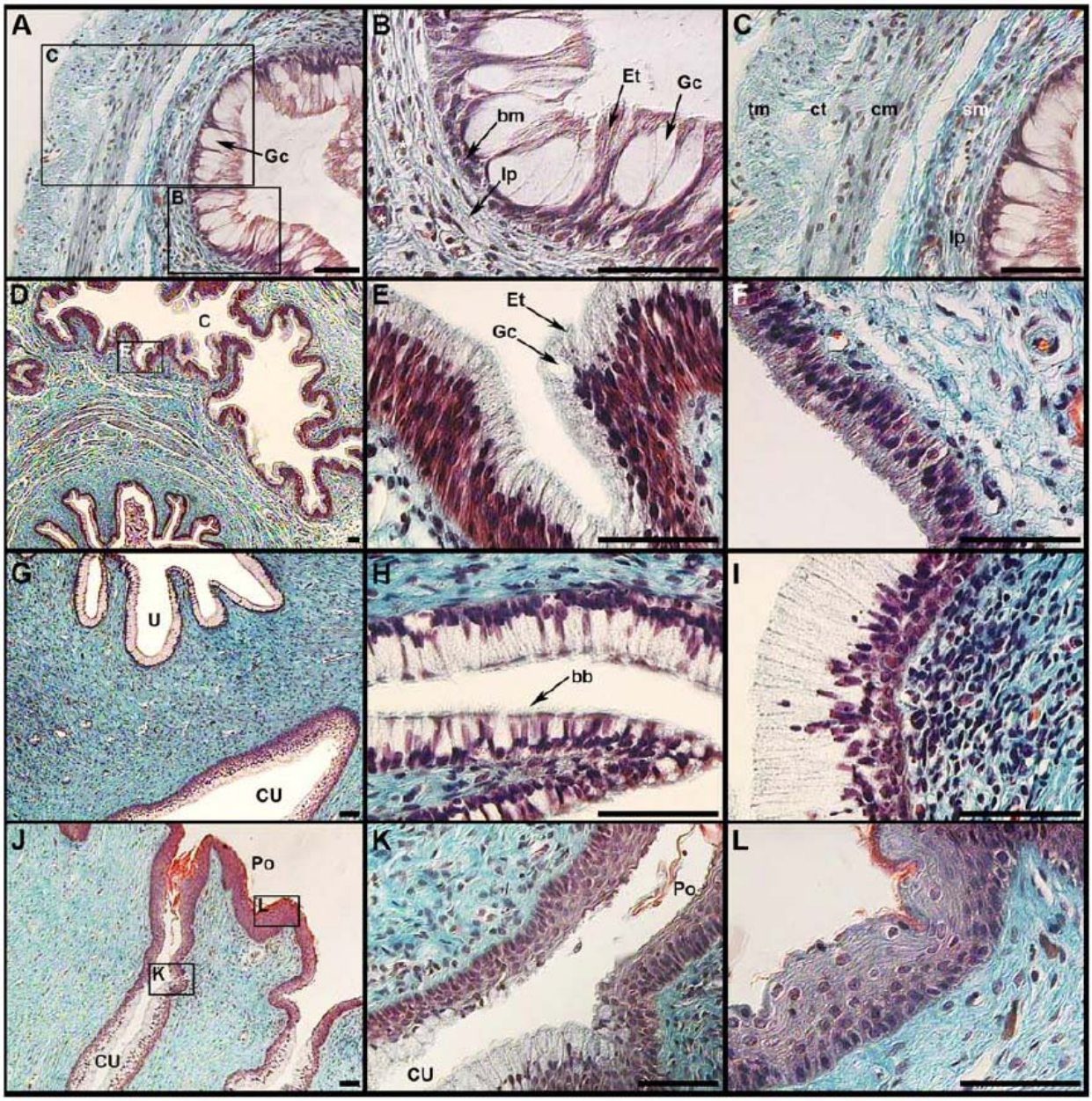

Figure 5-2. Representative sections of colon (A-C), coprodaeum (D-F), urodaeum (G-I), and proctodaeum (J-L) of watersnakes. No differences in morphology were detected between species. Areas of higher magnification (typically middle and right panels) are indicated by the boxed areas in low-magnification images (typically left panels). Abbreviations: basement membrane (bm), brush border (bb), circular muscle (cm), common urodaeum (CU), connective tissue (ct), coprodaeum (C), enterocyte (Et), goblet cell (Gc), lamina propria (lp), L/R urodael chambers (U), proctodaeum (Po), submucosa (sm), transverse muscle (tm). Images produced using Masson Trichrome stain and differential interference microscopy. Scale bars = 50 μm.

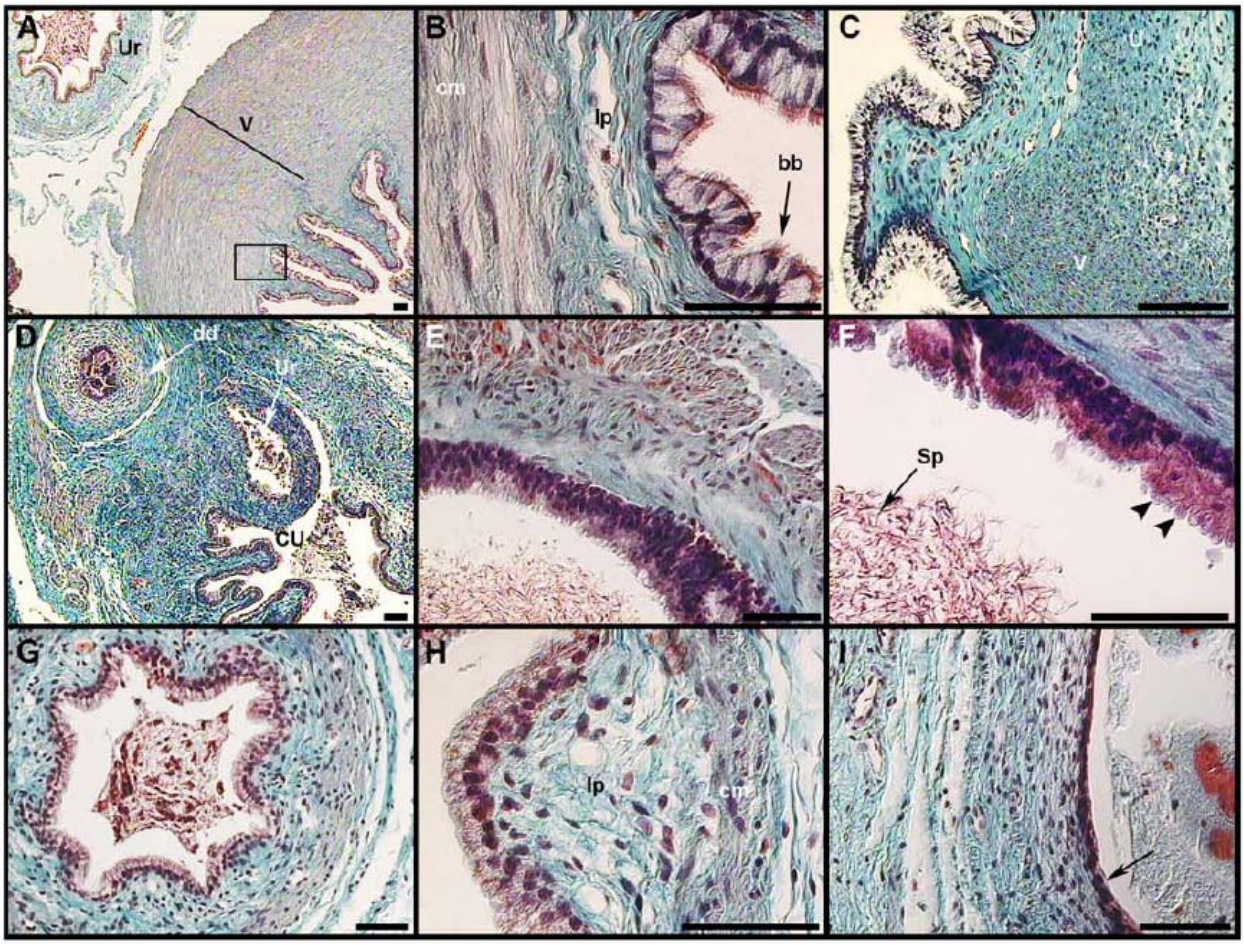

Figure 5-3. Representative sections of the posterior vaginal (A-C), ductus deferens (D-F), and ureters (G-I) of watersnakes. Arrowheads in F indicate convex apical membranes of epithelial cells in the ductus deferens. The arrow in I points to the low stratified squamous epithelium of the ureter where it meets the common urodael chamber. Abbreviations: brush border (bb), circular muscle (cm), common urodael chamber (CU), ductus deferens (dd), lamina propria (lp), L/R urodael chamber (U), ureter (Ur), vagina (V), sperm (Sp). Images produced using Masson Trichrome stain and differential interference microscopy. Scale bars = 50 µm.

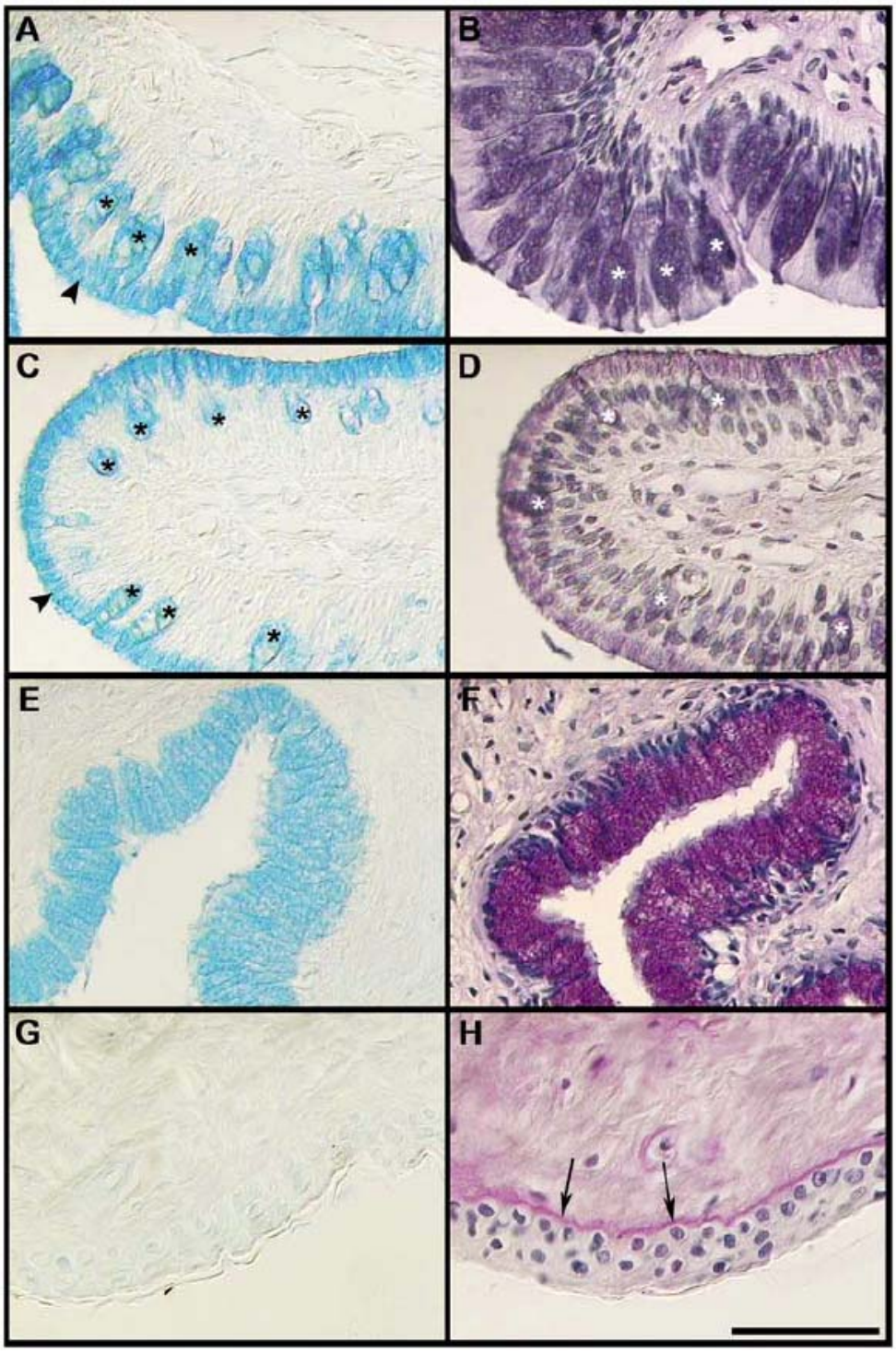

Figure 5-4. Representative sections of epithelium from the colon (A,B), coprodaeum (C,D), urodaeum (E,F), and proctodaeum (G,H) stained using Alcian blue (A,C,E,G) and PAS (B,D,F,H). Stars indicate the position of goblet cells and arrowheads point to apical mucin-rich cytoplasm. Arrows in H point to basement membrane, staining positively for PAS. Images produced via differential interference microscopy. Scale bars = 50 μm.

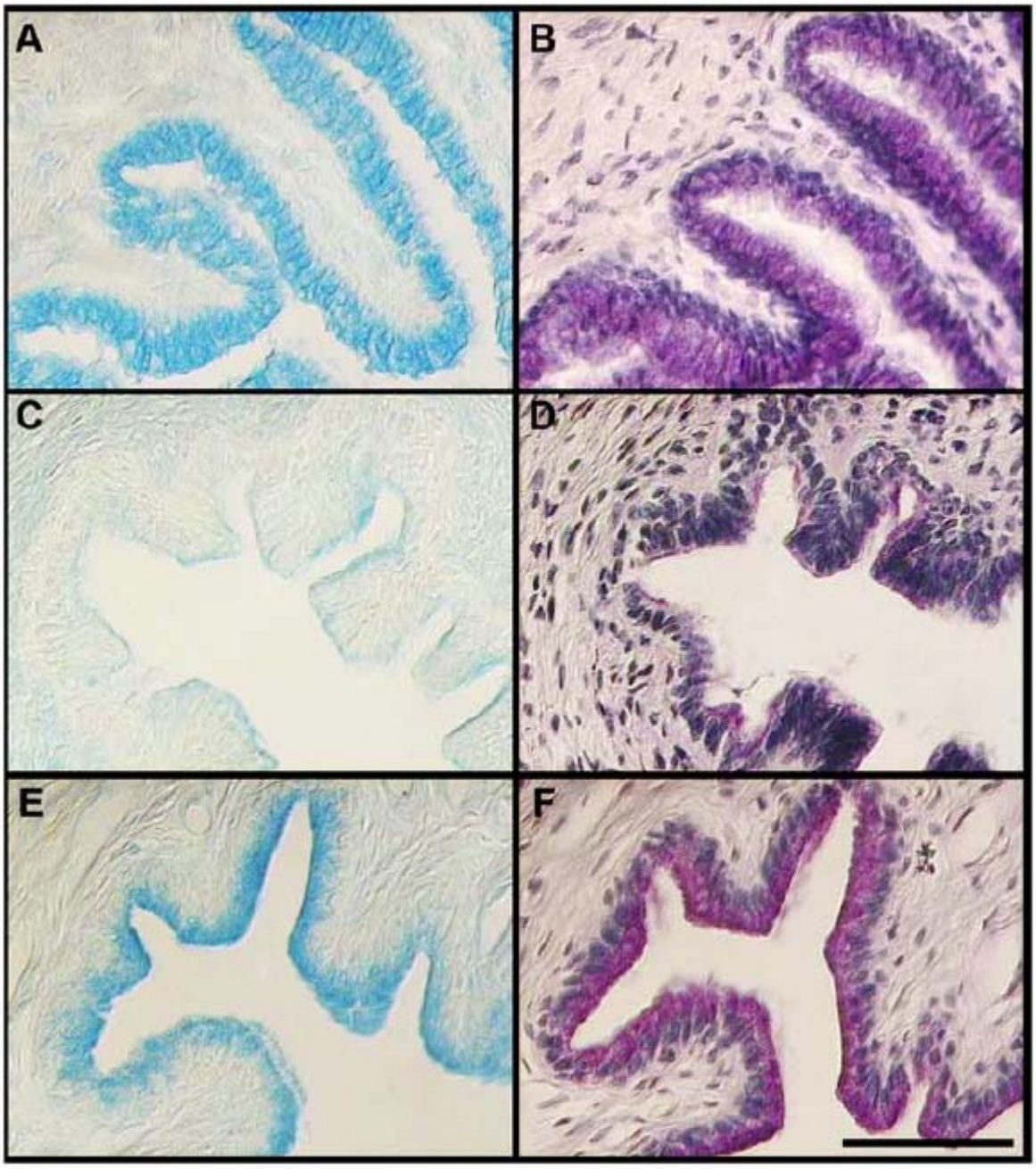

Figure 5-5. Representative sections of epithelium from the vagina (A,B), ductus deferens (C,D), and ureters (E,F) stained using Alcian blue (A,C,E) and PAS (B,D,F). Images produced via differential interference microscopy. Scale bars = 50 μm.

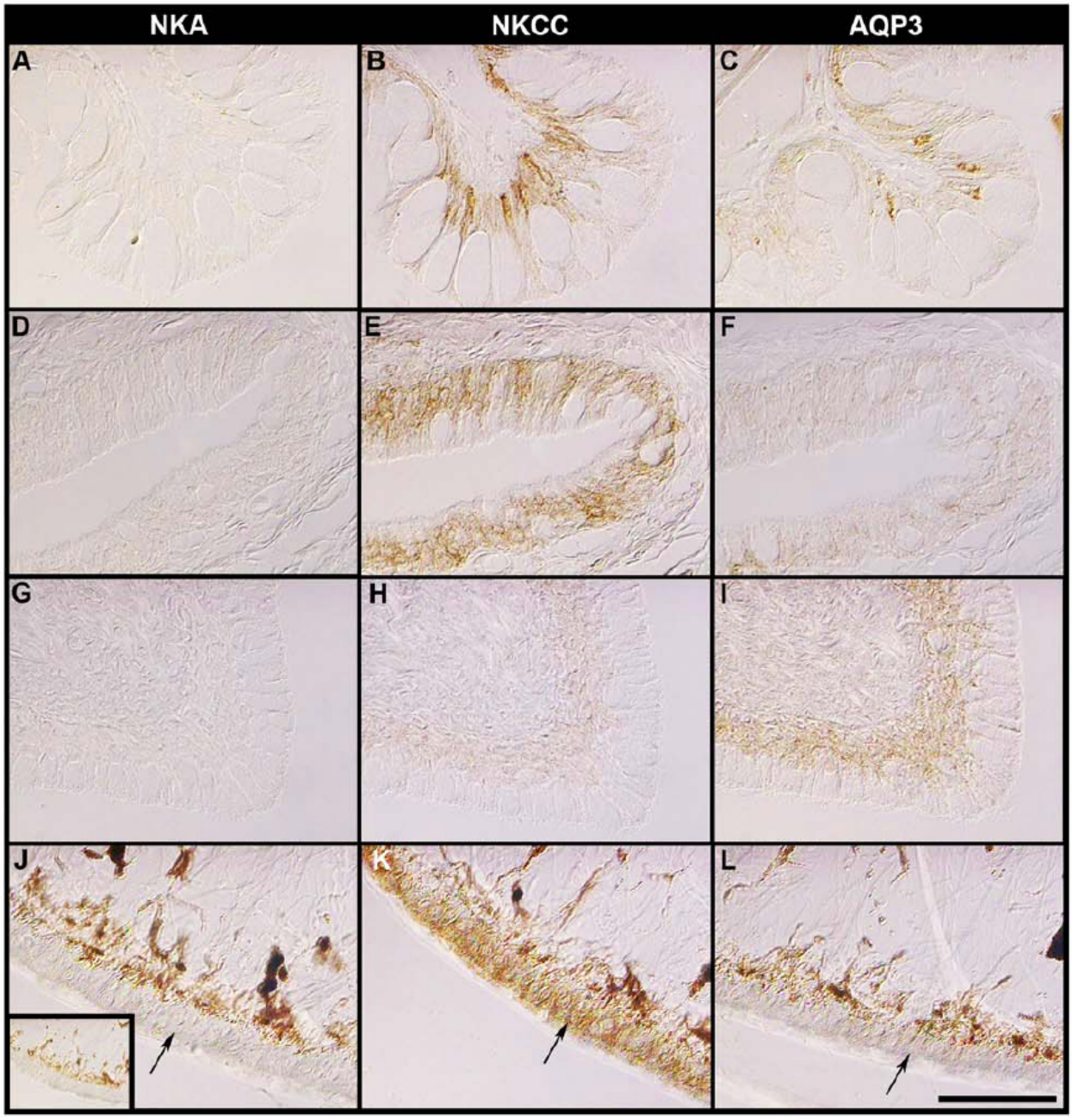

Figure 5-6. Immunolocalization of NKA, NKCC, and AQP3 in the colon (A-C), coprodaeum (D-F), urodaeum (G-I), and proctodaeum (J-L). The inset in panel J shows the negative control section for NKA, NKCC, and AQP3 in the proctodaeum and the arrows in J, K, and L point to the proctodael epithelium (positive for NKCC only). Images produced via differential interference microscopy. Scale bar = 50 μm.

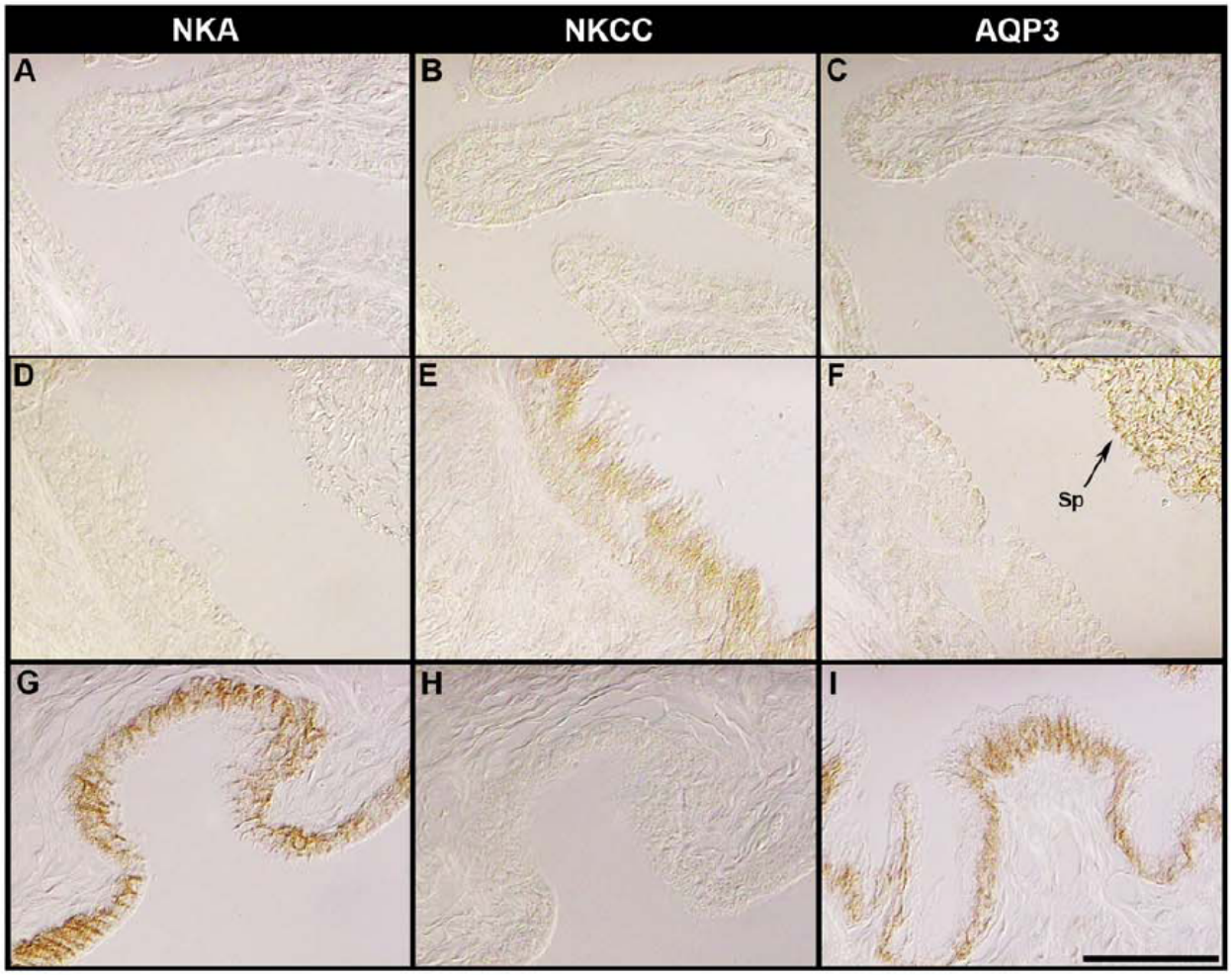

Figure 5-7. Immunolocalization of NKA, NKCC, and AQP3 in the vagina (A-C), ductus deferens (D-F), and ureters (G-I). Arrow in F points to AQP3-positive sperm. Images produced via differential interference microscopy. Scale bar = 50 μm.

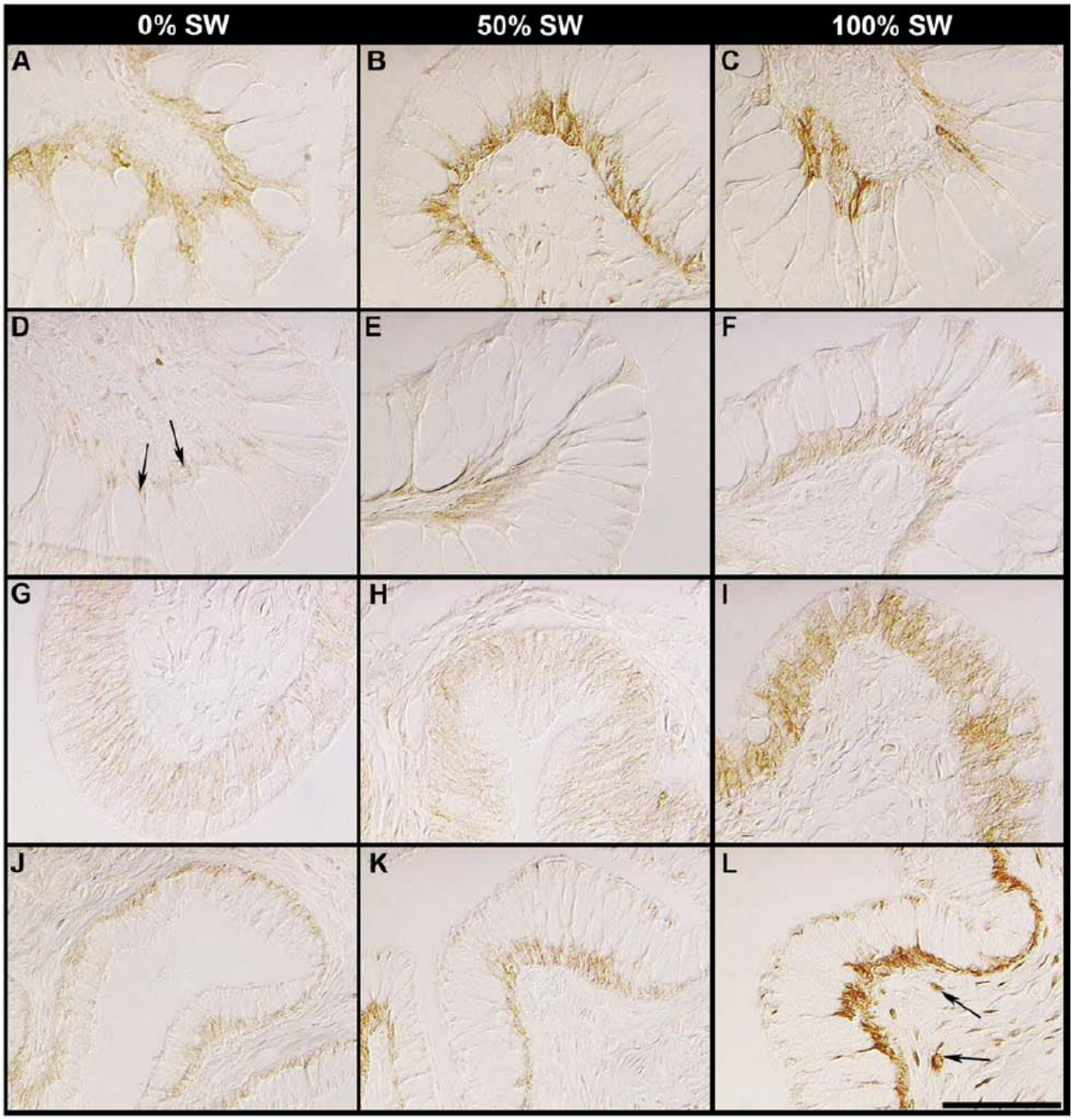

Figure 5-8. Immunolocalization of NKA, NKCC, and AQP3 was not affected by treatment. (A-C) NKCC is basal in the colonic epithelium across treatments. (D-F) AQP3 is basal (though nearly absent in the 0% SW treatment) in the colon of animals from all treatments. (G-I) NKCC is basal in the coprodaeum from all treatments and appears to increase in abundance in the 100% SW treatment, relative to the 0 and 50% SW treatments. (J-L) AQP3 is basolateral in the urodaeum in all salinities but also appears to increase in the 100% SW treatment relative to 0 and 50%. Images produced via differential interference microscopy. Scale bar = 50 μm.

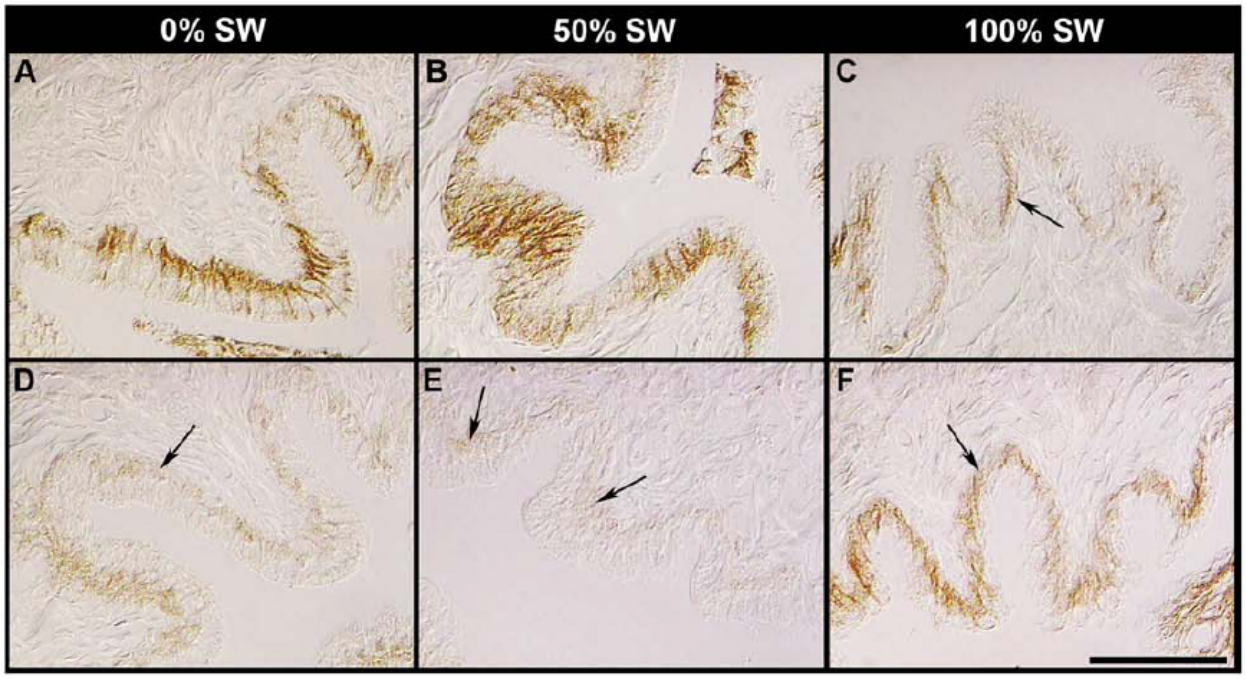

Figure 5-9. Immunolocalization of NKA and AQP3 in the ureters was not affected by treatment. (A-C) NKA is basolateral in the ureter and appears lower in abundance in the 100% SW treatment, relative to 0 and 50% treatments. (D-F) AQP3 is basolateral in all treatments but is very weak in 0 and 50% whereas the abundance of AQP3 appears to increase in 100% SW. Images produced via differential interference microscopy. Scale bar = 50 μm.

CHAPTER 6
CONCLUSIONS

Phylogeny Recapitulates Ontogeny?

Ernst Haeckel's famous Biogenic Law, though flawed in its explanation of the process of evolution, underscores the value of using data that *are* available (e.g., from detailed studies of the development of a single species) to make inferences about data that *aren't* available (e.g., a detailed understanding of the relationships among diverse taxa). The studies presented herein make use of phylogeny (comparisons of divergent taxa) to hypothesize about the evolution of hypo-osmoregulation in snakes. This approach assumes that contemporary marine snakes (i.e., those with a salt gland) are descendents of semi-marine/estuarine species which were themselves, descendents of freshwater species (a hypothesis originally proposed by Dunson and Mazzotti, 1989). By comparing the form and function of various tissues in the fully marine sea snake, *Laticauda semifasciata*, with homologous tissues from the semi-marine salt marsh snake, *Nerodia clarkii clarkii*, I develop several hypotheses about the evolution of hypo-osmoregulation in snakes. To ensure that the commonalities identified between these two groups are associated with marine habitat use, I make further comparisons with homologous tissues from an ecological "outgroup" (the freshwater species, *Nerodia fasciata*.)

While it would have been ideal to extend the studies presented herein to include comparisons between *L. semifasciata* and its closest freshwater relative, a study of this kind was not feasible for various reasons (including the difficulty associated with collecting/maintaining Elapids). Future studies of the morphology and biochemistry of the cephalic glands of terrestrial and freshwater Elapids (perhaps through use of

museum specimens) as well as detailed studies of the form and function of the cephalic glands in the various lineages of marine/estuarine Homalopsids (old world watersnakes) would be very informative in testing the hypotheses outlined in these studies.

Why Study Reptiles?

Despite decades of study, the osmoregulatory physiology of reptiles remains poorly understood (Dantzler and Bradshaw, 2009). Following the discovery of salt glands in this group (Schmidt-Nielsen and Fange, 1958), much attention was directed toward examining the osmoregulatory capacity of reptiles from desiccating environments, particularly deserts and oceans. Interest in the osmoregulatory physiology of reptilian taxa, however, appears to have dwindled over the last few decades, such that modern studies (in the last ~10 years) are largely restricted to those of a single group studying the physiology and plasticity of the saltwater crocodile (*Crocodylus porosus*) from marine and freshwater environments in Australia (Kuchel and Franklin, 2000; Franklin et al., 2005; Cramp et al., 2007; 2008; 2010a; 2010b). Thus, many of the modern techniques for examining the distribution and abundance of membrane regulatory proteins (e.g., NKA and AQP3) and their underlying mRNA have not been used in the study of reptiles (but, see: Cramp et al., 2010b).

The studies presented herein represent, to my knowledge, the first to use immunohistochemistry and molecular biology to describe the biochemical morphology of the osmoregulatory tissues in snakes and to examine the effects of environmental salinity on membrane water and ion transport in a range of reptiles from marine and freshwater environments. Furthermore, I am the first to isolate and characterize AQPs from any reptile. In many ways, my data support the results of similar studies from other vertebrate taxa. Important differences, however, were also identified and have the

potential to influence an understanding of the evolution of hypo-osmoregulatory mechanisms among vertebrates. Provided below is a summary of my findings with a discussion of how these results fit with the state of knowledge of the field of vertebrate osmoregulatory physiology.

Physiology and Evolution of Salt Glands

Although the morphology of the salt glands has been studied previously in some species of Laticaudine sea snake (Dunson et al., 1971; Burns and Pickwell, 1972), I am the first to examine the morphology of the glands in *L. laticaudata* (Chapter 2) and the first to examine the relationship between the biochemistry/morphology of the salt glands and habitat use (Chapter 2) across species in this lineage. Because NKA and NKCC were found to be basolateral in the salt glands of all three species of *Laticauda,* I can infer that the function of these two proteins is similar to the role they play in facilitating the secretion of NaCl in other vertebrate secretory epithelia (Haas and Forbush, 2000; Kaplan, 2002). Despite many attempts at localizing CFTR protein, I was unable to detect this protein in the apical membrane of the secretory cells, where it regulates apical Cl^- transport in other vertebrate secretory epithelia (Kunzelmann, 1999). This is especially surprising considering the CFTR gene is transcribed in the salt gland (Chapter 3) and that positive immunoreaction was detected in the mucus-secreting goblet cells of the gastrointestinal tract (Fig A-1; Appendix). Clearly, further studies aimed at understanding apical Cl^- transport in the ionosecretory cells of reptilian osmoregulatory tissues, in particular, salt glands, are necessary.

Surprisingly, I did not detect an effect of environmental salinity on the abundance or distribution of NKA, NKCC, CFTR, or AQP3 in the salt glands of *L. semifasciata*. A recent study of crocodilian salt gland plasticity suggested that NKA mRNA and protein

increased in abundance in SW acclimated animals though, like mine, this study failed to detect significant differences between FW and SW animals (Cramp et al., 2010b). Importantly, the activity of NKA (as well as NKCC and CFTR) can be modified by phosphorylation. Thus, while further studies of the activity and/or the phosphorylation status of NKA, NKCC, and CFTR (via enzyme immunoassay or western blot) would be of interest, previous studies of both snakes and crocodiles suggest that NKA activity is unaffected by salinity treatment (Dunson and Dunson, 1975; Cramp et al., 2010b). Clearly much remains to be learned about the plasticity of ion transport in the secretory epithelia of reptiles.

Although AQP3 was not detected in the salt gland of *L. semifasciata*, AQPs 1 and 5 have been identified from salt glands of birds (Muller et al., 2006) and AQP3 has been identified from a variety of other tissues in snakes (Chapter 4). Additionally, AQP3 was detected in the harderian gland of *L. semifasciata* (Chapter 3) as well as several of the cephalic glands from the *Nerodia* (Chapter 3) suggesting this protein may play a role in the production of dilute watery secretion, potentially in concert with the production of mucus (Lignot et al., 2002). Since I am the first to examine the distribution of any AQPs in reptiles, additional studies of AQP distribution and function (in particular, studies of the regulation of the various AQPs in osmoregulatory tissues) are necessary before comparisons can be made across vertebrate taxa. Of particular interest is the isolation and characterization of the full suite of AQPs present in the cephalic glands of all three species studied herein and the relationship between the localization/abundance of these proteins during time of water and salt stress.

Another significant contribution of this work to the field of evolutionary physiology is examination of the cephalic glands in the marine and freshwater species of *Nerodia*. Following failure to collect salty secretion from the cephalic glands in *N. c. compressicauda,* this group was generally considered to lack salt glands (Schmidt-Nielsen and Fange, 1958). Detailed studies of the morphology and biochemistry of the head glands, though warranted (Dunson, 1984), were never undertaken until now. The results from the studies presented in Chapter 3 enabled us to expand on early hypotheses about the evolution of salt glands to include explicit steps through which an unspecialized gland may have been co-opted to form a salt gland. Implicit in my evolutionary co-option hypothesis is the evolution of homogeneity in cell type within a gland, a feature that appears to be more extreme among marine snake salt glands than in other vertebrate taxa (Dunson et al., 1971; Dunson and Dunson, 1975; Babonis et al., 2009). What is lacking, is an understanding of the mechanism by which this homogeneity of cell type may have arisen during the evolution of salt glands.

A recent study of sublingual gland development in mice suggest that specific transcription factors in the NK-2 family may be responsible for conferring mucous cell fate on the cells populating the glandular epithelia (Biben et al., 2002). The posterior sublingual glands in both *N. c. clarkii* and *N. fasciata*, like the posterior sublingual salt gland in *L. semifasciata,* appear to be populated by a single mucus-secreting cell type; in contrast with this, many of the other cephalic glands in the *Nerodia* were heterogeneous assemblages of both serous and mucous cell types (Chapter 3). In future studies, it would be interesting to examine the effect of mis-expression of Nkx 2.3 on the phenotype of developing cephalic glands. Specifically, a study of this type would

aid in understanding the evolutionary mechanisms underlying co-option of a heterogeneous unspecialized precursor gland to form a homogeneous derived salt-secreting gland.

Physiology of the Kidneys and Gut/Cloaca

Because the salt gland is the primary means by which marine reptiles excrete salt (Holmes and McBean, 1964; Dunson, 1968), I expected the renal response to salinity acclimation to differ in animals with and without salt glands. In particular, kidneys from animals with salt glands were expected to vary little with changes in environmental salinity, reflecting the dominant role of the salt gland in responding to perturbations in plasma homeostasis. By contrast, those species that do not have a salt gland may be expected to (i) minimize the reabsorption of ions from the renal, gastrointestinal, and cloacal membranes following acclimation to high salinity, and/or (ii) continue to reabsorb ions to get the solute-linked water while simply tolerating a slow/steady increase in plasma osmolality. This latter case has been observed in both desert lizards and tortoises (Bradshaw and Shoemaker, 1967; Nagy and Medica, 1986) but does not appear to be the case for *N. c. clarkii*. *N. c. clarkii,* unlike its freshwater congener *N. fasciata*, maintained low plasma ion concentrations even following acclimation to 50% and 100% SW (Chapter 4).

The survival and plasma homeostasis differences observed in *N. c. clarkii* and *N. fasciata* do not, at first approximation, appear to be related to differences in the renal/post-renal osmoregulatory tissues between these two species. It is important to note, though, that the studies described herein examined the distribution and abundance of only a few ion/water transporters and a thorough analysis of membrane ion/water transport in these species will require further testing. In particular, future

studies aimed at identifying the apical ion/water transporters in both the proximal and distal nephron and in the cloaca will be highly informative. Additionally, studies focused on investigating the stimulatory signals regulating ion/water secretion in the kidneys and gut/cloaca as well as the salt glands of snakes will greatly advance the state of knowledge in this field.

Despite the fact that I largely found no effects of salinity acclimation on the morphology or biochemistry of the kidneys and colon/cloaca, several interesting results did come out of these studies. In particular, and as mentioned above, I am the first to localize AQP3 protein in the renal (Chapter 4) and gastrointestinal (Chapter 5) tissues of any reptiles. Much like the distribution of this protein in other taxa, the basolateral localization of AQP3 in the collecting ducts suggests a role for this water channel in modification of the urine through reabsorption of water from the filtrate. I also identified a putative apical/cytoplasmic localization of AQP3 in the distal tubules of *L. semifasciata* which was unexpected, but is similar to the apical/cytoplasmic localization of AQP3 in the proximal tubule of *Xenopus* (Mochida et al., 2008) and the gill of *Anguilla* (Lignot et al., 2002). The distribution of AQP3 in the tissues of fishes is known to be quite variable (for a review, see: Deane and Woo, 2006); thus, the differences I find in the distribution of AQP3 in the distal tubules of *Laticauda* and *Nerodia* may provide further support the species-specific nature of AQP3-mediated water transport.

The results of these studies clearly underscore the need for additional studies of AQP distribution and function in the reptile kidney. In particular, it would be of interest to examine the distribution of AQP1 and AQP2 (both apical water channels) in the renal tubules in comparison with the distribution of AQP3 and other potential basolateral

AQPs. Of note, AQP4 is known from the mammalian kidney to be localized to the basolateral membranes of the distal nephron (distal tubules and collecting ducts) where it plays a redundant/complimentary role with AQP3 in facilitating the passage of water from the cytoplasm to the peritubular blood supply (see:Nielsen et al., 2002, for a review of kidney aquaporins). In concert with this, I detected AQP4 in the basement membranes of the distal nephron (late distal tubule, renal sex segment, and collecting duct) and blood supply in the kidneys of all three species of snake (Fig A-2; Appendix). While the anti-AQP4 antibody (SC-20812; Santa Cruz Biotechnology, Santa Cruz, CA, USA) appears to be specific in all three species (Fig A-3; Appendix), the presence of two bands in *L. semifasciata* suggests that AQP4 might undergo post-translational modification, a process that has been hypothesized to regulate AQP4-mediated water transport in rats (Han et al., 1998). Since AQP4 was not detected in the kidney of *L. semifasciata* using IHC (Fig A-2A; Appendix). Further studies of the distribution and regulation of AQP4 in the kidney of sea snakes are necessary to understand these discordant results.

Another interesting result from these studies was the localization of AQP3 in the urothelium of snakes (Chapter 5). Although there have been very few studies of the function of the urothelium in regulating water and ion transport in reptiles, my results suggest that the ureters are potentially and important site of water reclamation in snakes, a process also known to be AQP3-mediated in the urothelium of mammals (Spector et al., 2002). Dehydration of the feces in aquatic snakes may also be facilitated by AQP3, as evidenced by the localization of AQP3 to the colonic and coprodael epithelium. This hypothesis is consistent with early hypotheses that the formation of

fecal pellets in the various parts of the coprodaeum was associated with water reabsorption across the coprodael epithelium (Seshadri, 1959; Minnich and Piehl, 1972). Taken together, the results of these studies suggest that snakes in the genus *Nerodia* may well have the ability to vary water reabsorption in the production/modification of urinary and fecal waste, potentially contributing to their ability to maintain water balance in desiccating environments. Importantly, however, no specializations for the secretion of excess salt were found in either species of *Nerodia*. Despite the lack of effects of salinity acclimation the results of these studies are novel and contribute much to a deeper understanding of membrane ion and, especially, water transport in reptiles.

The combined results of the studies presented herein suggest that, in the evolution of marine habitat use among reptiles, development of a salt gland, even one with a limited initial capacity for ion secretion, may have figured more prominently than modifications to the function of the renal and post-renal tissues. Indeed, across vertebrate taxa, the kidney appears to be a critical component of the water regulatory system while it is only among mammals that the kidneys also serve as the sole ion regulatory system. Considering that the ability of the mammalian kidney (and the mammalian-type nephrons in the kidneys of some birds) to produce concentrated urine derives, in part, from the parallel organization of the nephrons and collecting ducts, the diversity of vertebrate taxa that have evolved extra-renal means of secreting concentrated salts may, in fact, suggest that evolution of a salt-secreting gland (perhaps via co-option of an unspecialized precursor) may be ‘easier’ than reorganization of the kidney. It is interesting to note that the concentrating mechanism of the renal tubules

relies on countercurrent flow and this is not the case for vertebrate salt glands. Thus, the evolution of this simple system for ion secretion may require fewer steps (fewer modifications to existing structures) than evolutionary modification of the kidney.

Future Directions in this Research

In general, there are several limitations to these studies presented herein that the use of additional techniques could rectify. In particular, throughout these studies, the localization of specific ion/water transporters (NKA, NKCC, AQP3, etc) was examined but as has been shown in other taxa, many of these proteins undergo post-translational modification that affects the function without changing the localization. Thus, additional studies of the activity of NKA and/or the phosphorylation/glycosylation state of these ion transporters and aquaporins following acclimation to 0% and 100% SW would help to refine the issue of how these ionoregulatory proteins respond to environmental salinity. Additionally, though I was unsuccessful in localizing CFTR in either the salt gland or harderian gland, I was able to extract the mRNA from these tissues. Using *in situ* hybridization to localize the cells in which this mRNA is transcribed would enable us to make further comparisons between the distribution of CFTR and putative gland function (and these data would help to further inform my hypothesis regarding the co-option of a salt gland from an unspecialized precursor). Additionally, functional studies of apical Cl^- transport would be informative in confirming the presence of CFTR in these tissues, in the absence of antibodies that can detect the protein *in situ*.

These same comments regarding further analyses of protein regulation in the cephalic glands would also further our understanding of the form and function of the snake kidney. In addition, further characterization of the identity, distribution, and response to changes in environmental salinity of the various aquaporins in the renal

tubular epithelia are necessary before the water regulatory function of snake kidneys can be fully assessed. Finally, my studies of the putative function of the cloaca are only a meager start to uncovering the potential contribution of this organ to whole-animal osmoregulatory balance. Two classes of study would be most informative in furthering an understanding of the function of the snake cloaca: (i) physiological studies of membrane ion transport, making use of ion channel blocking agents, to definitively assess the role of each chamber in facilitating reabsorption of water/ions during times of hypo- and hyper-saline stress, and (ii) the use of chemical/radioactive tracers to follow the storage of urinary and fecal wastes in the various cloacal compartments would further aid in partitioning the relative importance of the various chambers.

Beyond the contributions of additional techniques, several complimentary studies would augment the results presented herein. Foremost, I suggest that a comparative study of the development of salt glands and unspecialized gland would contribute much to a continued understanding of the development of this specialized osmoregulatory organ and, importantly, may shed light on the mechanism by which this tissue evolved from an unspecialized precursor. Importantly, these studies would be highly unfeasible in snakes but may be quite straightforward in other model taxa. The other major contribution to advancing the field of reptile osmoregulation would be studies of the neural and hormonal regulation of ion and water transport across the tissues examined in these studies. While few studies of hormonal control of transport in the kidney and cloaca have been performed, little is known regarding the nervous control of secretion in the salt glands of reptiles, despite the potential for these data to help resolve issues regarding the evolution of salt glands from unspecialized glands. Thus, further

examinations of the potential relationship between hormonal and nervous control would contribute greatly to understanding the intricacies of evolutionary co-option.

In addition to the studies proposed above examining the development of various specialized and unspecialized cephalic glands, a critical next step in this line of research is to collect and characterize (biochemically) the secretion produced by each type of gland studied herein. While the definition of a salt gland may well lie in the binary state of the gland as either capable or incapable of secreting a salt solution that is hypertonic to the blood plasma, characterization of the secretion may actually reveal much more about the evolution of hypertonic secretory capacity in reptilian cephalic glands. In particular, collection of secretion that is higher in concentration in *N. c. clarkii* than in *N. fasciata* would provide initial support for the hypothesized trajectory of salt gland evolution proposed in Chapter 3. Conversely, isolation of identical secretory products from *N. c. clarkii* and *N. fasciata* would suggest that the hypotheses proposed herein regarding the abundance of ion transporters in the sublingual glands of the *Nerodia* must be re-evaluated.

As regards potential ecological and behavioral differences between the freshwater and semi-marine species of water snake, an interesting follow-up study would involve the quantification of differences in the volume of water consumed incidentally while feeding in an aquatic habitat (so-called "incidental drinking"; Dunson, 1985). In contrast with marine turtles (Bjorndal, 1985), snakes are not known to have any morphological features that allow them to expel water from the mouth before swallowing a prey item. As such, incidental drinking of salt water during prey capture may well serve as an important means of salt uptake. The semi-marine species of watersnake (*N. c. clarkii*)

may experience a selective advantage over their freshwater counterparts if they have developed an ability to reduce the amount of water taken in while feeding. Thus, additional studies should be aimed at assessing the detailed feeding behavior of these two species, including observations of where prey capture/swallowing occur (e.g., under water or above) and whether this behavior is modified when animals capture prey in salt- vs. freshwater. Additionally, detailed studies of the microhabitat use in these two species would enable a more detailed analysis of the potential salt and water stress experienced by each species in the wild. In particular, basking behavior may result in increased cutaneous water loss and, thus, it might be expected that *N. c. clarkii* exhibits modified basking behavior to minimize this potential dehydration stress.

APPENDIX
IMMUNOLOCALIZATION OF CFTR AND AQP4 IN THE OSMOREGULATORY TISSUES OF *NERODIA*

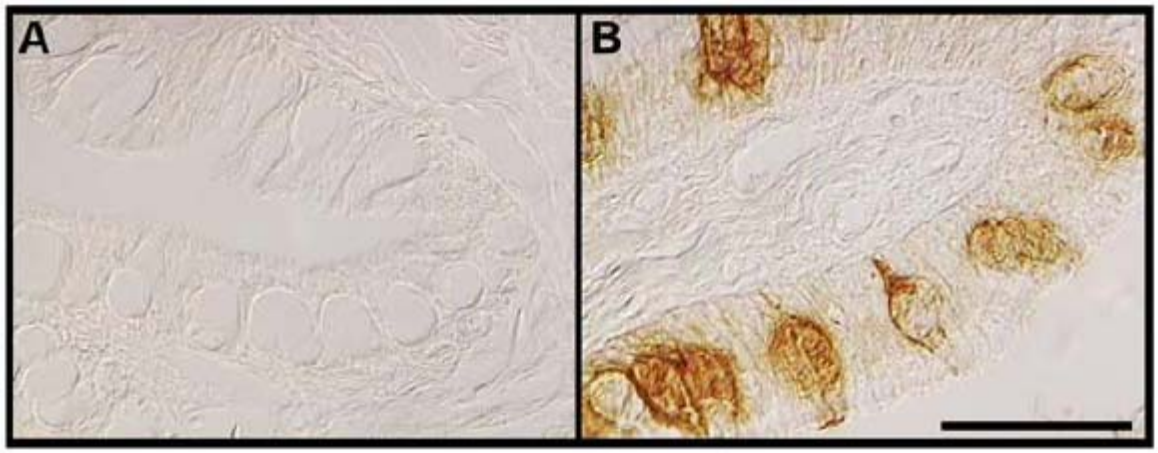

Figure A-1. Immunolocalization of CFTR (antibody 60) in the coprodael epithelium of watersnakes. (A) CFTR is absent from the coprodaeum of *N. c. clarkii* but appears to be present in the goblet cells of *N. fasciata* (B). Images produced by differential interference microscopy. Scale bar = 50μm.

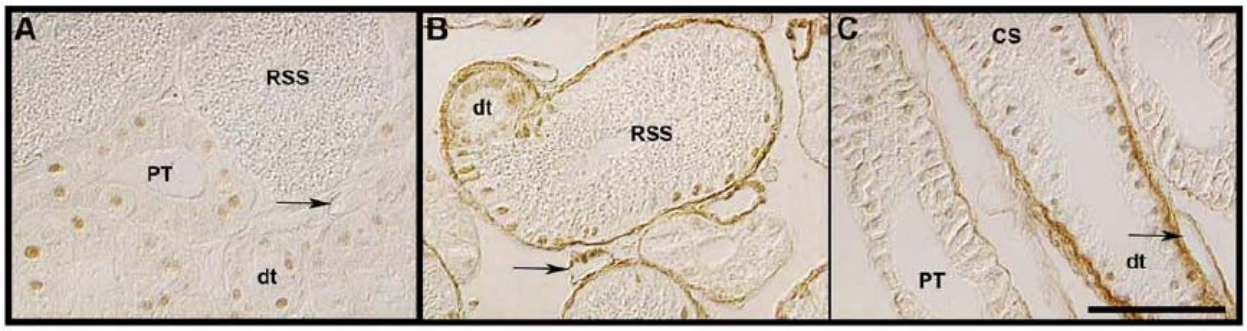

Figure A-2. Immunolocalization of AQP4 (SC-20812) in the nephron of aquatic snakes. (A) Positive reaction for AQP4 is evident only in the nuclei of the cells in the proximal and distal tubules in *L. semifasciata*. Among (A) *N. c. clarkii* and (B) *N. fasciata*, AQP4 is positive in the basement membrane of the distal nephron (distal tubule, renal sex segment, connecting segment, and collecting duct) as well as the nuclei in these tissues. Furthermore, AQP4 was detected in the blood vessels (arrows) of *N. c. clarkii* and *N. fasciata* only. Images produced by differential interference microscopy. Scale bar = 50μm.

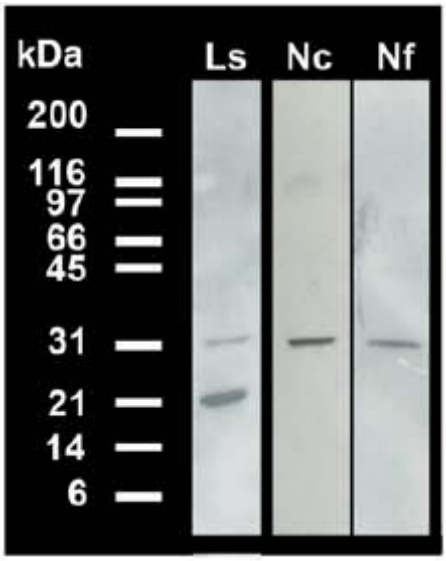

Figure A-3. Representative western blots showing the specificity of AQP4 (antibody SC-20812) which detects a protein of approximately 34 kDa in the tissues of *L. semifasciata* (Ls), *N. c. clarkii* (Nc), and *N. fasciata* (Nf). The additional band in the Ls lane suggests a second, smaller, product is also detected by this antibody.

LIST OF REFERENCES

Akabane G, Ogushi Y, Hasegawa T, Suzuki M, Tanaka S. 2007. Gene cloning and expression of an aquaporin (AQP-h3BL) in the basolateral membrane of water-permeable epithelial cells in osmoregulatory organs of the tree frog. Am J Physiol Regul Integr Comp Physiol 292(6):R2340-2351.

Babonis LS, Hyndman KA, Lillywhite HB, Evans DH. 2009. Immunolocalization of Na^+/K^+-ATPase and $Na^+/K^+/2Cl^-$ cotransporter in the tubular epithelia of sea snake salt glands. Comp Biochem Physiol Part A Mol Integr Physiol 154(4):535-540.

Baccari GC, Ferrara D, Di Matteo L, Minucci S. 2002. Morphology of the salivary glands of three *Squamata* species: *Podarcis sicula sicula*, *Tarentola mauritanica,* and *Coluber viridiflavus*. Acta Zool (Stockh) 83(2):117-124.

Barnitt AE, Goertemiller CC. 1985. Nasal salt-secreting glands of normal and hyperkalemically stressed *Sauromalus obesus* - histology and cytology. Copeia(2):403-409.

Bennett DC, Hughes MR. 2003. Comparison of renal and salt gland function in three species of wild ducks. J Exp Biol 206(18):3273-3284.

Bentley PJ. 1959. Studies on the water and electrolyte metabolism of the lizard *Trachysaurus rugosus* (Gray). Journal of Physiology-London 145(1):37-47.

Bentley PJ, Bradshaw SD. 1972. Electrical potential difference across the cloaca and colon of the Australian lizards *Amphibolurus ornatus* and *A. inermis* Comp Biochem Physiol 42(NA2):465-471.

Bentley PJ, Bretz WL, Schmidt-Nielsen K. 1967. Osmoregulation in the diamondback terrapin, *Malaclemys terrapin centrata*. J Exp Biol 46(1):161-167.

Benyajati S, Dantzler WH. 1988. Enzymatic and transport characteristics of isolated snake renal brush-border membranes. Am J Physiol 255(1):R52-R60.

Bertorello AM, Aperia A, Walaas SI, Nairn AC, Greengard P. 1991. Phosphorylation of the catalytic subunit of Na^+/K^+-ATPase inhibits the activity of the enzyme. Proc Natl Acad Sci U S A 88(24):11359-11362.

Beyenbach KW. 1984. Water-permeable and water-impermeable barriers of snake distal tubules. Am J Physiol 246(3):F290-F299.

Beyenbach KW, Dantzler WH. 1978. Generation of trans-epithelial potentials by isolated perfused reptilian distal tubules. Am J Physiol 234(3):F238-F246.

Biben C, Wang CC, Harvey RP. 2002. NK-2 class homeobox genes and pharyngeal/oral patterning: Nkx2-3 is required for salivary gland and tooth morphogenesis. Int J Dev Biol 46(4):415-422.

Billon-Bruyat J-P, Lécuyer C, Martineau F, Mazin J-M. 2005. Oxygen isotope compositions of Late Jurassic vertebrate remains from lithographic limestones of western Europe: implications for the ecology of fish, turtles, and crocodilians. Palaeogeogr Palaeoclimatol Palaeoecol 216(3-4):359-375.

Bjorndal KA. 1985. Nutritional Ecology of Sea Turtles. Copeia 1985(3):736-751.

Blanco G, Mercer RW. 1998. Isozymes of the Na^+/K^+-ATPase: Heterogeneity in structure, diversity in function. Am J Physiol 275(5 Pt 2):F633-650.

Borgnia M, Nielsen S, Engel A, Agre P. 1999. Cellular and molecular biology of the aquaporin water channels. Annu Rev Biochem 68:425-458.

Bradshaw SD, Shoemaker VH. 1967. Aspects of water and electrolyte changes in field population of *Amphibolurus* lizards. Comp Biochem Physiol 20(3):855-865.

Braun EJ. 1999. Integration of organ systems in avian osmoregulation. J Exp Zool 283(7):702-707.

Braysher M, Green B. 1970. Absorption of water and electrolytes from cloaca of an Australian lizard, *Varanus gouldii* (Gray). Comp Biochem Physiol 35(3):607-614.

Burns B, Pickwell GV. 1972. Cephalic glands in sea snakes (*Pelamis*, *Hydrophis* and *Laticauda*). Copeia(3):547-559.

Choe KP, Kato A, Hirose S, Plata C, Sindic A, Romero MF, Claiborne JB, Evans DH. 2005. NHE3 in an ancestral vertebrate: Primary sequence, distribution, localization, and function in gills. Am J Physiol Regul Integr Comp Physiol 289(5):R1520-1534.

Conant R, Lazell Jr JD. 1973. The Carolina salt marsh snake: a distinct form of *Natrix sipedon*. Brevoria, Museum of Comparative Zoology(400):1-11.

Cramp RL, De Vries I, Anderson WG, Franklin CE. 2010a. Hormone-dependent dissociation of blood flow and secretion rate in the lingual salt glands of the estuarine crocodile, *Crocodylus porosus*. J Comp Physiol B Biochem Syst Environ Physiol 180(6):825-834.

Cramp RL, Hudson NJ, Franklin CE. 2010b. Activity, abundance, distribution and expression of Na+/K+-ATPase in the salt glands of *Crocodylus porosus* following chronic saltwater acclimation. J Exp Biol 213(8):1301-1308.

Cramp RL, Hudson NJ, Holmberg A, Holmgren S, Franklin CE. 2007. The effects of saltwater acclimation on neurotransmitters in the lingual salt glands of the estuarine crocodile, *Crocodylus porosus*. Regul Pept 140(1-2):55-64.

Cramp RL, Meyer EA, Sparks N, Franklin CE. 2008. Functional and morphological plasticity of crocodile (*Crocodylus porosus*) salt glands. J Exp Biol 211(Pt 9):1482-1489.

Cuellar HS, Roth JJ, Fawcett JD, Jones RE. 1972. Evidence for sperm sustenance by secretions of the renal sexual segment of male lizards, *Anolis carolinensis*. Herpetologica 28(1):53-57.

Cutler CP. 2007. Cloning and identification of four aquaporin genes in the dogfish shark (*Squalus acanthias*). Bull Mt Desert Isl Biol Lab 46:19-20.

Cutler CP, Cramb G. 2002. Branchial expression of an aquaporin 3 (AQP-3) homologue is downregulated in the European eel *Anguilla anguilla* following seawater acclimation. J Exp Biol 205(Pt 17):2643-2651.

Dantzler WH. 1967a. Glomerular and tubular effects of arginine vasotocin in water snakes (*Natrix sipedon*). Am J Physiol 212(1):83-91.

Dantzler WH. 1967b. Stop-flow study of renal function in conscious water snakes (*Natrix sipedon*). Comp Biochem Physiol 22(1):131-140.

Dantzler WH. 1972. Effects of incubations in low potassium and low sodium media on Na^+/K^+-ATPase activity in snake and chicken kidney slices. Comp Biochem Physiol B Comp Biochem 41(1B):79-88.

Dantzler WH. 1976. Renal function (with special emphasis on nitrogen excretion). In: Gans C, Dawson WR, editors. Biol Reptil New York: Academic Press. p 447-503.

Dantzler WH, Bentley SK. 1978. Fluid absorption with and without sodium in isolated perfused snake proximal tubules. Am J Physiol 234(1):F68-79.

Dantzler WH, Bradshaw SD. 2009. Osmotic and ionic regulation in reptiles. In: Evans DH, editor. Osmotic and ionic regulation: Cells and animals. Boca Raton, FL: CRC Press. p 443-503.

Dantzler WH, Wright SH, Brokl OH. 1991. Tetraethylammonium transport by snake renal brush-border membrane-vesicles. Pflug Arch Eur J Phy 418(4):325-332.

Deane EE, Woo NY. 2006. Tissue distribution, effects of salinity acclimation, and ontogeny of aquaporin 3 in the marine teleost, silver sea bream (*Sparus sarba*). Mar Biotechnol (NY) 8(6):663-671.

Dunson MK, Dunson WA. 1975. Relation between plasma Na^+ concentration and salt gland Na^+/K^+-ATPase content in the diamondback terrapin and the yellow-bellied sea snake. J Comp Physiol 101(2):89-97.

Dunson W. 1968. Salt gland secretion in the pelagic sea snake *Pelamis*. Am J Physiol 215(6):1512-1517.

Dunson WA. 1969. Reptilian salt glands. In: Botelho SY, Brooks FP, Shelley WB, editors. The exocrine glands. Philadelphia: University of Pennsylvania Press. p 83-103.

Dunson WA. 1978. Role of the skin in sodium and water exchange of aquatic snakes placed in seawater. Am J Physiol 235(3):R151-159.

Dunson WA. 1980. The relation of sodium and water balance to survival in sea water of estuarine and freshwater races of the snakes *Nerodia fasciata*, *Nerodia sipedon* and *Nerodia valida*. Copeia(2):268-280.

Dunson WA. 1984. The contrasting roles of the salt glands, the integument and behavior in osmoregulation of marine reptiles. In: Pequeux A, Gilles R, Bolis L, editors. Osmoregulation in estuarine and marine animals: Lecture notes on coastal and estuarine studies.

Dunson WA. 1985. Effect of water salinity and food salt content on growth and sodium-efflux of hatchling diamondback terrapins (*Malaclemys*). Physiol Zool 58(6):736-747.

Dunson WA, Dunson MK. 1973. Convergent evolution of sublingual salt glands in the marine file snake and true sea snakes. J Comp Physiol 86(3):193-208.

Dunson WA, Dunson MK. 1974. Interspecific differences in fluid concentration and secretion rate of sea snake salt glands. Am J Physiol 227(2):430-438.

Dunson WA, Dunson MK. 1979. Possible new salt gland in a marine Homalopsid snake (*Cerberus rhynchops*). Copeia(4):661-673.

Dunson WA, Mazzotti FJ. 1989. Salinity as a limiting factor in the distribution of reptiles in Florida Bay: A theory for the estuarine origin of marine snakes and turtles. Bull Mar Sci 44(1):229-244.

Dunson WA, Packer RK, Dunson MK. 1971. Sea snakes: An unusual salt gland under the tongue. Science 173(3995):437-441.

Dunson WA, Robinson GD. 1976. Sea snake skin: Permeable to water but not to sodium. J Comp Physiol 108(3):303-311.

Dunson WA, Taub AM. 1967. Extrarenal salt excretion in sea snakes (*Laticauda*). Am J Physiol 213(4):975-982.

Ellis RA, Delellis RA, Goertemiller CC, Kablotsky YH. 1963. Effect of a salt water regimen on development of salt glands of domestic ducklings. Dev Biol 8(3):286-308.

Ellis RA, Goertemiller CC, Jr. 1974. Cytological effects of salt-stress and localization of transport adenosine triphosphatase in the lateral nasal glands of the desert iguana, *Dipsosaurus dorsalis*. Anat Rec 180(2):285-297.

Ernst SA, Crawford KM, Post MA, Cohn JA. 1994. Salt stress increases abundance and glycosylation of CFTR localized at apical surfaces of salt gland secretory cells. Am J Physiol 267(4 Pt 1):C990-1001.

Ernst SA, Goertemiller CC, Ellis RA. 1967. Effect of salt regimens on development of (Na^+/K^+)-dependent ATPase activity during growth of salt galnds of ducklings. Biochim Biophys Acta 135(4):682-692.

Evans DH, Claiborne JB. 2009. Osmotic and ionic regulation in fishes. In: Evans DH, editor. Osmotic and ionic regulation: Cells and animals. Boca Raton, FL: CRC Press. p 295-366.

Evans DH, Piermarini PM, Choe KP. 2004. Homeostasis: Osmoregulation, pH regulation, and nitrogen excretion. In: Carrier JC, Musick JA, Heithaus MR, editors. Biology of sharks and their relatives. Boca Raton, FL: CRC Press. p 247-268.

Fernandez M, Gasparini Z. 2000. Salt glands in a Tithonian metriorhynchid crocodyliform and their physiological significance. Lethaia 33(4):269-276.

Franklin CE, Taylor G, Cramp RL. 2005. Cholinergic and adrenergic innervation of lingual salt glands of the estuarine crocodile, *Crocodylus porosus*. Aust J Zool 53(6):345-351.

Frigeri A, Gropper MA, Turck CW, Verkman AS. 1995. Immunolocalization of the mercurial-insensitive water channel and glycerol intrinsic protein in epithelial cell plasma membranes. Proc Natl Acad Sci U S A 92(10):4328-4331.

Gerzeli G, De Stefano GF, Bolognani L, Koenig KW, Gervaso MV, Omodeo-Sale MF. 1976. The rectal gland in relation to the osmoregulatory mechanisms of marine and freshwater elasmobranchs. In: Thorson TB, editor. Investigations of the ichthyofauna of Nicaraguan lakes. Lincoln, Nebraska: School of Life Sciences, University of Nebraska. p 619-627.

Giménez I, Forbush B. 2003. Short-term stimulation of the renal $Na^+/K^+/Cl^-$ cotransporter (NKCC2) by vasopressin involves phosphorylation and membrane translocation of the protein. J Biol Chem 278(29):26946-26951.

Goldstein DL. 2002. Water and salt balance in seabirds. In: Schreiber EA, Burger J, editors. Biology of Marine Birds. Boca Raton, FL: CRC Press. p 467-483.

Guggino WB, Oberleithner H, Giebisch G. 1988. The amphibian diluting segment. Am J Physiol Renal Physiol 254(5):F615-627.

Haas M, Forbush B, 3rd. 2000. The Na-K-Cl cotransporter of secretory epithelia. Annu Rev Physiol 62:515-534.

Hackett SJ, Kimball RT, Reddy S, Bowie RCK, Braun EL, Braun MJ, Chojnowski JL, Cox WA, Han KL, Harshman J, Huddleston CJ, Marks BD, Miglia KJ, Moore WS, Sheldon FH, Steadman DW, Witt CC, Yuri T. 2008. A phylogenomic study of birds reveals their evolutionary history. Science 320(5884):1763-1768.

Han ZQ, Wax MB, Patil RV. 1998. Regulation of aquaporin-4 water channels by phorbol ester-dependent protein phosphorylation. J Biol Chem 273(11):6001-6004.

Hazard LC. 1999. Ion secretion by the nasal salt gland of an herbivorous desert lizard, *Dipsosaurus dorsalis*. [Dissertation]. Riverside, CA: University of California. 148 p.

Hildebrandt JP. 1997. Changes in Na^+/K^+-ATPase expression during adaptive cell differentiation in avian nasal salt gland. J Exp Biol 200(Pt 13):1895-1904.

Hildebrandt JP. 2001. Coping with excess salt: Adaptive functions of extrarenal osmoregulatory organs in vertebrates. Zoology 104(3-4):209-220.

Holmes WN, McBean RL. 1964. Some aspects of electrolyte excretion in the green turtle *Chelonia mydas mydas*. J Exp Biol 41(1):81-90.

Hughes MR. 1970. Relative kidney size in nonpasserine birds with functional salt glands. Condor 72(2):164-168.

Hughes MR. 2003. Regulation of salt gland, gut and kidney interactions. Comp Biochem Physiol A Mol Integr Physiol 136(3):507-524.

Humason GL. 1972. Animal tissue techniques. San Francisco: W.H. Freeman and Company.

Ishibashi K, Sasaki S, Fushimi K, Uchida S, Kuwahara M, Saito H, Furukawa T, Nakajima K, Yamaguchi Y, Gojobori T, et al. 1994. Molecular cloning and expression of a member of the aquaporin family with permeability to glycerol and urea in addition to water expressed at the basolateral membrane of kidney collecting duct cells. Proc Natl Acad Sci U S A 91(14):6269-6273.

Johnson OW, Skadhauge E. 1975. Structural-functional correlations in the kidneys and observations of colon and cloacal morphology in certain Australian birds. J Anat 120(Pt 3):495-505.

Junqueira LCU, Malnic G, Monge C. 1966. Reabsorptive function of the ophidian cloaca and large intestine. Physiol Zool 39(2):151-159.

Kaplan JH. 2002. Biochemistry of Na,K-ATPase. Annu Rev Biochem 71:511-535.

Katoh F, Cozzi RR, Marshall WS, Goss GG. 2008. Distinct $Na^+/K^+/2Cl^-$ cotransporter localization in kidneys and gills of two euryhaline species, rainbow trout and killifish. Cell Tissue Res 334(2):265-281.

Kinne RKH, Zeidel ML. 2009. Osmotic and ionic regulation in mammals. In: Evans DH, editor. Osmotic and ionic regulation: Cells and animals. Boca Raton, FL: CRC Press. p 525-565.

Kirschner LB. 1980. Comparison of vertebrate salt-excreting organs. Am J Physiol 238(3):R219-223.

Kuchel LJ, Franklin CE. 2000. Morphology of the cloaca in the estuarine crocodile, *Crocodylus porosus*, and its plastic response to salinity. J Morphol 245(2):168-176.

Kunzelmann K. 1999. The cystic fibrosis transmembrane conductance regulator and its function in epithelial transport. Reviews of Physiology, Biochemistry and Pharmacology, Volume 137: Springer Berlin Heidelberg. p 1-70.

Lau KK, Yang Y, Cook GA, Wyatt RJ, Nishimura H. 2009. Control of aquaporin 2 expression in collecting ducts of quail kidneys. Gen Comp Endocrinol 160(3):288-294.

Lauren DJ. 1985. The effect of chronic saline exposure on the electrolyte balance, nitrogen metabolism, and corticosterone titer in the American alligator, *Alligator mississippiensis*. Comp Biochem Physiol Part A Mol Integr Physiol 81(2):217-223.

Lebrie SJ, Sutherland ID. 1962. Renal function in water snakes. Am J Physiol 203:995-1000.

Lignot JH, Cutler CP, Hazon N, Cramb G. 2002. Immunolocalisation of aquaporin 3 in the gill and the gastrointestinal tract of the European eel *Anguilla anguilla* (L.). J Exp Biol 205(Pt 17):2653-2663.

Lillie RD. 1940. Further experiments with the Masson trichrome modification of the Mallory connective tissue stain. Stain Technology 15:17-22.

Lillywhite HB, Babonis LS, Sheehy CM, Tu MC. 2008. Sea snakes (*Laticauda* spp.) require fresh drinking water: Implication for the distribution and persistence of populations. Physiol Biochem Zool 81(6):785-796.

Lillywhite HB, Menon JG, Menon GK, Sheehy CM, Tu MC. 2009. Water exchange and permeability properties of the skin in three species of amphibious sea snakes (*Laticauda* spp.). J Exp Biol 212(12):1921-1929.

Lowy RJ, Dawson DC, Ernst SA. 1989. Mechanism of ion transport by avian salt gland primary cell cultures. Am J Physiol 256(6 Pt 2):R1184-1191.

Lytle C, Xu JC, Biemesderfer D, Forbush B, 3rd. 1995. Distribution and diversity of $Na^+/K^+/Cl^-$ cotransport proteins: A study with monoclonal antibodies. Am J Physiol 269(6 Pt 1):C1496-1505.

Marples BJ. 1932. The structure and development of the nasal glands of birds. Proc Zool Soc Lond Part 4:829-844.

Minnich JE. 1970. Water and electrolyte balance of the desert iguana, *Dipsosaurus dorsalis*, in its natural habitat. Comp Biochem Physiol 35(4):921-933.

Minnich JE, Piehl PA. 1972. Spherical precipitates in urine of reptiles. Comp Biochem Physiol 41(3A):551-554.

Mobasheri A, Wray S, Marples D. 2005. Distribution of AQP2 and AQP3 water channels in human tissue microarrays. J Mol Hist 36(1-2):1-14.

Mochida H, Nakakura T, Suzuki M, Hayashi H, Kikuyama S, Tanaka S. 2008. Immunolocalization of a mammalian aquaporin 3 homolog in water-transporting epithelial cells in several organs of the clawed toad *Xenopus laevis*. Cell Tissue Res 333(2):297-309.

More NK. 1977. Histochemistry of mucopolysaccharides from snake kidney and their possible role in excretion. Cell Mol Biol (Noisy-Le-Grand) 22(2):151-161.

Muller C, Sendler M, Hildebrandt JP. 2006. Downregulation of aquaporins 1 and 5 in nasal gland by osmotic stress in ducklings, *Anas platyrhynchos*: implications for the production of hypertonic fluid. J Exp Biol 209(20):4067-4076.

Nagy KA, Medica PA. 1986. Physiological ecology of desert tortoises in southern Nevada. Herpetologica 42(1):73-92.

Nielsen S, Chou CL, Marples D, Christensen EI, Kishore BK, Knepper MA. 1995. Vasopressin increases water permeability of kidney collecting duct by inducing translocation of aquaporin-CD water channels to plasma membrane. Proc Natl Acad Sci U S A 92(4):1013-1017.

Nielsen S, Frokiaer J, Marples D, Kwon TH, Agre P, Knepper MA. 2002. Aquaporins in the kidney: From molecules to medicine. Physiol Rev 82(1):205-244.

Nishimura H, Fan Z. 2002. Sodium and water transport and urine concentration in avian kidney. In: Hazon N, Flik G, editors. Osmoregulation and drinking in vertebrates. Oxford, UK: BIOS Scientific Publishers Ltd. p 129-151.

Oguri M. 1964. Rectal glands of marine and fresh-water sharks - comparative histology. Science 144(3622):1151-1152.

Ogushi Y, Mochida H, Nakakura T, Suzuki M, Tanaka S. 2007. Immunocytochemical and phylogenetic analyses of an arginine vasotocin-dependent aquaporin, AQP-h2K, specifically expressed in the kidney of the tree frog, *Hyla japonica*. Endocrinology 148(12):5891-5901.

Ortiz RM. 2001. Osmoregulation in marine mammals. J Exp Biol 204(Pt 11):1831-1844.

Pandey RN, Yaganti S, Coffey S, Frisbie J, Alnajjar K, Goldstein D. 2010. Expression and immunolocalization of aquaporins HC-1, -2, and -3 in Cope's gray treefrog, *Hyla chrysoscelis*. Comp Biochem Physiol A Mol Integr Physiol 157(1):86-94.

Peaker M, Linzell JL, editors. 1975. Salt glands in birds and reptiles. London, New York: Cambridge University Press. 307 p.

Pettus D. 1963. Salinity and subspeciation in *Natrix sipedon*. Copeia(3):499-504.

Piermarini PM, Verlander JW, Royaux IE, Evans DH. 2002. Pendrin immunoreactivity in the gill epithelium of a euryhaline elasmobranch. Am J Physiol Regul Integr Comp Physiol 283(4):R983-992.

Pough FH. 1979. Summary of oxygen transport characteristics of reptilian blood. Smithsonian herpetological information service. p 1-18.

R Development Core Team R. 2008. R: A language and environment for statistical computing. Vienna, Austria.

Reina RD, Jones TT, Spotila JR. 2002. Salt and water regulation by the leatherback sea turtle *Dermochelys coriacea*. J Exp Biol 205(13):1853-1860.

Riordan JR, Forbush B, 3rd, Hanrahan JW. 1994. The molecular basis of chloride transport in shark rectal gland. J Exp Biol 196:405-418.

Roberts JS, Schmidt-Nielsen B. 1966. Renal ultrastructure and excretion of salt and water by three terrestrial lizards. Am J Physiol 211(2):476-486.

Rose TM, Henikoff JG, Henikoff S. 2003. CODEHOP (COnsensus-DEgenerate Hybrid Oligonucleotide Primer) PCR primer design. Nucleic Acids Res 31(13):3763-3766.

Russell JM. 2000. Sodium-potassium-chloride cotransport. Physiol Rev 80(1):211-276.

Schmidt-Nielsen B, Skadhauge E. 1967. Function of the excretory system of the crocodile (*Crocodylus acutus*). Am J Physiol 212(5):973-980.

Schmidt-Nielsen K, Fange R. 1958. Salt glands in marine reptiles. Nature 182(4638):783-785.

Seshadri C. 1959. Structural modification of the cloaca of *Lycodon aulicus aulicus*, Linn., in relation to urine excretion and the presence of sexual segment in the kidney of male. Proc Natl Inst Sci India Part B Biol Sci 25B(5):271-278.

Sever DM, Ryan TJ. 1999. Ultrastructure of the reproductive system of the black swamp snake (*Seminatrix pygaea*): Part I. Evidence for oviducal sperm storage. J Morphol 241(1):1-18.

Shoemaker VH, Nagy KA. 1984. Osmoregulation in the Galapagos marine iguana, *Amblyrhynchus cristatus*. Physiol Zool 57(3):291-300.

Shuttleworth TJ, Hildebrandt JP. 1999. Vertebrate salt glands: Short- and long-term regulation of function. J Exp Zool 283(7):689-701.

Shuttleworth TJ, Thompson JL. 1987. Secretory activity in salt glands of birds and turtles: Stimulation via cyclic AMP. Am J Physiol 252(2 Pt 2):R428-432.

Skadhauge E, Duvdevani I. 1977. Cloacal absorption of NaCl and water in the lizard *Agama stellio*. Comp Biochem Physiol Part A Mol Integr Physiol 56(3):275-279.

Smith PR, Mackler SA, Weiser PC, Brooker DR, Ahn YJ, Harte BJ, McNulty KA, Kleyman TR. 1998. Expression and localization of epithelial sodium channel in mammalian urinary bladder. Am J Physiol Renal Physiol 274(1):F91-F96.

Spector DA, Wade JB, Dillow R, Steplock DA, Weinman EJ. 2002. Expression, localization, and regulation of aquaporin-1 to -3 in rat urothelia. Am J Physiol Renal Physiol 282(6):F1034-F1042.

Staaland H. 1967. Anatomical and physiological adaptations of the nasal glands in Charadriiformes birds. Comp Biochem Physiol Part A Mol Integr Physiol 23(3):933-944.

Stokes GD, Dunson WA. 1982. Permeability and channel structure of reptilian skin. Am J Physiol 242(6):F681-689.

Sugiura K, Aste N, Fujii M, Shimada K, Saito N. 2008. Effect of hyperosmotic stimulation on aquaporins gene expression in chick kidney. Comp Biochem Physiol A Mol Integr Physiol 151(2):173-179.

Sullivan MX. 1907. The physiology of the digestive tract of elasmobranchs. Contributions from the biological laboratory of the Bureau of Fisheries at Woods Hole, MA 27(3):3-27.

Takeyasu K, Tamkun MM, Renaud KJ, Fambrough DM. 1988. Ouabain-sensitive Na^+/K^+-ATPase activity expressed in mouse L cells by transfection with DNA encoding the alpha-subunit of an avian sodium pump. J Biol Chem 263(9):4347-4354.

Taplin LE. 1985. Sodium and water budgets of the fasted estuarine crocodile, *Crocodylus porosus*, in seawater. J Comp Physiol B Biochem Syst Environ Physiol 155(4):501-513.

Taplin LE, Grigg GC. 1981. Salt glands in the tongue of the estuarine crocodile *Crocodylus porosus*. Science 212(4498):1045-1047.

Taplin LE, Grigg GC, Harlow P, Ellis TM, Dunson WA. 1982. Lingual salt glands in *Crocodylus acutus* and *Crocodylus johnstoni* and their absence from *Alligator mississipiensis* and *Caiman crocodilus*. J Comp Physiol 149(1):43-47.

Terris J, Ecelbarger CA, Nielsen S, Knepper MA. 1996. Long-term regulation of four renal aquaporins in rats. Am J Physiol 271(2 Pt 2):F414-422.

Tipsmark CK, Sorensen KJ, Madsen SS. 2010. Aquaporin expression dynamics in osmoregulatory tissues of Atlantic salmon during smoltification and seawater acclimation. J Exp Biol 213(Pt 3):368-379.

Untergasser A, Nijveen H, Rao X, Bisseling T, Geurts R, Leunissen JA. 2007. Primer3Plus, an enhanced web interface to Primer3. Nucleic Acids Res 35(Web Server issue):W71-74.

Uribe MC, Gonzalez-Porter G, Palmer BD, Guillette LJ. 1998. Cyclic histological changes of the oviductal-cloacal junction in the viviparous snake *Toluca lineata*. J Morphol 237(2):91-100.

Winne CT, Ryan TJ, Leiden Y, Dorcas ME. 2001. Evaporative water loss in two natricine snakes, *Nerodia fasciata* and *Seminatrix pygaea*. J Herpetol 35(1):129-133.

Yokota SD, Benyajati S, Dantzler WH. 1985. Renal function in sea snakes. I. Glomerular filtration rate and water handling. Am J Physiol 249(2 Pt 2):R228-236.

Zachos NC, Tse M, Donowitz M. 2005. Molecular physiology of intestinal Na^+/H^+ exchange. Annu Rev Physiol 67(1):411-443.

Zardoya R, Villalba S. 2001. A phylogenetic framework for the aquaporin family in eukaryotes. J Mol Evol 52(5):391-404.

BIOGRAPHICAL SKETCH

After completing a Bachelor of Science degree in biology with a specialization in marine science at the University of Miami (Coral Gables, FL) in May of 2003, Leslie S. Babonis began an internship jointly sponsored by the Student Conservation Association and the National Park Service. She spent a year at Biscayne National Park (Homestead, FL) studying the effects of coastal land use on overland freshwater flow and, during this time, became interested in understanding the physiology of animals that were able to tolerate the hypersaline coastal habitats she studied. In August of 2004, Leslie entered the Ph.D. program in the Department of Zoology (later named: Department of Biology) at the University of Florida to study the physiology and evolution of marine habitat use in snakes and advanced to candidacy in May of 2007. In the course of completing her Ph.D. research, Leslie traveled to Taiwan four times during the summers of 2005-2008. In October of 2010, she accepted a position as a postdoctoral researcher in the laboratory of Dr. Mark Q. Martindale at the Kewalo Marine Laboratory (University of Hawaii) where she will work to understand the origins of cell identity by examining the evolution and development of neurons in basal marine invertebrates.